

University of Alberta

New Biodegradable Elastomers for Interferon- γ Delivery

By

Husam Mohammed Younes



A thesis submitted to the Faculty of Graduate Studies and Research in partial fulfillment
of the requirements for the degree of *Doctor of Philosophy*

In

Pharmaceutical Sciences

Faculty of Pharmacy and Pharmaceutical Sciences

Edmonton, Alberta

Spring 2003

National Library
of Canada

Acquisitions and
Bibliographic Services

395 Wellington Street
Ottawa ON K1A 0N4
Canada

Bibliothèque nationale
du Canada

Acquisitons et
services bibliographiques

395, rue Wellington
Ottawa ON K1A 0N4
Canada

Your file *Votre référence*

ISBN: 0-612-82188-9

Our file *Notre référence*

ISBN: 0-612-82188-9

The author has granted a non-exclusive licence allowing the National Library of Canada to reproduce, loan, distribute or sell copies of this thesis in microform, paper or electronic formats.

The author retains ownership of the copyright in this thesis. Neither the thesis nor substantial extracts from it may be printed or otherwise reproduced without the author's permission.

L'auteur a accordé une licence non exclusive permettant à la Bibliothèque nationale du Canada de reproduire, prêter, distribuer ou vendre des copies de cette thèse sous la forme de microfiche/film, de reproduction sur papier ou sur format électronique.

L'auteur conserve la propriété du droit d'auteur qui protège cette thèse. Ni la thèse ni des extraits substantiels de celle-ci ne doivent être imprimés ou autrement reproduits sans son autorisation.

Canada

University of Alberta

Library Release Form

Name of Author: **Husam Mohammed Younes**

Title of Thesis: **New Biodegradable Elastomers for Interferon- γ Delivery**

Degree: **Doctor of Philosophy**

Year this Degree Granted: **2003**

Permission is hereby granted to the University of Alberta Library to reproduce single copies of this thesis and to lend or sell such copies for private, scholarly or scientific research purposes only.

The author reserves all other publication and other rights in association with the copyright in the thesis, and except as herein before provided, neither the thesis nor any substantial portion thereof may be printed or otherwise reproduced in any material form whatever without the author's prior written permission.



.....

School of Pharmacy
Health Science Center
Memorial University of Newfoundland
St. John's, NF
Canada A1B 3V6

Date: *Nov 4, 2002*

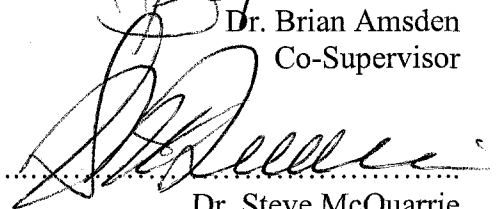
University of Alberta

Faculty of Graduate Studies and Research

The undersigned certify that they have read, and recommend to the Faculty of Graduate Studies and Research for acceptance, a thesis entitled *New Biodegradable Elastomers for Interferon- γ Delivery* submitted by *Husam Mohammed Younes* in partial fulfillment of the requirements for the degree of *Doctor of Philosophy in Pharmaceutical Sciences*.



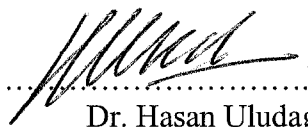
.....
Dr. Brian Amsden
Co-Supervisor



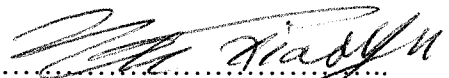
.....
Dr. Steve McQuarrie
Co-Supervisor



.....
Dr. Len I. Wiebe
Committee Chair



.....
Dr. Hasan Uludag
Committee Member



.....
Dr. Shirley Wu
External

Date: *November 4/02*

*Dedicated to the Memory of My Father:
because if I had been with him,
as I wished, and he deserved,
this thesis would not have
been studied or written.
Whatever its quality,
it is a poor substitute.*

Abstract

Maintaining a localized sustained concentration of Interferon- γ (IFN- γ) at the tumor site represents a promising immunotherapy methodology for cancer treatment and would provide distinct advantages. By restricting this cytokine to the vicinity of the neoplasm, minimal side effects and maximum therapeutic outcome can be realized. Different strategies have been utilized to deliver IFN- γ to the tumor site, including gene therapy and polymeric drug delivery systems. Some of the polymeric delivery systems investigated to date include liposomes, hydrogels and biodegradable microspheres made from poly (lactide-co-glycolide). These delivery strategies have inherent problems in maintaining the required therapeutic effect over time and/or in preserving their content of the loaded IFN- γ and/or in maintaining its stability.

Our objectives were first, to formulate a delivery system capable of providing a constant and sustained IFN- γ delivery rate by utilizing the osmotic release mechanism. Second, to maintain its stability and activity while within the delivery device and prior to it being released, and finally to eventually degrade and become bioabsorbed.

The delivery device has been formed by homogeneously distributing intimately mixed IFN- γ and stabilizing excipient particles throughout the polymer which has the required physical properties. The activity of IFN- γ in each step in the process, *i.e.* forming the excipient solution, lyophilization, and after release from the device has been determined using murine BV-2 Microglial cells and the quantification of the induced nitric oxide release. *In vitro* release studies in phosphate buffer saline of pH 7.4 were also undertaken

to demonstrate the osmotic mechanism and to determine the time frame for the drug release.

Our delivery system released IFN- γ in an almost zero order fashion and maintained its activity within the device until being released. This promising and effective delivery system may have application with other peptide and protein drugs which need to be delivered at a constant rate in a site-specific manner.

Acknowledgement

My thanks go firstly, as they should always be, to The Unique God (whom Muslims call *ALLAH*), the one who blessed me with the ability to undertake and finally complete this work. Whatever good may come of this work, the credit belongs to Him. After all, He already knows how diseases can be cured.

My most sincere gratitude goes to my supervisor Dr. Brian Amsden for his great efforts, guidance, attention and encouragement through the study. This invaluable help that he offered is beyond simple acknowledgement.

Thanks are also due to Dr. Steve McQuarrie for his support and helpful efforts. Further thanks should be expressed to Dr. Ayman El-Kadi whom without his help and support the completion of this work would have been far from over. My appreciation also goes to Dr. Len Wiebe for participating in my dissertation committee.

My deepest thanks go to Mr. Kassem Abouchehade for all the beautiful days we spent studying and shopping for computer parts. It is not easy in life to gain a unique friend like him.

The assistance provided by the support staff at the Faculty of Pharmacy, University of Alberta is highly appreciated. My special thanks also go to the followings for their assistance: Mr. Jeff Turchinsky, Mr. Don Whyte and Dr. Somayaji.

Finally, my special appreciation is extended to the members of my family and particularly my mother, sisters and wife for their endless love, care, encouragement, moral and spiritual support and their never failing patience. Their love and inspiration have made this task a pleasant one.

TABLE OF CONTENTS

Library Release Form

Title

Signed Examining Committee Signature

Dedication

Abstract

Acknowledgement

Table of Contents

List of Tables

List of Figures

List of Abbreviations

CHAPTER 1: Interferon- γ Therapy: Evaluation of Routes of Administration and Delivery Systems

1. Introduction	1
1.1. Background	2
1.2. Mechanism of Action of Interferon- γ	4
1.3. Physical Properties	7
1.4. Pharmacokinetics	9
1.5. Systemic Versus Local Delivery	11
1.6. Intermittent Versus Sustained Release	16
1.7. Dosage Forms: Advantages and Limitations	19
1.8. References	29

CHAPTER 2: Synthesis, Characterization and In Vitro Degradation of Biodegradable Elastomer.

2.1. Introduction	52
2.2. Experimental Section	53
2.2.1. Materials	54
2.2.2. Preparation of 50:50 poly (ϵ -caprolactone-dl-lactide) SCP	54

2.2.3. Preparation of 2,2-bis(ϵ -caprolactone-4-yl)-propane (BCP)	55
2.2.4. Synthesis of the Elastomer	57
2.2.5. BCP and Polymer Characterization	58
2.2.6. In Vitro Degradation Study	59
2.3. Results and Discussion.....	60
2.4. Conclusions	75
2.5. References	75

CHAPTER 3: Synthesis, Characterization and In Vitro Degradation of Photo-crosslinked Biodegradable Elastomer

3.1. Introduction	78
3.2. Experimental Section	80
3.2.1. Materials	80
3.2.2. Preparation of poly (ϵ -caprolactone-dl-lactide) Star Copolymer.....	81
3.2.3. Preparation of Acrylated SCP	82
3.2.4. UV-Crosslinking of Acrylated SCP	83
3.2.5. Polymer Characterization	84
3.2.6. In Vitro Degradation Study	86
3.3. Results and Discussion	86
3.4. Conclusions	96
3.5. References	97

CHAPTER 4: Osmotically Controlled Drug Delivery from a New Photo-cured Biodegradable Elastomer

4.1. Introduction	101
4.2. Materials and Methods	105
4.2.1. Materials.....	105
4.2.2. Preparation of poly (ϵ -caprolactone-dl-lactide) Star Copolymer	105
4.2.3. Preparation of Acrylated SCP	106
4.2.4. Preparation of Pilocarpine Nitrate Loaded Cylinders	107
4.2.5. Osmotic Activity measurements	108

4.2.6. In Vitro Release Study and UV Analysis	108
4.3. Results and Discussion	109
4.4. Conclusions	118
4.5. References	119

CHAPTER 5: Osmotically Release Delivery and Activity Assessment of Interferon- γ From a New Biodegradable Elastomer

5.1. Introduction	124
5.2. Materials and Methods	127
5.2.1. Materials	127
5.2.2. Preparation of poly (ϵ -caprolactone-dl-lactide) Star Copolymer	128
5.2.3. Preparation of Acrylated SCP	129
5.2.4. Lyophilization of Protein with Excipient	130
5.2.5. Preperation of Drug Loaded Elastomer	130
5.2.6. In Vitro Release Study	131
5.2.7. Cell Lines and Culture	131
5.2.8. Nitrite Assay and Protein Analysis	132
5.3. Results and Discussion	132
5.4. Conclusions	140
5.5. References	141

CHAPTER 6: General Discussion

6.1. General Discussion.....	147
6.2. Conclusions	155
6.3. References	158

APPENDICES

Appendix 1: Compatibility Assessment of a Biodegradable Elastomer

1. Introduction	163
2. Materials and Methods	165

2.1. Preparation of 50:50 poly (ϵ -caprolactone-dl-lactide)	166
2.2. Elastomer Synthesis	166
2.3. Sterilization.....	167
2.4. Compatibility Studies	167
2.4.1. In vitro Cytotoxicity	167
2.4.2. Intracutaneous Extract Injection	168
2.4.3. Systemic Extract Injection	169
2.4.4. Implantation Test	170
3. Results and Discussion	172
4. Conclusions	177
5. References	178
Appendix 2: Raw Data of the reported results	180

LIST OF TABLES

Table	Title	Page
2.1	Ratios of SCP and BCP used in preparing the elastomers	57
2.2	Elemental analysis for C, H, and O in BCP sample	66
2.3	Glass transition temperatures of the prepared elastomers	67
2.4	Summary of the mechanical properties of the elastomers. Values are means (standard deviation)	74
2.5	Summary of the changes in the extension ratio values with time for the tested slabs. Values are mean (standard deviation).	74
3.1	List of the star copolymers and their corresponding molecular weights prepared using different monomer/initiator molar ratios	83
3.2	List of the acrylated prepolymers prepared using different amounts of acryloyl chloride to react with the SCP prepolymer	88
3.3	The area under the peak for the OH and C=O stretching vibrations for SCP and the acrylated prepolymers and the % of conversion of the terminal hydroxyl to the vinyl groups.	90
3.4	Summary of the mechanical properties of the tested slabs of the corresponding prepared elastomers. Values are mean (SD)	94
3.5	Summary of the changes in the mechanical properties during in vitro degradation of elastomers prepared by photo-crosslinking of SCP-1A prepolymers. Values are mean (standard deviation)	95
4.1	Osmolality of pilocarpine nitrate solutions and the release media	110
4.2	Slopes of the linear phase of release shown in Figures 4.5 and 4.6.	

Values are mean \pm SD

112

LIST OF FIGURES

Figure	Title	Page
1.1	A proposed mechanism of direct action of IFN- γ on cellular membranes	5
1.2	Three-dimensional structure of bovine IFN- γ showing the dimeric inter-subunit 4-helix bundles	7
2.1	^1H -NMR of the prepared star copolymer	61
2.2	DSC thermogram of SCP	62
2.3	The ^1H -NMR of the prepared BCP	63
2.4	^{13}C -NMR of the prepared BCP	64
2.5	^{13}C -NMR of the prepared Diketone	65
2.6	Mass Spectrum of BCP	65
2.7	Stress-strain behaviour of the prepared elastomers	68
2.8	Percentage increase in weight of the tested slabs of the corresponding elastomers	69
2.9	Change in Young's modulus with time	70
2.10	Change in weight of the tested elastomers with time after drying	71
2.11	Change in pH of the degradation media with time	72
2.12	Change in ultimate tensile stress with time	73
3.1	Stacked FT-IR Spectra of the acrylated star copolymers reacted with different amounts of acryloyl chloride	88
3.2	Overlapped FT-IR spectra of SCP before and after the acrylation process showing the corresponding peaks	89
3.3	^1H -NMR spectra of the SCP-0 before acrylation (upper left) and the	

	acrylated SCP-01A (lower)	90
3.4	The stress-strain profile for the tested specimens of the elastomers prepared by photo-crosslinking of the SCP-1A prepolymers	93
4.1	Osmotic release mechanism. (a) water diffusion through polymer to first layer of agent particles; (b) swelling of particle capsules due to water imbibition under an osmotic activity gradient; (c) interconnected pore network formation and agent release as a result of capsule rupturing; (d) the elastomer eventually start significant degradation which overlaps with stage C	103
4.2	Method of loading PCN into the photoset elastomer	108
4.3	Cumulative percent PCN released from 5% v/v loaded cylinders (2 cm length) using distilled water, PBS and 3% NaCl as release media. Values are means of 4 samples \pm standard deviation	111
4.4	Cumulative percent PCN released from 5 % v/v loaded cylinders (1 cm length) using distilled water, PBS and 3% NaCl as release media. Values are means of 4 samples \pm standard deviation	112
4.5	Regression of the data obtained during the linear release phase (7-42 days) from 5% v/v cylinders of 2 cm length	113
4.6	Regression of the data obtained during the linear release phase (7-42 days) from 5% v/v cylinders of 1 cm length	115
4.7	Cumulative percent PCN released for 5% v/v of 1:1 intimately mixed PCN and trehalose in PBS of pH=7.4.(1 cm length). Values are means	

	of 4 samples \pm standard deviation	116
4.8	Regression fitting for the data obtained during the linear release phase (7-42days) from 5% v/v cylinders of 1 cm length in comparison with the linear phase (5-42 days) from 5% v/v loaded cylinders of 1 cm length of 1:1 intimately mixed PCN and trehalose	118
5.1	Nitrite concentration detected in culture medium of BV-2 Microglial cell. Cultures were incubated for 24 hours with various concentrations of rmIFN- γ , or LPS. <i>Data are means \pm SEM from 6 cell cultures. * $p < 0.05$ compared to control</i>	135
5.2	Nitrite concentration detected in culture medium of BV-2 Microglial cell. Cultures were incubated for 24 hours with 2 ng/ml rmIFN- γ during different preparation steps. LPS was used as a positive control. <i>Data are means \pm SEM from 6 cell cultures. * $p < 0.05$ compared to control. * $p < 0.05$ compared to lyophilized rmIFN-γ</i>	136
5.3	Nitrite concentration detected in culture medium of BV-2 Microglial cell. Cultures were incubated for 24 hours with the released rmIFN- γ at different time intervals	138
5.4	Cumulative amount of rmIFN- γ released in PBS medium at 37 °C detected using ELISA assay from stored frozen aliquots. Cylinders are of 1 mm diameter and 10 mm length with 0.5 % v/v rmIFN- γ loading. Values are mean \pm SD	139
5.5	Correlation between the percentage cumulative amount released of	

mIFN- γ and the cumulative activity detected between 1 to 15 days
period of release ($r^2=0.974$)

140

LIST OF ABBREVIATIONS AND SYMBOLS

σ	Tensile Stress
ϵ	Strain
λ_b	Extension Ratio
ϵ -CL	epsilon-Caprolactone
^{13}C -NMR	Carbon-13 Nuclear Magnetic Resonance
^1H -NMR	Proton Nuclear Magnetic Resonance
ACRL	Acryloyl Chloride
AUP	Area Under Peak
BCP	2,2-bis(ϵ -caprolactone-4-yl)-propane
CHO	Chinese Hamster Ovary
CSO	Cotton Seed Oil
Da	Dalton
DCM	Dichloromethane
DL-LA	D,L-Lactide
DMAP	4-Dimethyl Aminopyridine
DMPA	2,2-Dimethoxy-2-Phenyl-Acetophenone
DSC	Differential Scanning Calorimetry
DW	Distilled Water
E	Young's Modulus
EA	Elemental Analysis
EI	Electron Impact

Elast	Elastomer
EVA	Ethylene Vinyl Acetate
FDA	Food and Drug Agency
FT-IR	Fourier Transfer Infrared
GM-CSF	Granulocyte-Macrophage Colony Stimulating Factor
GPC	Gel Permeation Chromatography
hIFN- γ	Human Interferon-gamma
HLA	Human Leukocytes Antigen
IA	Intra-arterial
IFNs	Interferons
IFN- α	Interferon-alpha
IFN- β	Interferon-beta
IFN- γ	Interferon-gamma
IFN- γ R	Interferon-gamma receptors
IL-2	Interlukin-2
IM	Intramuscular
IU	International Unit
IV	Intravenous
KN	Kilo Newton
LWUV	Low Wave Ultra Violet
<i>m</i> CPBA	<i>m</i> -Chloroperoxybenzoic Acid
MHC	Major Histocompatibility Complex
MHz	Megahertz

mm	Millimetre
MS	Mass Spectroscopy
NK	Natural Killer
PBS	Phosphate Buffer Saline
PCN	Pilocarpine Nitrate
PDMS	Poly-Dimethoxysiloxane
PK	Pharmacokinetics
PLA-PEG	poly(lactic acid-block-ethyleneglycol)
PLG	poly(lactide-co-glycolide)
rhIFN- γ	Recombinant Human Interferon-gamma
rmIFN- γ	Recombinant Murine Interferon-gamma
SC	Subcutaneous
SCP	Star Copolymer Prepolymer
sIFN- γ R	Soluble Interferon-gamma receptors
SnOct	Stannous Octoate
$t^{1/2}$	Half-Life
TEA	Triethylamine
Tg	Glass Transition Temperature
THF	Tetrahydrofuran
TLC	Thin Layer Chromatography
TNF	Tumour Necrosis Factor
USP	United States Pharmacopoeia
UV	Ultra Violet

CHAPTER 1

INTRODUCTION

INTERFERON- γ THERAPY: EVALUATION OF ROUTES OF ADMINISTRATION AND DELIVERY SYSTEMS.

Husam M. Younes¹ and Brian G. Amsden^{1,2}

Published in *Journal of Pharmaceutical Sciences* 91: 2-17 (2002)

1. Faculty of Pharmacy and Pharmaceutical Science, University of Alberta, Edmonton, Alberta, Canada T6G 2N8
2. Department of Chemical Engineering, Queens University, Kingston, Ontario, Canada, K7L 3N6

1.1. Background

A great interest in the clinical use of Interferons (IFNs) has gradually arisen since their introduction in 1957.¹ Several clinical studies have demonstrated them to be effective in the treatment of multiple viral and neoplastic diseases²⁻⁴ and many excellent reviews have reported different specifics on their preparation, classification, stability, amino acid sequence, immuno-biological properties and the mechanisms by which this group of cytokines exert their antiviral and anti-tumoral activities.⁵⁻¹³

There are three main types of IFNs, now designated as interferon-alpha (IFN- α), interferon-beta (IFN- β) and interferon-gamma (IFN- γ). The latter, which is also known as immune or type II interferon, has several properties related to immunoregulation that make it different from the other interferons. It is a potent activator of mononuclear phagocytes. It does this by inducing them to produce tumour necrosis factor (TNF).¹⁴ It also directly induces the enzymatic activity that mediates the respiratory burst, allowing macrophages to kill phagocytosed microbes and tumour cells. Further, it not only increases the expression of class I major histocompatibility complex (MHC) molecules, but it also induces the cellular expression of class II MHC molecules. Thus, IFN- γ amplifies the recognition phase of the immune responses through the activation of class II-restricted T-Cells. It acts directly on T- and B-lymphocytes to promote their differentiation, and it stimulates the cytolytic activity of natural killer (NK) cells by inducing the secretion of the T-lymphocyte-produced cytokine interleukin-2 (IL-2). It also activates neutrophils and inhibits the proliferation of vascular endothelial cells.¹⁵ For all

these activities, IFN- γ has attracted extensive attention and, in the last two decades, scientists have been exploring its clinical uses and therapeutic potential.

IFN- γ has applications in the treatment of a number of immunological, viral and neoplastic diseases. These include systemic sclerosis,¹⁶ asthma,¹⁷ atopic dermatitis,¹⁸ myelogenous leukemia,¹⁹ hairy cell leukemia,²⁰ cutaneous leishmaniasis,²¹ lepromatous leprosy,²² scleroderma,^{23,24} granuloma annulare,²⁵ melanoma,²⁶ and metastatic renal cell carcinoma.^{4,27,28} IFN- γ currently is FDA approved for reducing the frequency and severity of serious infections associated with chronic granulomatous disease and for delaying time to disease progression in patients with severe, malignant osteopetrosis. Chronic granulomatous disease is a group of rare, inherited disorders of the immune system that are caused by defects in the phagocytes. These defects leave patients vulnerable to severe recurrent bacterial and fungal infections and chronic inflammatory conditions such as gingivitis, enlarged lymph glands, or granulomas. While not malignant, granulomas can cause serious problems by obstructing passage of food through the oesophagus, stomach, and intestines as well as blocking urine flow from the kidneys and bladder.^{29,30} Malignant osteopetrosis is another inherited disorder. This condition is characterized by an osteoclast defect leading to bone overgrowth and deficient phagocyte oxidative metabolism.^{31,32} In cancer immunotherapy, IFN- γ is injected along with irradiated autologous tumor cells. The IFN- γ acts as an adjuvant and enhances the immune response to the tumor cell challenge. A consistent finding in the studies regarding the delivery of IFN- γ for this latter purpose is that a stable and high concentration of the cytokine at the target site is required to elicit the desired response.^{13,33}

Although IFN- γ has been extensively investigated for a broad range of indications, it possesses properties which have limited its clinical use. Systemic delivery, which is the major route used to administer this interferon, of high concentrations yields significant side effects and toxicities. These side effects include fever, fatigue, nausea, vomiting, neurotoxicity, and leukopenia.

These limitations have prompted the investigation of alternate modes of delivering this cytokine to achieve higher therapeutic outcomes while minimizing its toxicity. In this review, emphasis will be placed on the different means of optimizing the antiviral and anticancer therapy of IFN- γ by utilizing an understanding of its physicochemical, pharmacokinetic, physiological and immunological aspects and relating this knowledge to the different routes and strategies used in delivering this interferon to its site of action.

1.2. Mechanisms of Action of IFN- γ

Several early hypotheses were proposed to explain the anti-tumour activities of IFNs. These hypotheses included inhibition of tumour viruses through the same mechanism that is involved in inhibition of other viruses³⁴ and/or acting as growth control regulators of the tumour cells³⁵ and/or acting on the immune system.³⁶ Currently, most of the issues relating to how IFNs exert their effects are fairly clear. In general, all IFNs exert their *in vivo* effects through their cellular action and/or stimulatory effects on the immune system. In the case of viral tumours, the cellular action includes binding to specific surface receptors. This results in transmembrane signalling and protein synthesis that either

reduces the translation of the viral protein and/or degrades the viral RNA, or blocks its replication.³⁷ Figure 1.1 summarizes some of the classical cellular pathways of IFN- γ . Upon interaction with its specific cell surface receptors, transmembrane signals are carried to the nucleus by a protein called Factor E. Factor E is a transcriptional activator that also plays a role in the internalization process. This series of events culminates in the production of different types of IFN- γ -induced proteins. It is these proteins that result in its antiproliferative and cytostatic actions.¹³

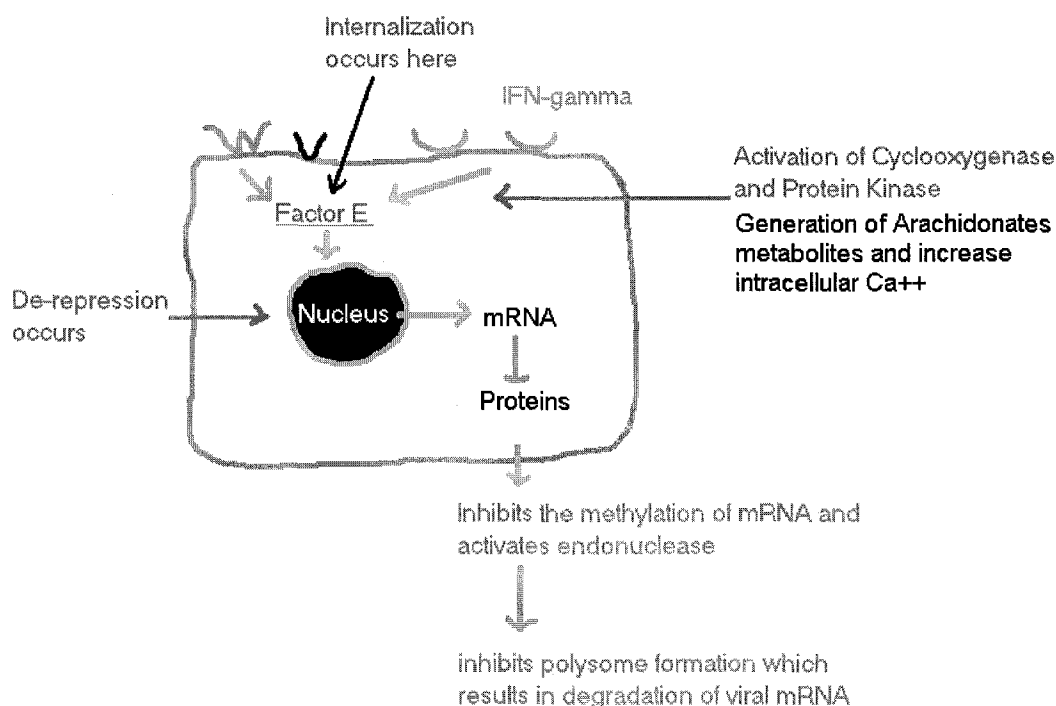


Figure 1.1 A proposed mechanism of direct action of IFN- γ on cellular membranes (Bocci, 1992 with permission).

It is well established now that IFN- γ receptors (IFN- γ R) are distributed and expressed on the membranes of almost all types of human cells and tissues.³⁸⁻⁴² It is this ubiquity of

receptors that results in the many side effects noted upon systemic administration of this cytokine. In some cases, the expression of the receptors was modulated by the effect of other cytokines that were simultaneously administered with IFN- γ for the treatment of cancer. For example, some *in vitro* studies reported that Granulocyte-Macrophage Colony Stimulating Factor (GM-CSF) significantly increased the expression of the IFN- γ receptor on human peripheral blood monocytes.⁴³

A soluble type of IFN- γ receptor (sIFN- γ R) has also been demonstrated to exist in the urine of healthy,⁴⁴ and the blood of arthritic,⁴⁵ patients. Such receptors were reported to either occur naturally or are formed by being cleaved from the intact cellular membrane receptors.⁴⁶ They are believed to have an immunoregulatory and neutralizing effect on both the biological and the immunological activity of IFN- γ . The administration of those soluble receptors would bind the free IFN- γ , thus prohibiting and /or competing with its binding with the membrane receptors, resulting in an inhibition of its biological activity.^{47,48}

IFN- γ also exerts its cytotoxic and cytostatic mechanisms by inducing the synthesis of indolamine 2,3-dioxygenase, which results in the degradation of the amino acid tryptophan causing tryptophan starvation of the cell.⁴⁹ Another means by which IFN- γ elicits its anti-tumour action is through its indirect stimulation of the immune system, causing a sequence of immunological reactions and stimulation of some of the immune system components. Both humoral and cellular effects are produced and these may

depend upon the dose of IFN- γ administered and its timing in relation to the immune process.⁵⁰

1.3. Physical Properties

IFN- γ is a homodimeric N-glycosylated glycoprotein with no sulphide bridges. It contains approximately 21-24 kD subunits that vary in their degree of glycosylation.⁵¹ IFN- γ is produced by T-Lymphocytes and natural killer (NK) cells, once these cells are induced by endogenous or exogenous stimulation.⁵² This glycoprotein is antigenically very different from both IFNs α and β . Unlike type I IFNs, it has an acid-labile bond, which is broken at pH 2.3 with subsequent loss of activity.⁵³ It is also heat sensitive and undergoes irreversible thermal denaturation in solution at a temperature range from 40-65 °C.⁵⁴ Moreover, it is basic with an isoelectric point at about pH 8.7.¹³ For reference, Figure 2 shows a representative three-dimensional structure of the dimeric form of bovine IFN- γ (bIFN- γ).

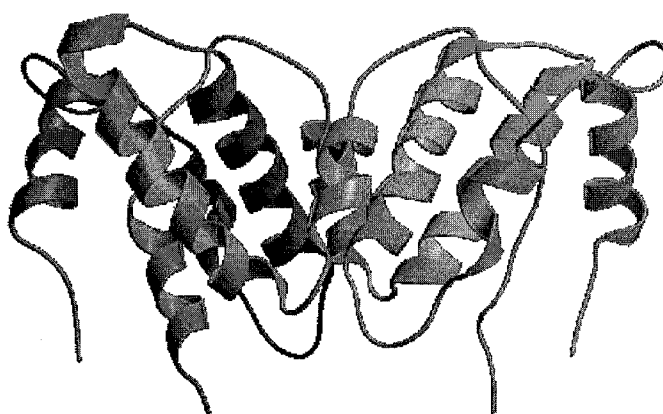


Figure 1.2 Three-dimensional structure of bIFN- γ showing the dimeric inter-subunit 4-helix bundles (From the cytokines web [www.psynix.co.uk/cytweb] with permission).

In the past, IFN- γ was obtained by purifying the naturally occurring protein produced by human leukocyte cells.⁵⁵ Presently, human IFN- γ (hIFN- γ) is produced via recombinant techniques in both *Escherichia coli* and cultured animal cells. This recombinant human IFN- γ (rhIFN- γ) has the same biological activity of natural hIFN- γ but, as with many recombinant proteins, possesses some differences in its glycosylation.⁵⁶ It is recognised that, in contrast to the naturally occurring hIFN- γ , rhIFN- γ lacks partially, or completely, the carbohydrate moieties attached to its structure.^{6,57,58}

hIFN- γ has two N-glycosylated sites at positions 25 and 97 of its 143 amino acid sequence.⁵⁸ This absence of carbohydrate moieties in the rhIFN- γ does not affect its biological activity but it does have a tremendous affect on both its physicochemical and pharmacokinetic properties. Bocci *et al.* were among the first to study and compare the pharmacokinetic differences of glycosylated and non-glycosylated IFN- γ . Their work showed that rhIFN- γ given by intravenous (IV) bolus injections disappeared from the bloodstream of rabbits at a faster rate than the glycosylated IFN- γ obtained from Chinese hamster ovary (CHO) cells.⁵⁹ Years later, Sareneva and co-workers compared the pharmacokinetics of natural hIFN- γ derived from human lymphocytes with that of glycosylated and non-glycosylated rhIFN- γ obtained from *Spodoptera frugipedra* insect cultures. Both forms were administered in equal doses by IV injection into rabbits. Interestingly, it was realized that not only did the lack of the glycan moieties decrease the half-life of the rhIFN- γ in the blood stream, but the type of the oligosaccharide moiety in the glycosylated form played a big role. It was found that since the glycosylated form of rhIFN- γ produced from insect cells possessed a mannose type oligosaccharide, it was

eliminated very rapidly from the circulation compared to the naturally occurring hIFN- γ . This was attributed to the faster rate of elimination of the mannose type (insect type) by the liver even when compared to the recombinant non-glycosylated IFN- γ .^{60,61} This discussion leads us to the conclusion that most of the differences in the elimination rate and in the other pharmacokinetic parameters reported in the next section with different modes of delivery resulted either completely or in part from the differences in the degree and type of glycosylation of IFN- γ .

1.4. Pharmacokinetics

The extent and rate at which the maximum IFN- γ concentration is reached in the bloodstream depends mainly on its physicochemical properties (molecular weight, size, and degree of glycosylation), the dosage form design, and its route of administration.^{13,62}

The primary route of administration of IFN- γ has been intravenous (IV). Other routes of administration evaluated in various clinical studies include intratumoral,^{63,64} intraarterial (IA),⁶⁵ intrathecal,⁶⁶ intraventricular,⁶⁷ intrabronchial⁶⁸ and intranasal.⁶⁹

Both hIFN- γ and rhIFN- γ have elimination half-lives in the bloodstream after IV administration of between 25-35 minutes and their serum concentrations are generally measurable for up to 4 hours.⁷⁰⁻⁷³ Their volume of distribution ranges from 12-40 L.^{72,74} This great range reflects the huge inequality in distribution between the body fluids and tissues.⁷⁰ Although hIFN- γ was not initially found to be absorbed significantly after SC and IM administration,^{75,76} rhIFN- γ given by the IM route had a peak level in the blood

stream between 4-8 hours with a half-life of 4.5 hours.⁷⁷ The SC and IM routes result in a more extended half-life, because these two routes form a depot after injection that allows a slower release of IFN- γ .

A factor that might have an effect on the pharmacokinetics (PK) of IFN- γ administered by the systemic route is the ubiquity of receptors,⁴⁰ including the soluble circulating receptors. Although there are many studies that report the distribution and other PK parameters of sIFN- γ R,^{46,47} to our knowledge, there are still no specific studies reporting the effect of circulating sIFN- γ R on the PK of IFN- γ itself. Nevertheless, it is most likely that their presence in the circulation would increase the half-life and the tissue distribution of IFN- γ , as has been reported to be the effect of soluble TNF- α receptors on the PK of TNF- α .⁷⁸

The goal of IFN- γ therapy is to deliver the cytokine to the interstitial fluid in the relevant tissue site. Many factors play an important role in the transfer of proteins such as IFNs from the bloodstream to interstitial fluids. Highly perfused organs including the liver, spleen, and lymph nodes contain a huge network of micro-capillaries that allow major transfer via extravasations of proteins. On the other hand, organ blood flow is also a critical factor in determining the transfer of proteins from plasma to the interstitial fluids. This factor has a major effect in determining the glomerular filtration rate and its contribution to the renal clearance of IFNs.¹³

The discussion above highlights the fact that IFN- γ has a short elimination half-life, whether given IV or SC or IM, and thus requires relatively frequent re-administration. For example, the dosing schedule for the treatment of chronic granulomatous disease is subcutaneous injection of 50 $\mu\text{g}/\text{m}^2$ three times weekly. This dosing regimen requires a health care professional, adding a health care burden, and is painful and inconvenient for the patient.

1.5. Systemic versus Local Delivery

Although, as has been noted, there is extensive literature concerning the uses of IFN- γ in different neoplastic, viral, immunological and other pathological conditions, little has been reported on the most efficient and least toxic sites, routes and modes of its delivery. The systemic delivery routes (IV, IM, SC, IA) constitute the vast majority of those used to deliver this cytokine to the human body.^{19,79,80} Nevertheless, such systemic routes possess tremendous disadvantages. Systemic administration will result in unequal and unpredictable distribution of IFNs throughout the body tissues and fluids and sometimes at a distance from the tumour site.^{70,81} Further, there is no direct dose-effect relationship. In other words, the concentration in the blood stream does not necessarily reflect the therapeutic outcome and/or the toxicity expected from the given dose.^{81,82} Also, the high concentration of IFN- γ to which different organs and cells are exposed might result in hypo- or hyper-responsiveness of the hormonal receptors. This response might have tremendous effects on the function of some vital organs.⁸³⁻⁸⁶ Finally, many of the side effects caused by INF- γ administration, which include fever, fatigue, nausea, vomiting, neurotoxicity, and leukopenia, are mainly caused by the high serum concentrations of the

cytokine.^{63,87} For a further discussion on the above issues, the reader is advised to refer to other excellent reviews.^{13,81}

In both the normal (physiological) and pathological (acute) conditions, IFN- γ produced or secreted from stimulated cells is characterized by two main features. First, it has a pleiotropic effect, *i.e.* it can exert the same effect on many different cell types and can also exert different actions on the same individual cell.⁸⁸ Second, it is produced in a paracrine fashion, that is, it is secreted locally from the producing cells and diffuses through the extra-cellular fluids to neighbouring cells in the surrounding microenvironment where it exerts its effect.^{89,90} The main difference between each situation is that in the pathological condition, the secretion of IFNs is described as acute.⁸⁹ In this case, the release mode switches to an endocrine secretion mode in which the high local concentrations of secreted IFNs manage to escape local (via internalization) and cellular catabolism. As a result, they will diffuse through the entire body and will be detected in the bloodstream. However, due to the dilution effect, hepatic metabolism and glomerular filtration, their presence will decline in a very short time. Thus, as has been noted in the pharmacokinetic section, secreted IFNs have a very short half-life in the bloodstream.^{59,75}

It has been proven that the regional mode of secretion of IFNs and the limited diffusion of this paracrine IFN to the bloodstream would minimize the exposure of many other cells and organs that do not need to be stimulated to switch to the antiviral state. In this manner, side effects and toxicity would be decreased.⁹¹ It has also been determined that

the lymphatic cells, after being activated by IFNs locally, in the microenvironment, would travel in the circulation producing defensive mechanisms without the need for the cytokines themselves to circulate.⁹²

Various studies have been aimed at studying the effectiveness and safety of localized delivery of cytokines compared to their systemic administration. Paralesional injections of TNF- α along with recombinant murine IFN- γ (rmIFN- γ) in phosphate buffer saline (PBS) in a murine tumour model was compared to their systemic administration in terms of their toxicity and anti-tumour effect. Tumour response after a single IV injection of 0-15 μ g of TNF- α and 5000 U of rmuIFN- γ was compared with five daily paralesional injections of exactly the same dose of TNF- α and rmIFN- γ . Although animals receiving the paralesional injections received five times the total of TNF- α and rmuIFN- γ dose compared with the IV animal, they had similar treatment-related mortality. On the other hand, the sustained local high concentration from the paralesional injections resulted in a dose-dependent improvement of the anti-tumour effect and a cure rate that was significantly greater than via the systemic administration.⁶³ In another study attempting to use rhIFN- γ in the treatment of granuloma annulare, local injection of IFN- γ in saline was well tolerated in all the patients participating in the clinical study and there were no flu-like symptoms or any changes in blood biochemistry. The treatment resulted in a significant reduction in granulomas compared to the control group.²⁵

Lepromatous leprosy, which is another form of granuloma, was efficiently treated with local intradermal injections of rhIFN- γ and such treatment resulted in a tremendous

leukocyte infiltration similar to a delayed-type hypersensitivity response.²² Surprisingly, this was not the case when an ethylene vinyl acetate copolymer used in the form of an implant loaded with rhIFN- γ was inserted subcutaneously. This controlled release drug depot failed to cause any local pathological responses.⁹³ This failure may have been due to the cytokine being inactivated by denaturation during the preparation of, or through interaction with, the polymeric device (see discussion below).

To solve the inability of systemically administered rhIFN- γ to reach the respiratory epithelial surface to cause activation of the alveolar macrophages, rhIFN- γ was targeted directly to the lung using an aerosol, which was inhaled once daily for 3 days. After this mode of localized delivery, rhIFN- γ was not detected in the circulation but was readily detectable in the respiratory epithelium lining fluids in a dose-dependent fashion. It was shown that this locally administered rhIFN- γ managed to augment the respiratory tract defence mechanism with no systemic toxicity.⁶⁸ Combination regional therapy using TNF- α plus IFN- γ with chemotherapy was also investigated in the treatment of melanoma. The immunohistological and immunological studies demonstrated efficacy and a minimization of toxicity.⁹⁴

Many other studies have reported the therapeutic potential and the advantages of a local/regional delivery of IFN- γ over a systemic mode in the treatment of cancer. Growth inhibition of human prostate carcinoma by local administration of the cytokines including IFN- γ has been demonstrated *in vitro* and *in vivo*.⁹⁵ The study showed the ability of IFN- γ to up-regulate HLA Class II expression on those cells tested, and other carcinoma

properties that are associated with tumour activity, suggesting that immunotherapy via the local delivery of the cytokines has a potentially therapeutic role in the treatment of prostate cancer.⁹⁵ The use of hIFN- γ in combination with hIFN- α was also explored for the treatment of breast carcinoma in two groups of patients who had failed radiotherapy. Both the IFNs were delivered by intralesional injections to the recurrent and metastatic lesions. The study demonstrated that non-injected lesions exposed to the systemic levels of the injected IFNs showed a non-appreciable clinical antitumor response with an immunological response that was less intense compared to those exposed to regional treatment. The study showed the usefulness of IFNs in controlling the loco-regional recurrence of breast carcinoma even in patients who were not responding to other forms of therapy.⁹⁶

The effect of regional therapy of rhIFN- γ on basal cell carcinoma in twenty-nine patients divided into two groups each receiving a different dose has also been reported.⁹⁷ The first group of 15 patients received 0.01 mg of rhIFN- γ intralesionally three times a week for three weeks, while the second group of 14 patients received 0.05 mg of rhIFN- γ following the same dosing schedule. The biopsies taken after 12 weeks of therapy showed a cure rate of 50% in the second group compared to 7% in the first group. The high local concentration of IFN- γ at the site of action was crucial in achieving a higher antitumor effect with mild adverse effects.⁹⁷

What can be concluded from this section is that a locally contained delivery system for IFN- γ would provide the best therapeutic outcome. This conclusion is based on the

manner in which IFN- γ is naturally secreted to elicit its effects, and on clinical data which demonstrate that fewer side-effects are achieved if IFN- γ is delivered in a site-specific manner, while at the same time its cytotoxic and cytolytic effects are magnified. It has also been demonstrated that local administration can exert potent immunological stimulation for the different components of the immune system without the need for the cytokine to circulate in the bloodstream

1.6. Intermittent Versus Sustained (Continuous) Release

In view of the above discussion, the questions that come to mind are: what is the maximum concentration required in the local microenvironment? Do we need an intermittent or a continuous release of IFNs? In the intermittent mode of administration, the cells are exposed to pulses or waves of the delivered IFN- γ followed by a time- and concentration-dependent decline in the effect. This mode of IFN- γ delivery was the focus of one of the studies carried out by a Japanese group exploring the effect of massive pulsatile administration of rhIFN- γ by IV infusion on an advanced renal cell carcinoma.⁹⁸ Although they concluded that this strategy of administration was successful in exerting a potentially active anti-tumour effect, it was obvious that the side effects were tremendous: ranging from as simple as fever to the deterioration of liver function, bronchial asthma and stiffness of the extremities.

In another study to determine the antileishmanial activity of recombinant murine IFN- γ (rmIFN- γ), Murray investigated the difference between intermittent and continuous

delivery of rmIFN- γ into *Leishmania donovani*-infected mice.⁹⁹ He compared once daily IP injections of 10^5 and 10^6 units (U) of rmIFN- γ with a subcutaneous osmotic pump of comparable dose (2.4×10^5 U/day). These researchers not only reported that intermittent IP administration of rmIFN- γ can induce antileishmanial activity, but also confirmed that this microbiostatic effect can be considerably enhanced by continuous administration of this cytokine. Forty Seven percent of the liver parasite killing effect was attributed to the rmIFN- γ being delivered continuously by a SC osmotic pump compared to 3 and 9% resulting from intermittent IP doses of 10^5 and 10^6 U respectively.⁹⁹

The rapid disappearance of rmIFN- γ from the mouse circulation after an intermittent IP dosing regimen may explain why continuous local delivery was more effective and resulted in enhanced activity.^{71,100} In addition, the constant presence of rmIFN- γ more closely mimicked the acute pathological mode of release in which the secretion of cytokines, like IFN- γ , would remain active as long as the stimulus, in this case cells parasitized by *L. donovani*, exists. On the other hand, the author in the previous study concluded that continuous delivery of rmIFN- γ might have initiated a separate antileishmanial mechanism in addition to the direct stimulation of macrophages and NK cells.⁹⁹

The preliminary results of an open randomized trial of rhIFN- γ in patients suffering from bowenoid papulosis –also known as penile intraepithelial neoplasia¹⁰¹ - and other pre-cancerous lesions were also reported. This genital disorder, caused by papilloma viruses, mainly affects young male adults. It is considered a high risk factor with respect to the

etiology of genito-anal carcinoma and believed to result in the deficiency in immunosurveillance mechanisms directed against viral-induced tumours.¹⁰² In this study, rhIFN- γ was given by SC injections to twelve patients divided into three groups at a daily dose of 4×10^6 I.U. The patients were assigned to a three-treatment schedule. Group A, with continuous therapy of rhIFN- γ administered 3 times per week for 13 weeks; Group B, with intermittent block therapy with four six-week cycles consisting of five injections on days 1, 3, 5, 7, and 9 of each cycle; and Group C, with intermittent single-dose therapy with six four-week cycles consisting of only one SC injection on the first day of each cycle. The study revealed that at the beginning of the treatment, there was no significant difference between the three groups. Nevertheless, six and a half months after the onset of therapy, the cure rates were significantly higher among group A in which the patients were treated with continuous administration of the cytokine.¹⁰²

Recently, it was reported that high local continuous cytokine therapy was more effective in the treatment of prostatic cancer¹⁰³ and also resulted in less toxicity.^{63,104} In another recent *in vitro* study, which explored the effect of high local intermittent and continuous treatment using TNF- α and IFN- γ , an isolated limb perfusion technique was used in which the human micro- and macrovascular endothelial cells were isolated and subjected to intermittent and high continuous delivery of TNF- α /IFN- γ . It was concluded that a continuous exposure to those cytokines for at least 24 hours was subsequently required to achieve a persistent antiproliferative effect on the endothelial cells.¹⁰⁵

Based on the preceding discussion, it can be concluded that the most efficient and least toxic delivery system for IFN- γ is a localized sustained release dosage form. Such a delivery strategy would minimize the exposure of the other cells and organs to the stimulatory and/or inhibitory effects of this potent cytokine.

1.7. Dosage Forms: Advantages and Limitations

Various strategies have been explored to formulate and deliver interferons while at the same time trying to achieve two major goals. The first is to deliver and target IFNs specifically and safely to their site of action to maximize their therapeutic efficacy while minimizing their toxicity. The other is to overcome stability issues during the preparation of dosage forms containing these cytokines, and to help in maintaining this stability during storage of the dosage form and after administration to the body. Work in this area is ongoing.

With respect to IFN- γ , which is acid sensitive and which possesses other stability problems, early studies focused mainly on achieving a localized and/or sustained/controlled release to help in increasing the therapeutic outcome, in extending its half-life in plasma and in decreasing the amount to which other non-tumour or non-infected tissues are exposed upon administering this potent IFN.^{106,107} Currently, studies concerning how efficient the methods and strategies used to formulate IFN- γ to achieve the two mentioned goals are running in parallel with efforts to use it in different neoplastic and viral diseases. Various means of achieving localized delivery of IFN- γ

have been investigated and include the use of liposomes, polymer gels, biodegradable microspheres, and gene therapy. Each of these formulation strategies will be examined individually.

Liposomal formulations of IFN- γ have been examined by a number of research groups. In these studies, IFN- γ has been found to be most efficiently incorporated by using negatively charged liposomes.¹⁰⁸⁻¹¹¹ Indications are that the cytokine resides primarily at the surface of the liposome, due to electrostatic interactions between the positively charged protein and the negatively charged liposomal components, and not in the aqueous interior. For example, van Slooten *et al.* determined that 75% of the IFN- γ incorporated into their phosphatidylcholine/phosphatidylglycerol liposomes resided at the surface.¹⁰⁹ Loading of the cytokine into the liposome formulations had been less than optimal. Initial studies by Goldbach *et al.* produced a loading efficiency of only 30%,¹¹⁰ while those obtained by Lachman *et al.* were only 23%.¹¹¹ However, in subsequent work by van Slooten *et al.* with recombinant murine IFN- γ , loadings of approximately 89% have been achieved.¹⁰⁹ Of the studies to date, only van Slooten *et al.* have examined IFN- γ stability upon desorption from the liposomes.¹¹² They found that the protein retained its secondary and tertiary structure upon desorption, but examined a release period of just 30 minutes, and so long term IFN- γ stability in this formulation has yet to be demonstrated. Furthermore, the release period of the IFN- γ from this liposomal formulation was relatively rapid, with a large burst of up to 75% of the initially loaded cytokine desorbed within the first eight hours.¹⁰⁹ This release behaviour has been noted with other proteins, such as interleukin-7¹¹³ in which approximately 50% of the initial drug load was

detectable in the urine of guinea pigs, and interleukin-2 which, after subcutaneous injection, was detectable in the plasma for 6 hours after administration.¹¹⁴

Liposomes have the distinct advantage of easy administration by injection. However, they also have distinct disadvantages. They produce relatively short drug release durations necessitating additional painful injections, and release rates are neither sustained nor controllable. Thus, they do not appear to be optimal for sustained, local delivery.

To date, only one study has focused on the incorporation and release of rhIFN- γ from hydrogels. Yu and Grainger examined the potential of poly (N-isopropylacrylamide-co-sodium acrylate-co-N-alkylacrylamide) as a release device.¹¹⁵ These gels were designed to be both pH and temperature responsive. rhIFN- γ release was almost constant, however, release durations were short (less than 7 days). Additionally, this hydrogel formulation is not biodegradable and so a surgical removal step would be required. Furthermore, the constant release achieved was attributed to hydrophobic interactions with the polymer, which may lead to denaturation of the cytokine. The advantages of hydrogels as a delivery vehicle are that they are as soft as tissue, and thus are considered to be very biocompatible, and can be made to be biodegradable. However, for protein drugs hydrogels possess drug stability issues with storage, due to the presence of a large degree of water in the device.

In gene therapy, a vector is used to insert a gene for the expression of a cytokine into a

cell. This process, termed transfection, can be accomplished using a number of vectors, which include viral vectors, polymers, and liposomes, and can be accomplished *in vivo* or *in vitro*.¹¹⁶ This approach has been used in numerous studies to obtain a sustained local IFN- γ concentration.¹¹⁷⁻¹²³ For example, Stoeckle *et al.* (1996) have demonstrated *in vitro* that IFN- γ can be secreted by transfected HeLa cells and fibroblasts using a replication-defective adenovirus for greater than 4 weeks.¹²⁰ The possible utility of the approach has also been demonstrated in Phase I clinical trials. In one study,¹²³ 13 patients received a single daily intra-tumoral injection of a retroviral vector containing the IFN- γ gene for 5 consecutive days. No toxicity related to the injected vector was observed, however, only 3 of 10 harvested tumour cell samples were found to be secreting IFN- γ , and DNA transduction was unable to be confirmed in six samples.

Gene therapy has potential, however, there are a number of unresolved problems surrounding it as a pharmaceutical approach. As noted in the example above, *in vivo* transfection rates, particularly for tumour cells, are low. This low transfection rate necessitates harvesting cells such as tumour infiltrating lymphocytes or tumour cells and treating them to express increased cytokines.³³ The cell population is then established *in vitro* and returned to the patient. Tumour cells are irradiated before being returned to the patient, to prevent reintroduction of replication competent tumour cells. This process is labour intensive, and difficult to achieve. Most human tumours are difficult to establish as *in vitro* cell lines, and extensive subcloning and *in vitro* replication might alter the original antigenic composition of the primary tumour. Moreover, it may take several months to transduce a tumour cell. Such patient-individualized therapy is therefore very

cost intensive. Finally, this approach is fraught with ethical issues.

Polymeric microspheres have been developed which are capable of delivering a virtually constant amount of an encapsulated protein. These formulations typically consist of a biodegradable polymer, poly (lactide-co-glycolide) (PLG), throughout which the protein is distributed as discrete solid particles. The protein is released in three phases: an initial burst; diffusion controlled release; and erosion controlled release. The initial burst is due to surface resident protein particles, while the diffusion controlled release is a result of dissolved protein diffusing through the water-filled pores and channels within the microspheres.^{124,125} To obtain a constant release rate from PLG microspheres, the diffusion phase must overlap with the erosion release phase such that new pores or channels are created. Polymeric microspheres have the advantages of not only providing a constant release, but of being easily injected to the target site, providing a long term release duration, of consisting of proven biocompatible materials, having a reasonable shelf-life and degrading to completely bioresorbable compounds. They thus appear to be a very promising formulation.

The main problem with this delivery system is maintenance of protein stability. The activity of a protein molecule is determined by its conformation in solution. Proteins are susceptible to aggregation, denaturation and adsorption at interfaces, deamidation, isomerization, cleavage, oxidation, thiol disulfide exchange, and β elimination in aqueous solutions. The major factors affecting these changes are mechanical forces such as shear, the presence of surfactants, buffers, ionic strength, the presence of oxidizers such as ions,

radicals and peroxide, light, pH and temperature. Thus, protein denaturation may result in a loss of potency and the conformation changes in the protein molecule may make the protein immunogenic.¹²⁶

IFN- γ possesses a number of stability problems. Firstly, IFN- γ is a prime candidate for acid degradation. It contains an acid-labile group (Asp-Pro bond at positions 2 and 3), which is broken at pH 2.3 with subsequent loss of activity. Furthermore, IFN- γ , as are many recombinant proteins, is particularly susceptible to aggregation when present in relatively high concentration in solution. This is because, as noted above, when produced through genetically engineered bacteria, post-translational glycosylation of the protein molecule does not take place.⁵³ Various means of stabilizing proteins in solution have been determined. These include the addition of compounds such as polyols, inorganic salts, and amino acids.¹²⁷

The problems of using the PLG microsphere formulation involve both acidic protein degradation, and denaturation at an organic solvent-water interface. When polymers such as PLG degrade, they liberate oligomers and monomers carrying carboxylic acid end groups. The presence of these oligomers and monomers has been found to decrease the local pH at the surface of the polymer and in the pores and channels of the device.¹²⁸⁻¹³⁰ In fact, a recent work has measured the pH at the centre of a PLG microspheres to be as low as 1.5.¹³¹ At this pH, IFN- γ is certain to undergo cleavage and deactivation. This reduction in the pH of the inner environment of the microspheres has been linked to inactivation and denaturation of other proteins within PLG microspheres prior to being

released. For example, when fast-degrading PLG microspheres were used to deliver interleukin-1 α , the cytokine lost its activity during incubation, and the extent of cytokine inactivation was consistent with the microsphere degradation rate.¹³² Other protein drugs for which this effect was noted are carbonic anhydrase,¹³³ atriopeptin III,¹³⁴ ovalbumin,¹³⁵ and trypsin and heparinase.¹³⁶ The protein-loaded microspheres are typically prepared using an water-in oil-in water(w/o/w) emulsification procedure in which the protein is dissolved in the aqueous phase. This preparation procedure has also been found to result in protein denaturation due to contact of the protein with the polymer solvent at the solvent-water interface.¹³⁷

There is one report in which rhIFN- γ has been incorporated into PLG microspheres and its stability after release studied.¹³⁸ These researchers examined the effects of microsphere preparation by w/o/w emulsion, buffer pH and buffer system on the release of IFN- γ . Using this emulsion procedure they successfully incorporated 100 % of the rhIFN- γ in the PLG microspheres. The stability of the cytokine was maintained during the fabrication procedure through the use of trehalose in the aqueous phase. However, they found that, although rhIFN- γ was stable after microsphere preparation and it was released for up to 50 days, after 7 days the released rhIFN- γ only had an activity of 30-38 %. Thus, maintaining stability of IFN- γ within PLG microspheres is still a problem.

This problem may be overcome by using a microsphere geometry that allows for virtually complete IFN- γ release before significant polymer degradation occurs. One possibility is the use of microporous microspheres wherein the cytokine is loaded completely into the

pores and not surrounded by polymer. Protein release would then proceed via diffusion through tortuous channels, which may proceed at a faster rate than polymer degradation. Alternatively, a different release mechanism could be employed. It has been demonstrated that a constant drug release rate is achievable from a rubbery polymer matrix in which the drug is distributed as discrete particles. Due to osmotic water imbibition, ruptures are formed in the polymer and dissolved drug solution is forced out of the device.^{139,140} Accomplishing this type of release mechanism with microspheres, however, may be quite difficult.

Another release system that has been employed with other proteins, but not IFN- γ to date, is the use of an injectable polymer vehicle. There have been two strategies developed for this purpose. One involves preparing a low molecular weight degradable polymer that is a viscous liquid at room temperature. The protein is mixed with the liquid polymer and then injected. Polymers that have been examined for this use include a block copolymer of poly(lactic acid – block – ethylene glycol) (PLA-PEG)¹⁴¹ and a poly(orthoester).^{142,143} The PLA-PEG system was composed of a PLA block of a molecular weight of 650 and a PEG block of molecular weight 200 Dalton. Bone morphogenic proteins were incorporated into the polymer and injected into the dorsal muscle of rats. The authors reported only a mild inflammatory response and that the polymer was completely absorbed within 3 weeks. The protein was apparently active as bone formation was noted, however no release data and no protein stability assays were done. Merkli *et al.*, synthesized a poly (orthoester) composed of 1,2,6-hexanetriol and trimethyl orthoacetate as an injectable polymer vehicle. At low molecular weights (3300 Dalton) the polymer

had a low viscosity (33 Pa·s) and the viscosity increased with increasing molecular weight to a maximum of 15,331 Pa·s at a molecular weight of 33,300. At these viscosities the polymers were relatively easily injected through a 20-gauge needle. The authors examined the release of 5-fluorouracil from these systems and observed an almost constant release period with no initial burst. The release duration ranged from 1 day to 7 days with the 3300 Dalton polymer and the 33,300 Dalton polymer respectively. This polymer breaks down by hydrolysis and the pH, as measured in saline, dipped to a low of 4.5 within the first 5 days. With the incorporation of a basic excipient, this pH decrease was reduced and the polymer degradation time extended. The polymer with the basic excipient (Mg(OH)₂) was well tolerated when tested in rabbit ocular tissue. This material has not been used to deliver proteins, but would appear to be a good candidate to examine, although possible stability issues would need to be resolved.

The other strategy employed to produce an injectable polymer depot is the dissolution of a biodegradable polymer in a physiologically acceptable solvent, suspending protein particles within this suspension, and then injecting the solution into tissue. Upon entering the tissue, the solvent dissipates and diffuses away in the aqueous environment, while the polymer precipitates, entrapping the protein particles. A number of research groups have explored this method, using poly(lactic acid – co – glycolic acid) dissolved in either N-methyl pyrrolidone^{144,145} or glycofurol.¹⁴⁶ Lambert and Peck examined the factors governing the release of BSA from such a system and noted that the initial burst of protein released from the depot could be reduced to about 5-10 % of the initially loaded amount by increasing the polymer solution viscosity.¹⁴⁴ Viscosity can be increased by

increasing either polymer molecular weight or polymer concentration in solution. BSA was released from this depot system for greater than 9 days at an approximately constant rate. Eliaz and Kost observed the same release characteristics but with a combination of BSA and human soluble tumor necrosis factor receptor.¹⁴⁶ These authors reported a constant release rate lasting almost 20 days after an initial burst of 5-10%. They also demonstrated that the release of the protein was controlled predominantly by the degradation time of the polymer. Although these results appear promising for IFN- γ delivery, there is still the undetermined effect of the delivery vehicle and release mechanism on the stability of this cytokine.

Based on the previous introduction, we conclude that a continuous localized release of IFN- γ is a desirable goal. Of the formulation strategies examined to date to achieve this condition, biodegradable polymers possess a number of desirable properties but are limited by protein stability issues.

A new formulation approach is presented here which was based on the following hypothesis. First, that a continuous release from a polymeric matrix can be achieved by employing an osmotic mechanism and a balance of polymer physical properties with polymer degradation. To accomplish this, a biodegradable polymer has been crosslinked to become elastomeric. Second, the use of a slowly degrading polymer which has also been demonstrated to be biocompatible, such as caprolactone, will reduce or eliminate acidic degradation of IFN- γ within the device. Third, aggregation of the IFN- γ within the delivery device can be eliminated or reduced by incorporating the protein as a solid

lyophilized with the appropriate agents. The lyophilization agents will also serve as the driving force for the osmotic drug delivery mechanism. Finally, to facilitate production of protein-loaded matrices, the crosslinking can be introduced via a photo-initiated terminal end group which is also biocompatible.

On the basis of the previous introduction, our objectives were first, to synthesize a new biomaterial that is a *biocompatible, biodegradable, and thermo or photocurable elastomer* consisting of a crosslinked star copolymer of caprolactone and D,L-lactide and to crosslink this prepolymer with either the synthesized crosslinker Bis-caprolactone or by having terminal acryloyl moieties. The polymer will have an extension ratio which remains constant during osmotic pressure driven drug delivery and a degradation time of greater than one month. Second, is to report the biocompatibility and biodegradability of the new biomaterial. Third, is to demonstrate the osmotic release mechanism from prepared cylinders of this new biodegradable photocured elastomer using Pilocarpine nitrate as a model drug. Fourth, is to incorporate in the biodegradable elastomer the intimate solid mixture of excipient and IFN- γ and to manufacture this matrix in cylindrical form. Finally, to examine the activity of the IFN- γ released from the elastomer using BV-2 Microglial cell cultures.

1.8. References

1. Isaacs A, Lindenmann J. 1957. Virus interference, I: The interferon. Proc R Ser B147: 258-267.

2. Strander H.1982. Interferon therapy for tumor disease in man: prospects for the near future. In Munk K, Kirchner H, editors. Interferon, contributions to oncology, 11th ed., Basel: Karger S. p 227-233.
3. Cesario TC.1983. The clinical implications of human interferon. *Med Clin North Am* 67: 1147-1162.
4. Ellerhorst JA, Kilbourn RG, Amato RJ, Zukiwski AA, Jones E, Logothetis C. 1994. Phase II trial of low dose γ -interferon in metastatic renal cell carcinoma. *J Urol* 152: 841-845.
5. Valle MJ, Jordan GW, Haar S, Merigan TC. 1975. Characterization of immune interferon produced by human lymphocyte culture compared to other human interferons. *J Immunol* 115: 230-233.
6. Arakawa T, Alton NK, Hsu Y-R. 1985. Preparation and characterization of recombinant DNA-derived human interferon- γ . *J Biol Chem* 260: 14435-14439.
7. Lauren SL, Arakawa T, Stoney K, Rohde MF. 1993. Covalent dimerization of recombinant human interferon- γ . *Arch Biochem Bioph* 306: 350-353.
8. Papermaster VM, Baron S. 1981. Immune interferon for clinical trials: condition for induction, purification and stability. *Tex Rep Biol Med* 41: 672-680.
9. Sedmak JJ, Grossberg SE. 1981. Approaches to the stabilization of interferons. *Tex Rep Biol Med* 41: 274-279.

10. Finter NB. 1986. The classification and biological functions of the interferons: a review. *J Hepat* 3: S157-S160.
11. Langer JA, Pestka S. 1985. Structure of interferons. *Pharmacol Ther* 27: 371-401.
12. Young AS, Cummins JM. 1990. The history of interferon and its use in animal therapy. *East Afr Med J* 67: SS31-SS63.
13. Bocci V. 1992. Physicochemical and biological properties of interferon and their potential uses in drug delivery systems. *Crit Rev Ther Drug Carrier Syst* 9: 91-133.
14. Philip R, Epstein LB. 1986. Tumor necrosis factor as immunomodulator and mediator of monocyte cytotoxicity induced by itself, γ -IFN and interleukin-1. *Nature* 323: 86-89.
15. Arai K, Lee F, Miyajima A, Miyatake S, Arai N, Yokota T. 1990. Cytokines: coordinators of immune and inflammatory responses. *Ann Rev Biochem* 59: 783-836.
16. Vlachoyiannopoulos PG, Tsifetki N, Dimitriou I, Galaris D, Papiris SA, Moutsopoulos HM. 1996. Safety and efficacy of recombinant γ interferon in the treatment of systemic sclerosis. *Am Rheum Dis* 55: 761-768.
17. Dow SW, Schwarze J, Heath TD, Potter TA, Glefand EW. 1999. Systemic and local interferon γ gene delivery to the lungs for treatment of allergen-induced airway hypersensitivity in mice. *Hum Gene Ther* 10: 1905-1924.

18. Schneider LC, Baz Z, Zarcone C, Zurakowski D. 1998. Long-term therapy with recombinant interferon-gamma (rIFN- γ) for atopic dermatitis. *Ann Allergy Asthma Immunol* 80: 263-268.
19. Stone RM, Spriggs DR, Arthur KA, Mayer RJ, Griffin J, Kulfe DW. 1993. Recombinant human gamma interferon administered by continuous intravenous infusion in acute myelogenous leukemia and myelodysplastic syndromes. *Am J Clin Oncol* 16: 159-163.
20. Gressler VH, Weinkauff RE, Franklin WA, Golomb HM. 1989. Is there a direct differentiation-inducing effect of human recombinant interferon on hairy cell leukemia in vitro? *Cancer* 64: 374-378.
21. Badro R, Falcoff E, Badro FS, Carvalho EM, Pedral Sampaio D, Barrel A, Carvalho JS, Barel Netto M, Brandely M, Silvia I. 1990 Treatment of visceral leishmaniasis with pentavalent actimony and interferon gamma. *N Eng J Med* 322:16-21.
22. Nathan CF, Kaplan G, Levis WR, Nusrat A, Witmer MD, Sherwin SA, Job CK, Horwitz CR, Steinman RM, Cohen ZA. 1986. Local and systemic effects of intradermal recombinant interferon- γ in patients with lepromatous leprosy. *N Eng J Med* 325: 6-15.
23. Varga J. 1997. Recombinant cytokine treatment for scleroderma. Can the antifibrotic potential of interferon-gamma be realized clinically? *Arch Dermatol* 33: 637-642.

24. Gillery P, Serpier H., Polette M, Bellon G, Cavel C, Wegrowski Y, Kalis P, Cariou R, Maquart FX. 1992. Gamma-interferon inhibits extracellular matrix synthesis and remodeling in collagen lattice cultures of normal and scleroderma skin fibroblasts. *Eur J Cell Biol* 57: 244-253.
25. Weiss JM, Muchenberger S, Schopf E, Simon C. 1998. Treatment of granuloma annulare by local injections with low-dose recombinant human interferon gamma. *J Am Acad Dermatol* 39: 117-119.
26. Maluish AE, Urba WJ, Longo DL, Overton WR, Coggin D, Crisp ER, Williams R, Sherwin SA, Gordon K, Steis RG. 1988. The determination of an immunologically active dose of interferon-gamma in patients with melanoma. *J Clin Oncol* 6: 434-445.
27. Aulitzky W, Gast G, Aulitzky WE, Herold M, Kemmler J, Mull B, Frick J, Huber Ch. 1989. Successful treatment of metastatic renal cell carcinoma with a biologically active dose of recombinant interferon-gamma. *J Clin Oncol* 7: 1875-1884.
28. Fujii A, Yui-En K, Ono Y, Yamamoto H, Gohi K, Takenaka A. 1999. Preliminary results of the alternating administration of natural interferon- α and recombinant interferon- γ for metastatic renal cell carcinoma. *BJU Int* 84: 399-404.
29. Conte D, Fraquelli M, Capsoni F, Giacca M, Zentilin L, Bardella MT. 1999. Effectiveness of IFN-gamma for liver abscesses in chronic granulomatous disease. *J Interferon Cytokine Res* 19: 705-710.

30. Condino-neto A, Muscara MN, Bellinati-Pires R, Carneiro-Sampaio MM, Brandao AC, Grumach AS, De Nucci G. 1996. Effect of therapy with recombinant human interferon-gamma on the release of nitric oxide by neutrophils and mononuclear cells from patients with chronic granulomatous disease. *J Interferon Cytokine Res* 16: 357-64 (1996).
31. Shankar L, Gerritsen EJA, Key LL. 1997. Osteopetrosis: pathogenesis and rationale for the use of interferon-gamma-1b. *Biodrugs* 7: 23-29.
32. Key LL, Rodriguiz RM, Willi SM, Wright NM, Hatcher HC, Eyre DR. 1995. Long-term treatment of osteopetrosis with recombinant human interferon gamma. *N Engl J Med* 24: 1594-1599.
33. Zhao Z, Leong KW. 1996. Controlled delivery of antigens and adjuvants in vaccine development. *J Pharm Sci* 85:1261-1270.
34. Friedman RM. 1977. Antiviral activity of interferons. *Bacteriol Rev* 41: 543-567.
35. Gresser I, Tovey MG, Maury C, Chouroulinkov I. 1975. Lethality of interferon preparations for newborn mice. *Nature* 258: 76-78.
36. Johnson HM, Smith BG, Baron S. 1975. Inhibition of the primary in vitro antibody response by interferon preparations. *J Immunol* 144: 403-410.
37. Pestka S, Langer JA, Zoon KC, Samuel CE. 1987. Interferons and their actions. *Ann Rev Biochem* 56: 727-777.

38. Valente G, Ozmen L, Novelli F, Geuna M, Plestro G, Forni G, Garotta G. 1992. Distribution of interferon- γ -receptor in human tissues. *Eur J Immunol* 22: 2403-2412.
39. Garotta G, Ozmen L, Fountoulakis M, Dembic Z, vanLoon AP, Stuber D.1990. Human interferon-gamma receptor. Mapping of epitopes recognized by neutralizing antibodies using native and recombinant receptor proteins. *J Biol Chem* 265: 6908-6915.
40. van Loon AG, Ozmen L, Fountoulakis M, Kania M, Haikar M, Garotta G.1991. High-affinity receptor for interferon-gamma (IFN-gamma), a ubiquitous protein occurring in different molecular forms on human cells: blood monocytes and eleven different cell lines have the same IFN-gamma receptor protein. *J Leukocyte Biol* 49: 462-473.
41. Finbloom DS, Hoover DL, Wahl LM.1985. The characteristics of binding of human recombinant interferon- γ to its receptors on human monocytes and human monocytes-like lines. *J Immunol* 135: 300-305.
42. Farrar MA, Schreiber RD.1993. The molecular biology of interferon- γ and its receptor. *Ann Rev Immunol* 11: 571-611.
43. Finbloom DS, Larner AC, Nakgawa Y, Hoover DL.1993. Culture of human monocytes with granulocyte-macrophage colony-stimulating factor results in enhancement of IFN-gamma receptors but suppression of IFN-gamma-induced expression of the gene IP-10. *J Immunol* 150: 2383-2390.

44. Novick D, Engelmann H, Wallach D, Rubinstein M. 1989. Soluble cytokine receptors are present in normal human urine. *J Exp Med* 170: 1409-1414.
45. Bello I, Perez A, Torres Am, Hernandez MV, Lopez Saura P. 1998. High levels of soluble IFN gamma receptor alpha chain in the plasma of rheumatoid arthritis patients. *Biotherapy* 11: 53-57.
46. Jacobs CA, Beckmann MP, Mohler K, Maliszewski CR, Fanslow WC, Lynch DH. 1993. Pharmacokinetic parameters and biodistribution of soluble cytokine receptors. *Int Rev Exp Pathol* 34B: 123-135.
47. Ozmen L, Gribaudo G, Fountoulakis M, Gentz R, Landolfo S, Garotta G. 1993. Mouse soluble IFN γ receptor as IFN γ inhibitor: distribution, antigenicity, and activity after injection in mice. *J Immunol* 150: 2698-2705.
48. Ozmen L, Roman D, Founoulakis M, Schmid G, Ryffel B, Garotta G. 1994. Soluble interferon- γ receptor: a therapeutically useful drug for systemic lupus erythematosus. *J Interferon Res* 14: 283-284.
49. Yasui H, Takai K, Yoshida R, Hayaishi O. 1986. Interferon enhances tryptophan metabolism by inducing pulmonary indolamine 2,3-dioxygenase: its possible occurrence in cancer patients. *Proc Natl Acad Sci USA* 83: 6622-6626.
50. Hansen LA. 1990. Immunotherapy of cancer. In Koeller J, Tami J, editors. *Concept in immunology and immunotherapeutics*, Bethesda: American Society of Hospital Pharmacists, p 325-344.

51. Fountoulakis M, Juranville J-F, Maris A, Ozmen L, Garotta G.1990. One interferon- γ receptor binds one Interferon- γ dimer. *J Biol Chem* 265: 19758-19767.
52. Baron S, Tyring SK, Fleischmann WR, Coppenhaver DH, Niesel DW, Klimpel GR, Stanton GJ, Hughes TK. 1991. The interferons: mechanism of action and clinical applications. *JAMA* 266: 1375-1383.
53. Estrov Z, Kurzrock R, Talpaz M.1993. Interferons, basic principles and clinical applications. Austin: Landes RG Co. p1-113.
54. Mulkerrin MG, Wetzel R. 1989. pH dependence of the reversible and irreversible thermal denaturation of γ -interferons. *Biochemistry* 28: 6556-6561.
55. Cantell K, Hirvonen S, Kauppinnen HL. 1986. Production and partial purification of human immune interferon. *Methods Enzymol* 119: 54-63.
56. Gray PW, Leung DW, Pennica D, Yelverton E, Najarian R, Simonsen CC, Derynck R, Sherwood PJ, Wallace DM, Berger SL, Levinson AD, Goeddel DV. 1982. Expression of human immune interferon cDNA in *E. coli* and monkey cells. *Nature* 295: 503-508.
57. Rinderknecht E, O'Conner BH, Rodriguez H. 1984. Natural human interferon- γ . *J Biol Chem* 259: 6790-6797.
58. Ealick SE, Cook WJ, Vijay-Kumar S, Carson M, Nagabhushan TL, Trotta PP, Bugg CE. 1991. Three-dimensional structure of recombinant human interferon- γ . *Science* 252: 698-702.

59. Bocci V, Pacini A, Pessina GP, Paulesu L, Muscettola M, Lunghetti G. 1985. Catabolic sites of human interferon- γ . *J Gen Virol* 66: 887-891.
60. Sareneva T, Cantell K, Pyhala L, Pirohenen J, Julkunen I. 1993. Effect of carbohydrates on the pharmacokinetics of human interferon- γ . *J Interferon Res* 13: 267-269.
61. Hooker A, James D. 1998. The glycosylation heterogeneity of recombinant human IFN- γ . *J Interferon Cytokine Res* 18: 287-295.
62. Fountoulakis M, Gentz R. 1992. Effect of glycosylation on properties of soluble interferon gamma receptors produced in prokaryotic and eukaryotic expression system. *Biotech* 10: 1143-1147.
63. Thom AK, Fraker DL, Taubenberger JK, Norton JA. 1992. Effective regional therapy of experimental cancer with paralesional administration of tumour necrosis factor- α + interferon- γ . *Surg Oncol* 1: 291-298.
64. Schneider HJ, Heddle RM, Downes MO, Wan KMB, Smedley HM. 1998. Intralesional interferon for the treatment of metastatic carcinoid tumours. *Clin Oncol* 10: 129-130.
65. Ramming KP. 1983. The effectiveness of hepatic artery infusion in treatment of primary hepatobiliary tumours. *Semin Oncol* 10: 199-205.

66. Xu XJ, Hao JX, Olsson T, Kristensson T, van der Meide PH, Wiesenfeld-Hallin Z. 1994. Intrathecal interferon-gamma facilitates the spinal nociceptive flexor reflex in the rat. *Neurosc Letters* 182: 263-266.
67. Voorthuis JA, Uitdehaag BM, De Groot CJ, Goede PH, van der Meide PH, Dijkstra CD. 1990. Suppression of experimental allergic encephalomyelitis by intraventricular administration of interferon-gamma in lewis rats. *Clin Exper Immunol* 81: 183-188.
68. Jaffe HA, Buhl R, Mastranageli A, Holroyd KJ, Saltini C, Czerski D, Jaffe HS, Kramer S, Sherwin S, Crystal RG. 1991. Organ specific cytokine therapy: long activation of mononuclear phagocytes by delivery of an aerosol of recombinant interferon- γ to the human lung. *J Clin Invest* 88: 297-302.
69. Li H-L, Shi F-D, Bai X-F, Y-M. Huang, van der Meide PH, Xiao B-G, Link H. 1998. Nasal tolerance to experimental autoimmune myasthenia gravis: tolerance reversal by nasal administration of minute amounts of interferon- γ . *Clin Immunol Immunopathol* 87: 15-22.
70. Wills RJ. 1990. Clinical pharmacokinetics of interferons. *Clin Pharmacokinet* 19: 390-399.
71. Kurzrock R, Rosenblum MG, Sherwin SA, Rios A, Talpaz M, Quesada JR, Gutterman JU. 1985. Pharmacokinetics, single-dose tolerance, and biological activity of recombinant gamma-interferon in cancer patients. *Cancer Res.* 45: 2866-2872.

72. Chen SA, Izu AE, Baughman RA, Ferraiolo BL, Mordenti J, Reed BR, Jaffe HS, Green JD. 1990. Pharmacokinetic disposition of recombinant human interferon-gamma following intravenous, subcutaneous and intramuscular administration in normal, male volunteers. *J Interferon Res* 10: S125.
73. Sherwin SA, Foon KA, Abrams PG, Heyman MR, Ochs JJ, Watson T, Maluish A, Oldham RK. 1984. A preliminary Phase I trial of partially purified interferon-gamma in patients with cancer. *J Biol Resp Mod.* 3:599-607.
74. Gutterman JU, Rosenblum MG, Rios A, Fritsche HA, Quesada JR. 1984. Pharmacokinetics study of partially pure interferon- γ in cancer patients. *Cancer Res* 44: 4164-4171.
75. Bocci V. 1985. Distribution, catabolism, and pharmacokinetics of interferons. In Finter NB, Oldham R, editors. *Interferon*, Amsterdam: Elsevier, p 47-72.
76. Perez R, Lipton A, Harvey HA, Simmonds MA, Romano PJ, Imboden SL, Giudice G, Downing MR, Alton NK. 1988. A phase I trial of recombinant human gamma interferon (IFN-gamma 4A) in patients with advanced malignancy. *J Biol Resp Mod* 7: 309-317.
77. Foon KA, Sherwin SA, Abrams PG, Stevenson HC, Holmes P, Maluish AE, Oldham RK, Herberman RB. 1985. A phase I trial of recombinant gamma interferon in patients with cancer. *Cancer Immunol Immunother* 20: 193-197.

78. Aderka D, Engelmann H, Maor Y, Brakebusch WD. 1992. Stabilization of the bioactivity of tumor necrosis factor by its soluble receptors. *J Exp Med* 175: 323-329.
79. Mani S, Poo WJ. 1996. Single institution experience with recombinant gamma-interferon in the treatment of patients with metastatic renal cell carcinoma. *Am J Clin Oncol* 19: 149-153.
80. Hillman GG, Younes E, Visscher D, Hamzavi F, Kim S, Lam JS, Montecillo EJ, Ali E, Pontes JE, Puri RK, Haas GP. 1997. Inhibition of murine renal cell carcinoma pulmonary metastases by systemic administration of interferon γ : mechanism of action and potential for combination with interleukin 4. *Clin Cancer Res* 3: 1799-1806.
81. Bocci V. 1984. Evaluation of routes of administration of interferon in cancer: a review and a proposal. *Cancer Drug Deliv* 1: 337-351.
82. Wagstaff J, Smith D, Nelmes P, Loynds P, Crowther D. 1987. *Cancer Immunol Immunother* 25: 54-58.
83. Zoon KC, Arnheiter H. 1984. Studies of the interferon receptors. *Pharmacol Ther* 24: 259-278.
84. Aguet M, Mogensen KE. 1983. Interferon receptors. In Gresser I, editor. *Interferon*, London: Academic Press, p 1-21

85. Goldstein D, Gockerman J, Krishnan R, Ritchie J Jr, Tso CY, L, Hood LE, Ellinwood E, Laszlo J. 1987. Effect of γ -interferon on the endocrine system: Results from a phase I study. *Cancer Res* 47: 6397-6401.
86. Bussiere JL, Hardy LM, Hoberman AM, Foss JA, Christian MS. 1996. Reproductive effects of the chronic administration of murine interferon-gamma. *Reprod Toxicol* 10: 379-391.
87. Quesada JR, Talpaz M, Rios A, Kurzrock R, Gutterman JU. 1986. Clinical toxicity of interferons in cancer patients: a review. *J Clin Oncol* 4: 234-243.
88. Stewart II WE. 1981 Non-antiviral actions of interferons. In Stewart II WE, editor. *The interferon system*, 2nd ed., Vienna: Springer-Verlag. p 223-256.
89. Bocci V. 1981. Production and role of interferon in physiological conditions. *Biol Rev* 56: 49-85.
90. Bocci V. 1988. Role of interferon produced in physiological conditions. A speculative review. *Immunology* 64: 1-9.
91. Bocci V. 1982. Catabolism of interferons. *Surv Immunol Res* 1:137-43.
92. Bocci V. 1985. The physiological interferon response. *Immunol Today* 6: 7-9.
93. Dunn CJ, Hardee MM, Gibbons AJ, Saite ND, Richard KA. 1989. Local pathological responses to slow-release recombinant interleukin-1, interleukin-2 and gamma-interferon in the mouse and their relevance to chronic inflammatory disease. *Clin Sci* 76: 261-263.

94. Lejeune F, Lienard D, Eggermont A, Koops HS, Rosenkaimer F, Gerain J, Klaase J, Kroon B, Vanderveken J, Schmitz P. 1994. Rationale for using TNF α and chemotherapy in regional therapy of melanoma. *J Cell Biochem* 5: 52-61.
95. Sokoloff MH, Tso CL, Kaboo R, Taneja S, Pang S, deKernion JB, Beldegrun AS. 1996. In vitro modulation of tumor progression-associated properties of hormone refractory prostate carcinoma cell line by cytokines. *Cancer* 77: 1862-1872.
96. Habif DV, Ozzello L, De Rosa CM, Cantell K, Lattes R. 1995. Regression of skin recurrences of breast carcinomas treated with intralesional injections of natural interferon alpha and gamma. *Cancer Invest* 13: 165-172.
97. Edwards L, Whiting D, Rogers D, Luck K, Smiles KA. 1990. The effect of intralesional interferon gamma on basal cell carcinomas. *J Am Acad Dermatol* 22: 496-500.
98. Hayakawa M, Hatano T, Miyazato T, Sato K, Saito S, Osawa A. 1987. Studies on antitumor effect of human interferon: (2) effect of massive pulsatile administration of rIFN-gamma on advanced renal cell carcinoma. *Jap J Urol* 78: 1784-1791.
99. Murray HW. 1990. Effect of continuous administration of interferon- γ in experimental visceral leishmaniasis. *J Infect Dis* 161: 992-994.
100. Cantell K, Hirvonen S, Pyhälä L, de Reus A, Schellekens H. 1983. Circulating interferon in rabbits and monkeys after administration of human gamma interferon by different routes. *J Gen Virol* 64: 1823-1826.

101. Levine RM, Crum CP, Herma F.1984. Cervical papilloma virus infection and intraepithelial neoplasia: a study of male sexual partners. *Obstet Gynecol* 64: 16-20.
102. Gross G, Roussaki A, Papendick U. 1990. Efficacy of interferon on bowenoid papulosis and other precancerous lesions. *J Invest Dermatol* 95: 152S-157S.
103. Hautmann SH, Huland E, Huland H.1999. Local intratumor immunotherapy of prostate cancer with interleukin-2 reduced tumor growth. *Anticancer Res* 19: 2661-2664.
104. Morales A, Johnston B, Emerson L, Heaton JW. 1997. Intralesional administration of biological response modifiers in the treatment of localized cancer of the prostate: a feasibility study. *Urology* 50: 495-502.
105. Yilmaz A, Bieler G, Spertini O, Lejeune FJ, Ruegg C. 1998. Pulse treatment of human vascular endothelial cells with high doses of tumor necrosis factor and interferon-gamma results in simultaneous synergistic and reversible effects on the proliferation and morphology. *Int J Cancer* 77: 592-599.
106. Eppstein DP, Kurahara CG, Bruno NA, van der Pas MA, Marsh YV, Schryver BB. Pathways to increase efficacy of interferons: drug synergy and sustained-release. 1985. In Stewart II WE, Schellekens H, editors. *The biology of the interferon system*. BV: Elsevier Science. p 401-409.
107. Golumbek T, Azhari R, Jaffee EM, Levitsky HI, Lazenby A, Leong K, Pardoll DM. 1993. Controlled release, biodegradable cytokine depots: a new approach in cancer vaccine design. *Cancer Res* 53: 5841-5844.

108. Ishihara H, Hara T, Aramaki Y, Tsuchiya S, Hosoi K. 1990. Preparation of asialofetuin-labeled liposomes with encapsulated human interferon-gamma and their uptake by isolated rat hepatocytes. *Pharm Res* 7: 542-546.
109. vanSlooten ML, Storm G, Zoepfel A, Kupcu Z, Boerman O, Crommelin DJA, Wagner E, Kircheis R. 2000. Liposomes containing interferon-gamma as adjuvant in tumor cell vaccines. *Pharm Res* 17: 42-48.
110. Goldbach P, Dumont S, Kessler R, Poindron P, Stamm A. 1995. Preparation and characterization of interferon-gamma containing liposomes. *Int J Pharm* 123: 33-39.
111. Lachman LB, Shih LC, Shao XM, Hu X, Bucana CD, Ulrich SE, Cleland JL. 1995. Cytokine-containing liposomes as adjuvants for HIV subunit vaccines. *AIDS Res Hum Retroviruses* 11:921-932.
112. van Slooten ML, Visser AJG, van Hoek A, Storm G, Crommelin DJA, Jiskoot W. 2000. Conformational stability of human interferon-gamma on association with and dissociation from liposomes. *J Pharm Sci* 89: 160-1619.
113. Bui T, Faltynek C, Ho RJY. 1994. Differential disposition of soluble and liposome-formulated human recombinant interleukin-7: Effects on blood lymphocyte population in guinea pigs. *Pharm Res* 11: 633-641
114. Anderson PM, Katsanis E, Sencer SF, Hasz D, Ochoa AC, Bostrom B. 1992. Depot characteristics and biodistribution of interleukin-2 liposomes: importance of route of administration. *J Immunother.* 12:19-31.

115. Yu H, Grainger DW. 1995. Modified release of hydrophilic, hydrophobic and peptide agents from ionized amphiphilic gel networks. *J Control Rel* 34: 117-127.
116. Kupfer J. 1997. DNA delivery vectors for somatic cell gene therapy. In Park E, editor. *Controlled drug delivery: challenges and strategies*, Washington DC: American Chemical Society. p 27-48.
117. Visse E, Siesjo P, Widegren B, Sjogren HO. 1999. Regression of intracerebral rat glioma isografts by therapeutic subcutaneous immunization with interferon-gamma, interleukin-7, or B7-1-transfected tumor cells. *Cancer Gene Ther* 6: 37-44.
118. Lei H, Ju D.W, Yu Y, Tao Q, Chen G, Gu S, Hamada H, Cao X. 2000. Induction of potent antitumor response by vaccination with tumor lysate-pulsed macrophages engineered to secrete macrophage colony-stimulating factor and interferon-gamma. *Gene Ther* 7: 707-713.
119. Stopeck AT, Vahedian M, Williams SK. 1997. Transfer and expression of the interferon gamma gene in human endothelial cells inhibits vascular smooth muscle cell growth in vitro. *Cell Transplant* 6: 1-8.
120. Stoeckle MY, Falk-Pederson E, Rubin BY, Anderson SL, Murrya, HW. 1996. Delivery of human interferon-g via gene transfer in vitro: prolonged expression and induction of macrophage antimicrobial activity. *J Interferon Cytokine Res* 16: 1015-1019.

121. Karavodin LM, Robbins J, Chong K, Hsu D, Ibanez C, Mento S, Jolly D, Fong TC. 1998. Generation of a systemic antitumor response with regional intratumoral injections of interferon gamma retroviral vector. *Hum Gene Ther* 9: 2231-2241.
122. Kanno H, Hattori S, Sato H, Murata H, Huang FH, Hayashi A, Suzuki N, Yamamoto I, Kawamoto S, Minami M, Miyatake S, Shui T, Kaplitt MG. 1999. Experimental gene therapy against subcutaneously implanted glioma with a herpes simplex virus-defective vector expressing interferon-gamma. *Cancer Gene Ther* 6: 147-154.
123. Nemunaitis J, Fong T, Robbins JM, Edelman G, Edwards W, Paulson RS, Bruce J, Ognoskie N, Wynne D, Pike M, Kowal K, Merritt J, Ando D. 1999. Phase I trial of interferon-gamma (IFN-gamma) retroviral vector administered intratumorally to patients with metastatic melanoma. *Cancer Gene Ther* 6: 322-330.
124. Splenehauer G, Vert M, Benoit J-P, Chabot F, Veillard M. 1988. Biodegradable cisplatin microspheres prepared by the solvent evaporation method: morphology and release characteristics. *J Control Rel* 7: 217-229.
125. Mehta C, Thanoo BC, Deluca PP. 1996. Peptide containing microspheres from low molecular weight and hydrophilic poly (d,l-lactide-co-glycolide). *J Control Rel* 41: 249-257.
126. Lee VHL. 1991. Changing needs in drug delivery in the era of peptide and protein drugs. In Lee VHL, editor. *Peptide and protein drug delivery*. New York: Marcel Dekker. p 1-56.

127. Oeswein JQ, Shire SJ. 1991. Physical biochemistry of protein drugs. In Lee VHL, editor. Peptide and protein drug delivery. New York: Marcel Dekker. p 167-202.
128. Gopferich A, Gref R, Minamitake Y, Shieh L, Alonso MJ, Tabata Y, Langer R. Drug delivery from bioerodible polymers: systemic and intravenous administration. 1994. In Cleland JL, Langer R, editors. Formulation and delivery of proteins and peptides. Washington: ACS. p 242-277.
129. Mader K, Gallez B, Liu KJ, Swartz HM. 1996. Non-invasive in vivo characterization of release processes in biodegradable polymers by low-frequency electron paramagnetic resonance spectroscopy. *Biomaterials* 17: 457-461.
130. Shenderova A, Bruke TG, Schwendeman SP. 1998. Evidence for an acidic microclimate PLGA microspheres. *Proceed. Int'l Symp Control Rel Bioact Mater* 25: 256-166.
131. Fu K, D. Pack W, Laverdiere A, Son S, R. Langer R. 1998. Visualization of pH in degrading polymer microspheres. *Proceed Int'l Symp Control Rel Bioact Mater* 25: 150-151.
132. Chen L, Apte RN, Cohen S. 1997. Characterization of PLGA microspheres for the controlled delivery of IL-1alpha for tumor immunotherapy. *J Control Rel* 43: 261-272.
133. Park G, Lu W, Crotts G. 1995. Importance of in vitro experimental conditions on protein release kinetics, stability and polymer degradation in protein encapsulated poly (D, L-lactic acid-co-glycolic acid) microspheres. *J Control Rel* 33: 211-222.

134. Johnson RE, Lanaski LA, Gupta V, Griffin MJ, Gaud HT. 1991. Stability of atriopentin III in poly (d,l-lactide-co-glycolide) microspheres. *J Control Rel* 17: 61-67.
135. Takahata H, Lavelle EC, Coombes AGA, Davis SS. 1998. The distribution of protein associated with poly (DL-lactide-co-glycolide) microparticles and its degradation in simulated body fluids. *J Control Rel* 50: 237-246.
136. Tabata Y, Gutta S, Langer R. 1993. Controlled delivery system for protein using polyanhydride microspheres. *Pharm Res* 10: 487-496.
137. Hora MS, Rana RK, Nunberg JH, Tice TR, Gilley RM. 1990. Release of human serum albumin from poly (lactide-co-glycolide) microspheres. *Pharm Res* 7: 1190-1194.
138. Yang J, Cleland JL. 1997. Factors affecting the in vitro release of recombinant human interferon-gamma (rhIFN- γ) from PLGA microspheres. *J Pharm Sci* 86: 908-914.
139. Michaels AS, Guilod MS. 1979. Osmotic bursting drug delivery device. US patent no. 4177256.
140. Amsden B, Cheng Y-L. 1995. A generic protein delivery system based on osmotically rupturable monoliths. *J Control Rel* 33: 99-105.

141. Miyamoto S, Takaoka K, Okada T, Yoshikawa H, Hashimoto J, Suzuki S, Ono K. 1993. Polylactic acid-polyethylene glycol block copolymer. A new biodegradable synthetic carrier for bone morphogenetic protein. *Clin Orthop* 294:333-343.
142. Merkli A, Heller J, Tabatabay C, Gurny R. 1994. Semi-solid hydrophobic bioerodible poly(ortho ester) for potential application in glaucoma filtering surgery. *J Control Rel* 29: 105-112.
143. Zignani M, Merkli A, Sintzel MB, Bernatchez SF, Kloeti W, Heller J, Tabatabay C, Gurny R. 1997. New generation of poly(ortho esters): Synthesis, characterization, kinetics, sterilization and biocompatibility. *J Control Rel* 48: 115-129.
144. Lambert WJ, Peck KD. 1995. Development of an in situ forming biodegradable poly-lactide-co-glycolide system for the controlled release of proteins. *J Control Rel* 33: 89-195.
145. Dunn RL, Tipton AJ, Southard GL, Rogers JA. 1997. Biodegradable polymer composition. US patent no. 5599552
146. Eliaz RE, Kost J. 2000. Characterization of a polymeric PLGA-injectable implant delivery system for the controlled release of proteins. *J Biomed Mater Res* 50: 388-396.

CHAPTER 2

SYNTHESIS, CHARACTERIZATION AND IN VITRO DEGRADATION OF BIODEGRADABLE ELASTOMER

Husam M. Younes¹ and Brian G. Amsden^{1,2}

A version of this chapter has been submitted to *Biomacromolecules*

1. Faculty of Pharmacy and Pharmaceutical Science, University of Alberta, Edmonton, Alberta, Canada T6G 2N8
2. Department of Chemical Engineering, Queens University, Kingston, Ontario, Canada, K7L 3N6

2.1. Introduction

Biodegradable elastomers have a number of possible uses in the biomaterials area, from scaffolds for engineering tissue *in vivo* or *in vitro*,¹⁻³ to localized drug delivery depots.^{4,5} Biodegradable elastomers have been prepared in either of two ways, using thermoplastic⁶⁻⁸ or thermoset materials.^{9,10} Thermoplastics have the advantage of being easily fabricated by melt processing. However, the crystalline crosslink regions these materials possess provide regions of much slower degradation *in vivo*, and produce a material whose physical properties degrade in a non-linear fashion with time while at the same time the dimensions of the material do not remain constant. Thermosets, although not as easily processed, degrade more homogeneously, and maintain their dimensions longer with time and their physical properties degrade in a more linear fashion.¹⁰ Thermosets, therefore, possess clear application advantages.

One approach to preparing a thermoset elastomer has been to first prepare star copolymer prepolymers, and then crosslink these prepolymers using a suitable method, such as via diisocyanate linkages or methacrylate groups on the termini. The advantages of using star polymers are that they have a reduced viscosity when in melt form, which allows for easier injection into molds for part manufacture, their architecture can be altered to achieve different physical properties, and they can form a network when their termini are reacted with difunctional crosslinkers. Star polymers and copolymers have been prepared using degradable monomers such as D,L-lactide (DL-LA), glycolide, ϵ -caprolactone (ϵ -CL), δ -valerolactone, dioxanone, dioxepanone, and trimethylene carbonate.⁹⁻¹⁷ Requirements for the formation of a useful elastomer using a star copolymer as a

prepolymer are that the prepolymer has a glass transition temperature (T_g) below room temperature and is amorphous. Thus, copolymers in which one monomer has a very low T_g are the most suitable. One example would be a copolymer of ϵ -caprolactone ($T_g = -60$ °C) and D, L-lactide ($T_g = 68$ °C).

Although elastomers have been prepared from star polymers by crosslinking with diisocyanate linkages^{9,13} or methacrylate groups on the termini,¹⁰ these approaches possess some disadvantages. Diisocyanate crosslinked elastomers, depending on the diisocyanate used, may degrade to potentially toxic compounds, can only be crosslinked in solution and require a potentially carcinogenic solvent in order to achieve a dispersion of the crosslinking agent in the polymer, which requires a further solvent removal step. Any residual solvent may jeopardize the biocompatibility of the material. Methacrylate end-capped star copolymers have been cured to form elastomers; however, the reaction requires cobalt naphthenate as a catalyst in an organic solvent. The catalyst raises questions about biocompatibility as does the use of a solvent.

In this work, we report on the synthesis, characterisation, mechanical properties and *in vitro* degradation of a newly synthesized biodegradable elastomer. This elastomer was prepared in two stages. The first involved the preparation of a star copolymer (SCP) utilizing ring opening polymerization of ϵ -CL with DL-LA using glycerol as initiator and SnOct as a catalyst. The second stage involved the reaction of this SCP with different ratios of the crosslinking monomer, 2,2-bis(ϵ -caprolactone-4-yl)-propane (BCP).

2.2. Experimental Section

2.2.1. Materials

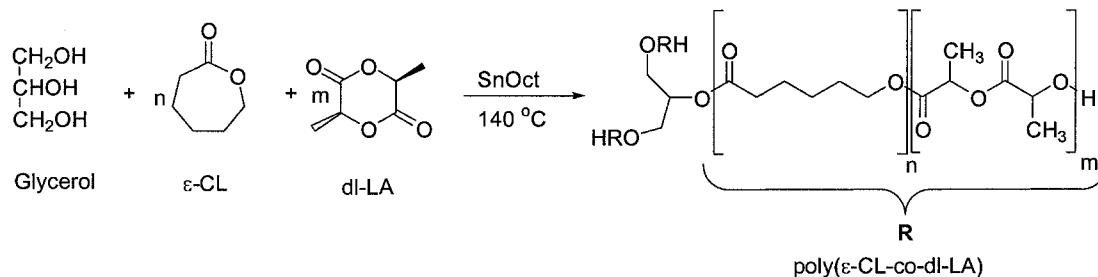
DL-lactide was obtained from Polysciences while ϵ -caprolactone was obtained from Lancaster and then dried over CaH_2 (Aldrich). Other chemicals used in the synthesis of the SCP were stannous octoate (Aldrich), and glycerol (BDH). The chemicals used in the synthesis of the crosslinker BCP include 2,2-bis(4-hydroxycyclohexyl)propane (TCI America), chromium trioxide, m-chloroperoxybenzoic acid (*m*CPBA), and 2-heptanone which were all obtained from Aldrich. Other chemicals used include 2-propanol (Fisher), benzene (BDH), dichloromethane (Fisher), glacial acetic acid (BDH), and methanol (Aldrich).

2.2.2. Preparation of 50:50 poly (ϵ -caprolactone-co-DL-lactide) (ϵ -CL/DL-LA) Star Copolymer (SCP)

Solvent-free polymerization was carried out in sealed silanized 20 ml ampoules. A representative polymerization is described as follows. Into a dry silanized ampoule, 0.005 mol of glycerol and 0.05 mol of ϵ -CL were transferred and mixed till homogeneous. An amount equivalent to 0.05 mol of DL-LA was transferred to the ampoule, the ampoule filled with nitrogen, then placed in an oven at 120 °C for 10 minutes allowing the DL-LA to melt. The mix was then stirred using a vortex mixer and SnOct was added in an amount equivalent to 1.4×10^{-4} mol for each 1 mol of the monomer. The ampoule was

filled with nitrogen, flame sealed under vacuum, and left in an oven at 140 °C for 18 hours. The prepared SCP was then purified by precipitation from dichloromethane (DCM) solution into cold methanol. The thermal behaviour and the composition of the prepared SCP were characterized using Differential Scanning Calorimetry (DSC), Nuclear Magnetic Resonance (NMR) and Gel Permeation Chromatography (GPC). Scheme 2.1 shows a representation of the synthesis of the poly(ϵ -CL/DL-LA) SCP.

Scheme 2.1



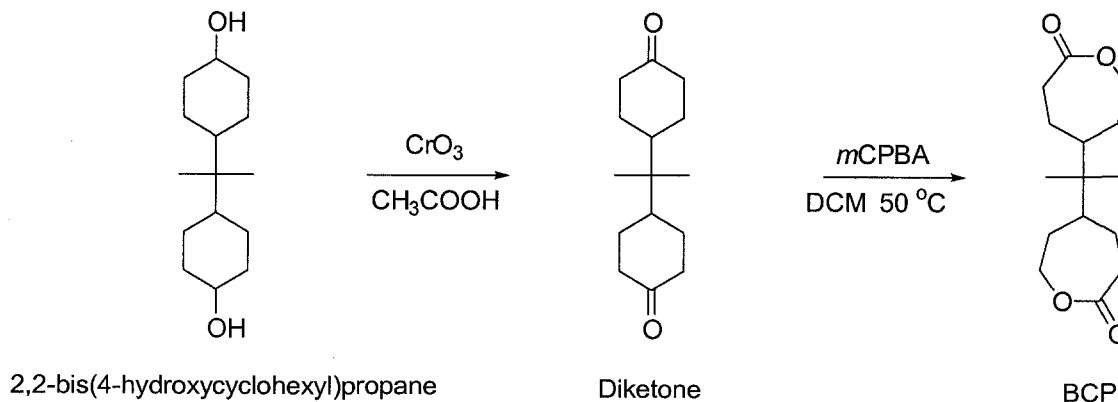
2.2.3. Preparation of 2,2-bis(ϵ -caprolactone-4-yl)-propane (BCP)

A detailed preparation method has been reported elsewhere.¹⁸ In summary, 5.4 g of 2,2-bis(4-hydroxyhexyl)propane was dissolved in 29.5 ml glacial acetic acid to which a solution of 5.5 g of chromium trioxide in dilute acetic acid (25 ml of glacial acetic acid mixed with 40 ml water) was added in drop-wise fashion over a period of 2 hours under stirring while maintaining a temperature of 17-18 °C using a circulating cooling system. After reactant addition, the solution was reacted for a further 30 minutes, and then 25 ml of 2-propanol was added to the solution. This solution was left under vacuum to concentrate overnight. The concentrated solution was then poured into 200 ml of distilled

water where a thick violet suspension was formed. The suspension was filtered using Whatman no. 1 filter paper and the cake was washed several times using distilled water. The resulting white dicyclohexyl-4,4'-dione (Diketone) powder product was dried in an oven at 50 °C overnight and later characterized using DSC and NMR.

A Baeyer-Villiger oxidation reaction was then carried out on the prepared diketone as has been previously reported.^{19,20} In summary, in a round bottom flask 3.9 g of *m*CPBA previously dried with MgSO₄/DCM was added in batches to DCM solution of the diketone (4.1 g in 200 ml) under reflux at 50 °C. The reaction was monitored using thin layer chromatography (TLC) and the final product was purified by washing with hot 2-heptanone. The final white powder product was characterized using DSC, NMR, Mass Spectroscopy (MS) and Elemental Analysis (EA). Scheme 2.2 summarizes the steps involved in preparing BCP.

Scheme 2.2



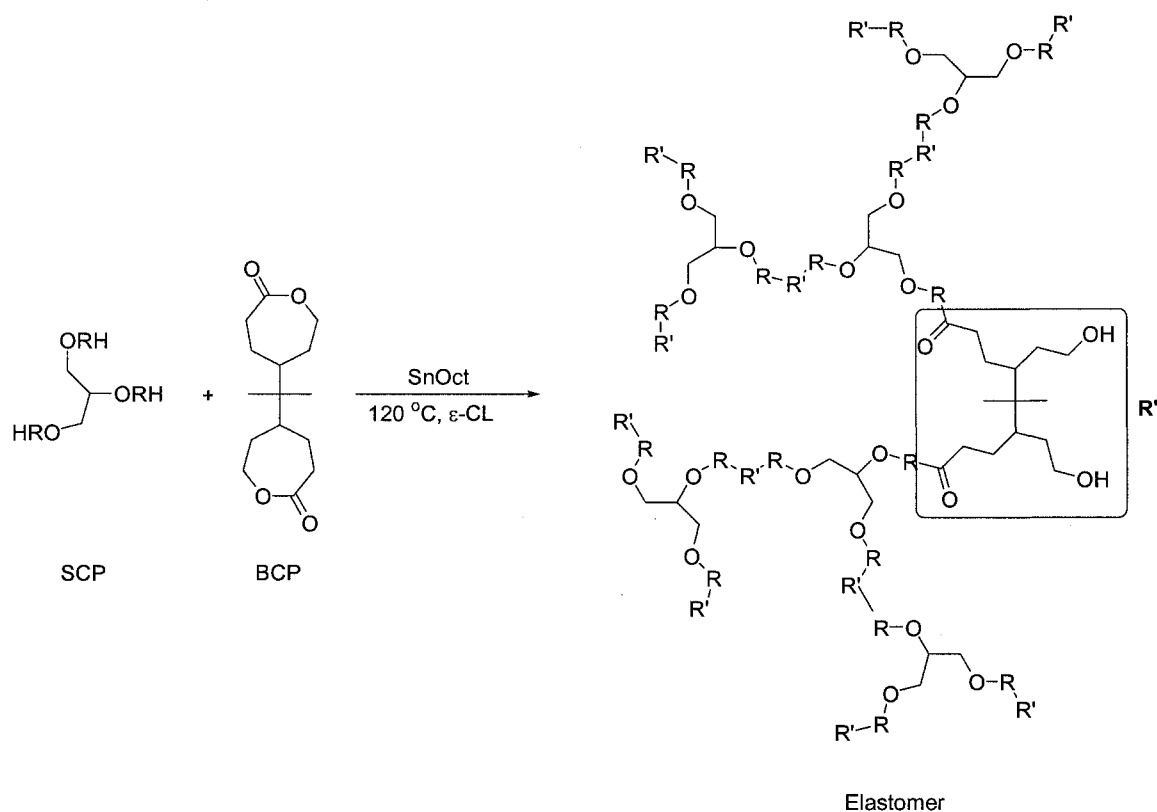
2.2.4. Synthesis of the Elastomer

The following procedure describes the steps involved in preparing the elastomer using a 3:1 weight ratio of SCP:BCP respectively. In a dry silanized glass ampoule, 1 g of BCP was dissolved in 1 g of ϵ -CL monomer at 140°C under a nitrogen blanket. The mixture was left in the oven for 5 to 10 minutes to dissolve. A molten mass of 3 g SCP and an amount of SnOct equivalent to $1.4 (10)^{-4}$ mol for each 1 mol of the monomer were added to the ampoule. The contents were mixed using a vortex mixer and the ampoule was sealed under vacuum. The ampoule was left in the vacuum oven at 125 °C for 10 minutes and then the seal was broken and the highly viscous liquid was poured into rectangular Teflon moulds (100 x 6 x 3 mm), covered, and left in the vacuum oven at 120 ± 5 °C under 10 mmHg vacuum for 18 hours. The elastomer was then removed from the mould and characterized using DSC, *in vitro* degradation and tensile testing before and during the degradation study. Table 2.1 reports the different ratios of both SCP and BCP used to prepare the elastomers while scheme 2.3 summarizes the steps involved in preparing the elastomer.

Table 2.1 Ratios of SCP and BCP used in preparing the elastomers.

Sample ID	SCP (g)	BCP (g)	SCP/BCP Weight Ratio
Elast 1	3.0	1.50	2.0/1.0
Elast 2	3.0	1.25	2.4/1.0
Elast 3	3.0	1.00	3.0/1.0
Elast 4	3.0	0.75	4.0/1.0
Elast 5	3.0	0.50	6.0/1.0

Scheme 2.3



2.2.5. BCP and Polymer Characterization

^1H and ^{13}C NMR spectra were recorded in CDCl_3 using a Varian VXR 500 MHz Spectrometer with an Oxford Instruments superconducting magnet. The DSC experiments were carried out using a Seiko SII SSC/5200 DSC with a cooling system. The samples were run at a heating rate of $10\text{ }^{\circ}\text{C}/\text{min}$ and the DSC was calibrated using indium and gallium standards. The enthalpies, glass transitions temperatures, and melting endotherms were determined using the internal DSC analysis program. MS analysis was run on an Electron Impact Kratos MS-50 spectrometer and analysed using the supplied software. EA was carried out using an EMGA-620W and EMGA-621W series Elemental Analyser. The GPC experiments were conducted using an Hewlett-Packard 1100 system

connected to a Precision Detectors PD 2000 DLS light scattering detector supplied with a Waters 410 Differential Refractometer. The mobile phase consisted of THF at a flow rate of 2 ml/min with the system at 35 °C. The concentration of the polymers used for the GPC measurements were 2 mg/ml and the injection volume was 20 μ l. The column configuration consisted of an HP guard column pre-attached to a Phenogel linear (2) 5 μ GPC column. Monodisperse Polystyrene Standards (Aldrich) were used for initial calibration. The mechanical properties of the elastomers were carried out on slabs (100 x 6 x 3 mm) using an Instron tensile tester model 4443 equipped with an extensometer. The extensometer gauge length was set to 25 mm while the specimen gauge length was set to 40 mm. Crosshead speed was set at 500 mm/min and the sample rate was set at 6.667 pts/secs (ASTM D412). All specimens were tested at room temperature. Data analysis was carried out using the Instron Merlin 4.11 Series IX software package.

2.2.6. In Vitro Degradation Study

Slab specimens of the different prepared elastomers reported in Table 2.1 were subjected to an *in vitro* degradation study. Each specimen had its weight recorded and was placed into a 15 ml tissue culture tube which was filled with 12 ml 1/15 M Phosphate Buffer Saline (PBS) of pH 7.4. The tubes were attached to a Glas-Col's rugged culture rotator. The rotator was set at 30% rotation speed and placed in an oven at 37 °C. The buffer was replaced on a bi-daily basis to ensure a constant pH of 7.4 during the whole period of the study. One set of samples representing each ratio was left without changing its buffer to monitor the change in the medium's pH with respect to time. Samples of the four ratios

prepared (each sample represents 4 specimens) were dried, weighed and subjected to tensile testing at time periods of 0, 1, 2, 4, 8 and 12 weeks.

2.3. Results and Discussion

Our goal was to prepare an amorphous elastomer that would have a T_g well below body temperature, and that would maintain its form stability for the intended time period. To accomplish this, a trifunctional alcoholic initiator (glycerol) was reacted with a 1:1 molar ratio of both DL-LA and ϵ -CL using SnOct as catalyst. A monomer:initiator molar ratio of 10:1 was used to prepare a SCP of a theoretically calculated number average molecular weight of 2700 Da. This theoretical molecular weight was calculated using equation (2.1) which was derived based on two assumptions. The first was that each of the three OH groups in the glycerol initiator initiate a polymer chain and secondly, that all the monomers are consumed in the reaction.

$$M_{n,c} = \left[\frac{m_{CL}}{m_i} \left(\frac{114 + r144}{114} \right) + 1 \right] 92.1 \quad (2.1)$$

In this equation $M_{n,c}$ is the theoretically calculated number average molecular weight M_n , m_{CL} is the mass of ϵ -CL, m_i is the mass of glycerol, and $r = \text{mole DL-LA} / \text{mole } \epsilon\text{-CL}$ (i.e. for a 50:50 ϵ -CL: DL-LA, $r = 1.0$) and the value of 92.1 corresponds to glycerol molecular weight. The polymer product was a living star-shaped 3-arm copolymer (scheme 2.1). The structure of this prepared SCP was further confirmed using $^1\text{H-NMR}$

as shown in Figure 2.1. NMR of the SCP confirmed its composition as being 53% DL-LA and 47% ϵ -CL as measured using the ratio of the integrals at the chemical shift of 5.1 ppm which correspond to the DL-LA methine protons resonances to that at 2.3 ppm which corresponds to the ϵ -CL methylene protons resonances. (Figure 2.1)

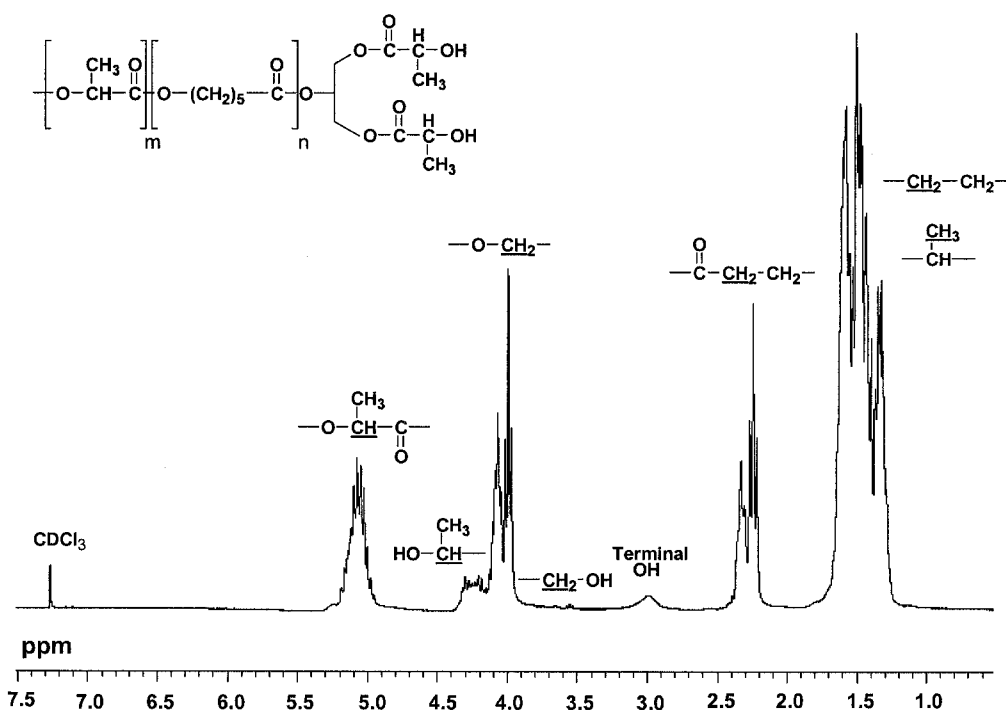


Figure 2.1 $^1\text{H-NMR}$ of the prepared star copolymer.

The GPC molecular weight analysis of the prepared SCP resulted in $M_w = 2430$ Da, $M_n = 1894$ Da and an M_w/M_n of 1.28. This M_n value was lower than the calculated $M_{n,c}$ value, possibly due to an error in the dn/dc value used in the light-scattering determination of molecular weight. As noted, the molar ratio of 10:1 of monomer:initiator resulted in a low molecular weight of the prepared SCP and narrow polydispersity. Similar results have previously been reported in the copolymerization of other polyesters using multifunctional initiators like pentaerythritol.^{11,12}

Figure 2.2 shows the DSC thermogram of the prepared SCP. The Figure illustrates that a completely amorphous polymer was prepared with a corresponding T_g of $-25.3\text{ }^{\circ}\text{C}$. The presence of only one T_g confirmed the random sequence of the copolymer chains.

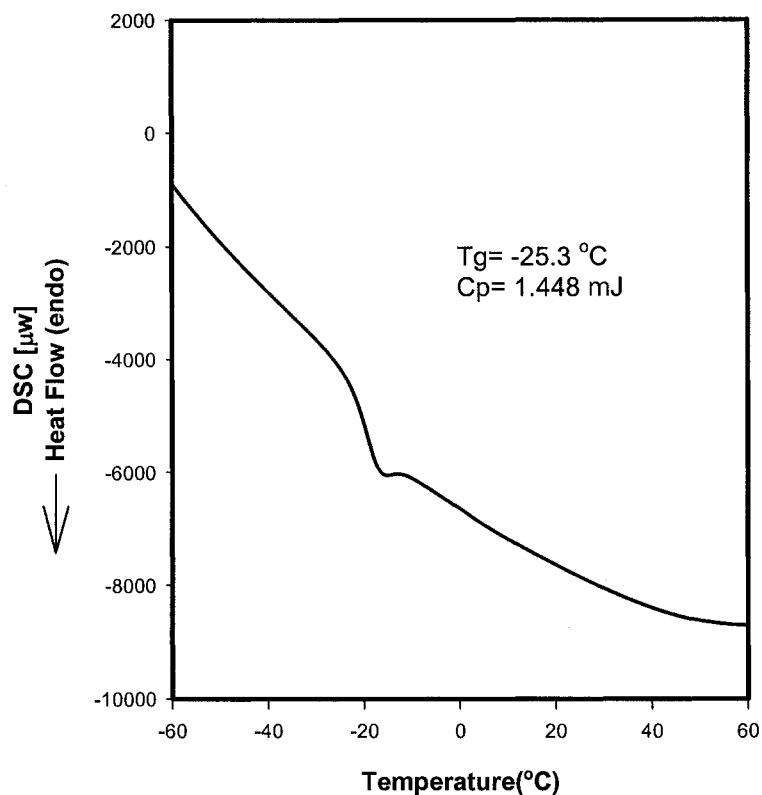


Figure 2.2 Differential Scanning Calorimetry thermogram of SCP.

The second stage involved the synthesis and characterization of the tetra- functional crosslinking monomer BCP (scheme 2.2). The yield of BCP was calculated to be 67 % with a purity exceeding 90% calculated from the elemental analysis difference between the actual value from the formula given by mass spectroscopy and the calculated formula given by the elemental analysis. This product was characterized by DSC and different spectroscopic methods. The DSC analysis of the prepared BCP batches always revealed a

sharp endothermic peak between 195 and 205 °C with no other interfering endotherms, which was an indication of the high purity that was later confirmed with TLC, NMR and EA data.

Figures 2.3 and 2.4 show the ^1H and ^{13}C NMR of the prepared BCP respectively in which each peak is labelled with the corresponding functional group. The ^1H -NMR confirms the purity by showing the complete absence of any interfering aromatic protons of *m*CPBA or other interfering impurities between 7-9 ppm.

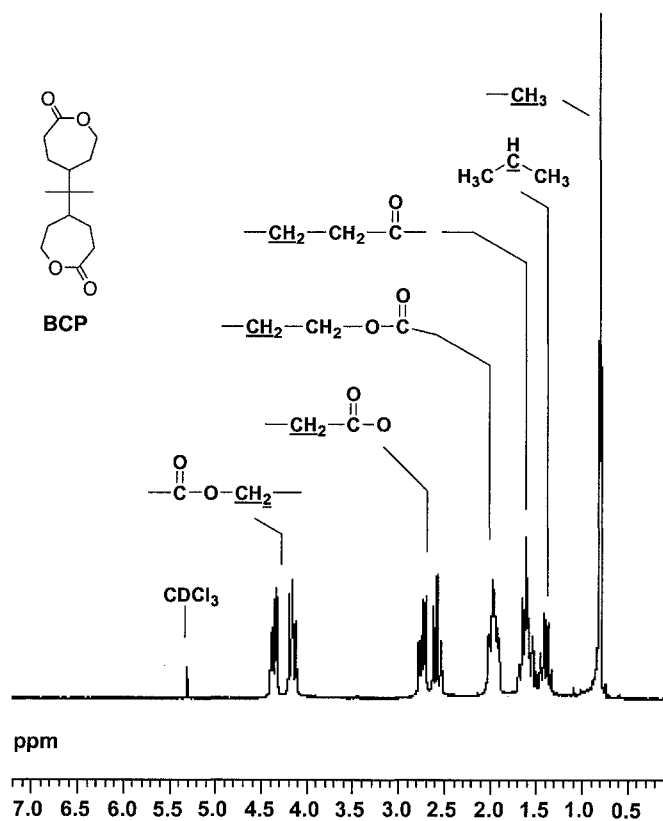


Figure 2.3 The ^1H -NMR of the prepared BCP

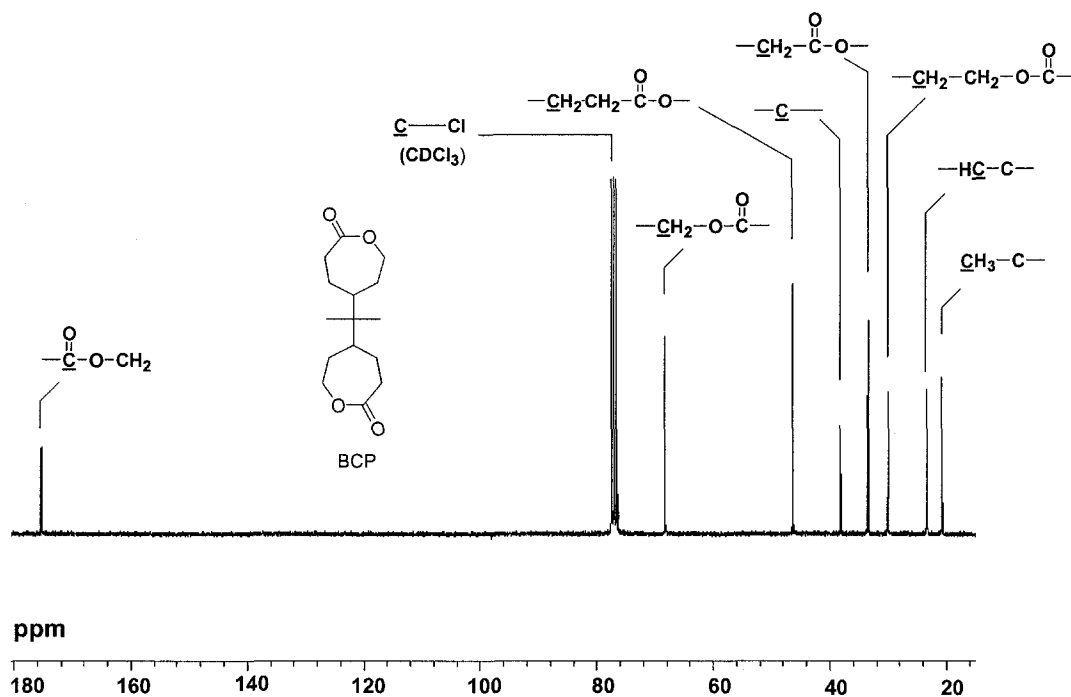


Figure 2.4 ^{13}C -NMR of the prepared BCP

The ^{13}C -NMR of BCP confirmed this conclusion and the formation of the lactone structure as well, indicated by the singlet peaks at 68.25 and 175.37 ppm. In addition, the absence of a peak at 210 ppm in the ^{13}C -NMR of the diketone as shown in Figure 2.5 excluded the possibility of a partial reaction in which only one ketone ring was converted to lactone, and the absence of residual diketone.

The MS analysis confirmed the molecular weight of the final product. Figure 2.6 shows the MS spectrum of BCP in which the parent ion appears at $m/z=269$ which corresponds to $M+1$ isotope peak of BCP due to the presence of oxygen in its structure. It seems that under the thermal conditions of MS, the stability of the parent ion was so low that it attained a very low abundance. The base peak of 100 % abundance appeared at m/z of 155.10.

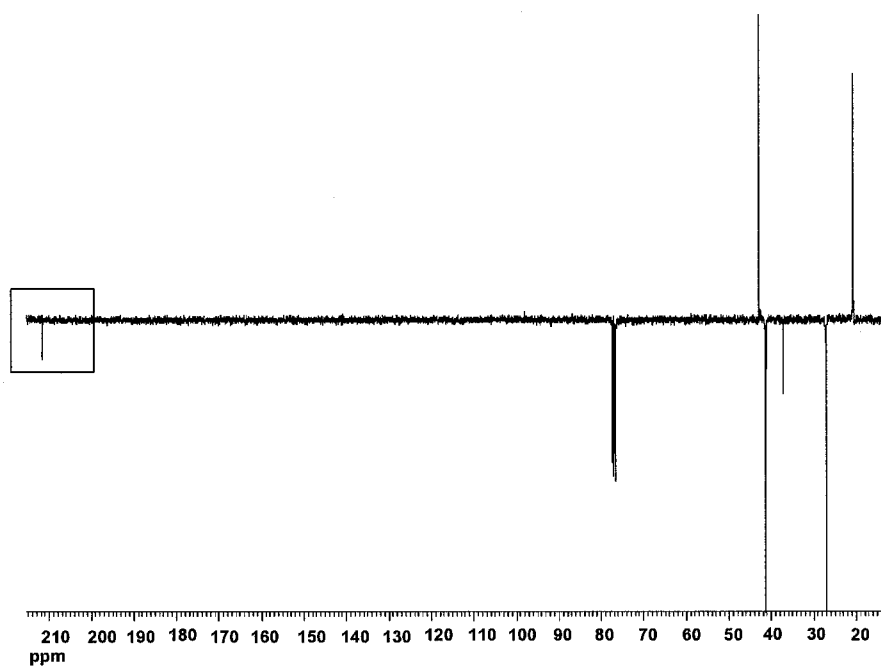


Figure 2.5 ^{13}C -NMR of the prepared Diketone

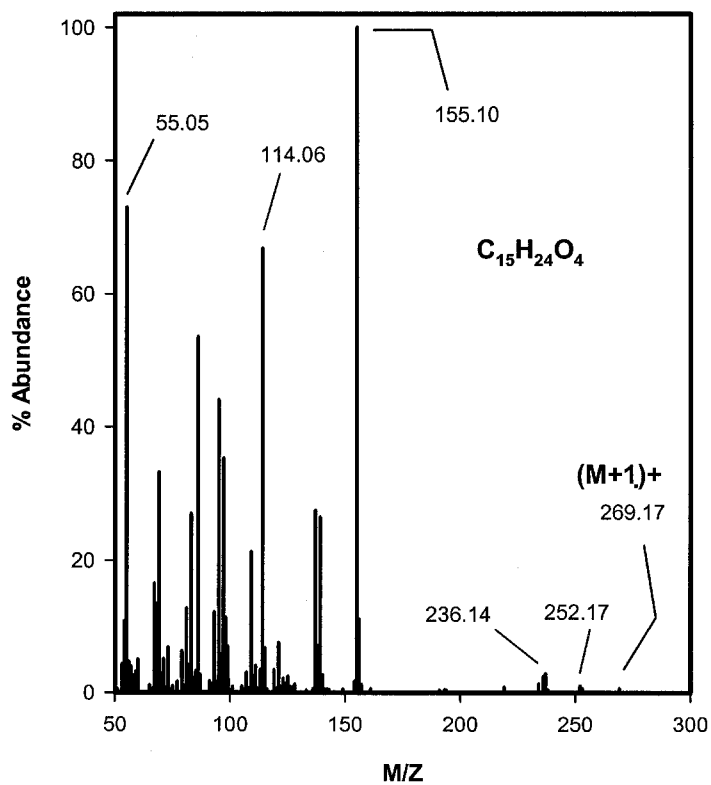


Figure 2.6 Mass Spectrum of BCP.

This conclusion was further confirmed by the elemental analysis (Table 2.2). There was no significant difference between the reported and the calculated percentages for C, H, and O.

Table 2.2 Elemental analysis for C, H, and O in BCP sample

Analysed Element	% Result	% Calculated
C	65.2	67.2
H	8.92	8.90
O	22.80	23.89

With the structure of the prepolymer and the crosslinking agent confirmed, elastomers were prepared. The purified SCP was crosslinked in different ratios with the BCP monomer (scheme 2.3). An amount equivalent to 1 g of ϵ -CL monomer was required to dissolve the amount used of BCP to decrease the crosslinking temperature from 180 °C, using only BCP, to 120 °C. At 180 °C, substantial oxidation of the BCP occurred during the crosslinking reaction, as was noted by the discoloration of the sample. It should be noted that solution polymerization using toluene as a solvent was attempted to undergo the reaction at a lower temperature, but with no success.

Table 2.1 reports the different ratios of SCP and BCP used to prepare 5 elastomers of different mechanical properties. A summary of the corresponding T_g for each of the prepared elastomers is provided in Table 2.3. The data show that the higher the amount of

BCP used in crosslinking the SCP, the higher the T_g of the elastomer, as would be expected due to the increase in crosslinking density.

Table 2.3 Glass transition temperatures of the prepared elastomers

Elastomer	T_g ($^{\circ}\text{C}$)
Elast 1	-11.3
Elast 2	-14.0
Elast 3	-18.1
Elast 4	- 21.0

For the purpose of determining the mechanical properties of the samples reported in Table 2.1, slabs of those samples were subjected to tensile testing as detailed under the experimental section. It was not possible to test the elastomer prepared with a weight ratio of SCP:BCP of 6:1 (Elast 5) because the specimens were too soft and weak to align properly in the Instron clamps. Figure 2.7 shows the stress-strain profiles for the tested slabs. These profiles reflect behaviour typical of amorphous elastomers tested above their T_g . In addition, as expected, incorporating higher amounts of the BCP crosslinker resulted in a highly crosslinked tough elastomer (Elast 1) indicated by higher Young's modulus (E) values and lower ultimate strain (ϵ). On the contrary, Elast 4 for example, with less crosslinker amount used, was a soft, weak elastomeric polymer with a low E and high ϵ .

In an attempt to determine the changes in the mechanical properties and the degradation patterns of the prepared elastomers as a function of time, slab specimens of recorded

weights of the different elastomers reported in Table 2.1 were subjected to an *in vitro* degradation. Figure 2.8 shows the percentage mean increase in weight of the tested slabs with respect to time over a period of 12 weeks. This increase in the slab weight over time is attributed to water absorption from the degradation media into the slabs' bulk. As the elastomer degrades, more water soluble products are formed which act as a driving force for the imbibition of water into the elastomer due to osmotic activity, and the elastomer then swells. Therefore, the weight gain of the elastomer with time can be used as a measure of the rate of degradation of the material. The elastomers prepared with less BCP degraded at a faster rate as indicated by their increased weight gain. Elast 4 and Elast 3 showed the most significant increase in weight with values around 110% and 65% respectively compared to those corresponding to Elast 1 and Elast 2.

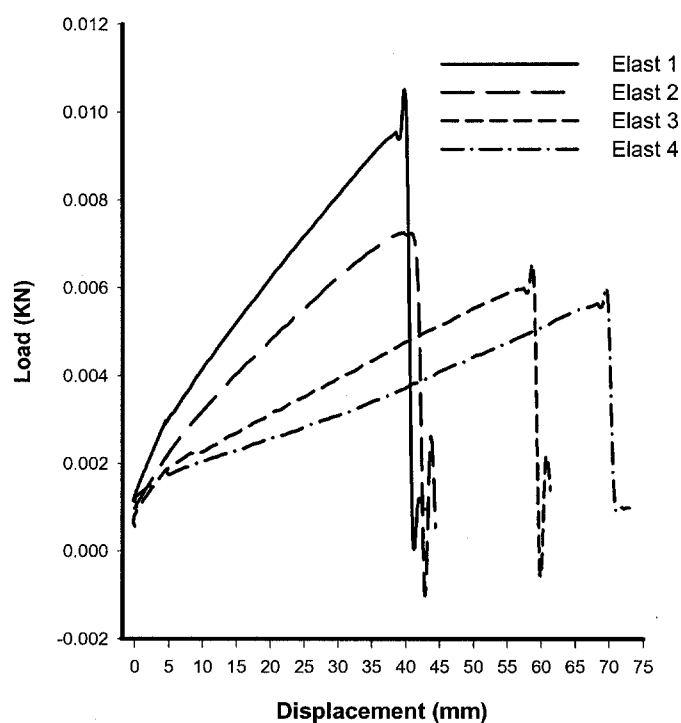


Figure 2.7 Stress-strain behaviour of the prepared elastomers.

The higher amount of the crosslinker BCP used in preparing Elast 1 and Elast 2 resulted in tougher elastomers that have higher crosslink density and therefore, a better ability to resist water penetration leading to hydrolysis. This conclusion was supported by the results reported in Figure 2.9 which show that a more significant decrease in Young's modulus accompanied the degradation of the less crosslinked elastomers. Young's modulus values for Elast 4 at twelve weeks were not reported because these specimens decomposed into pasty materials.

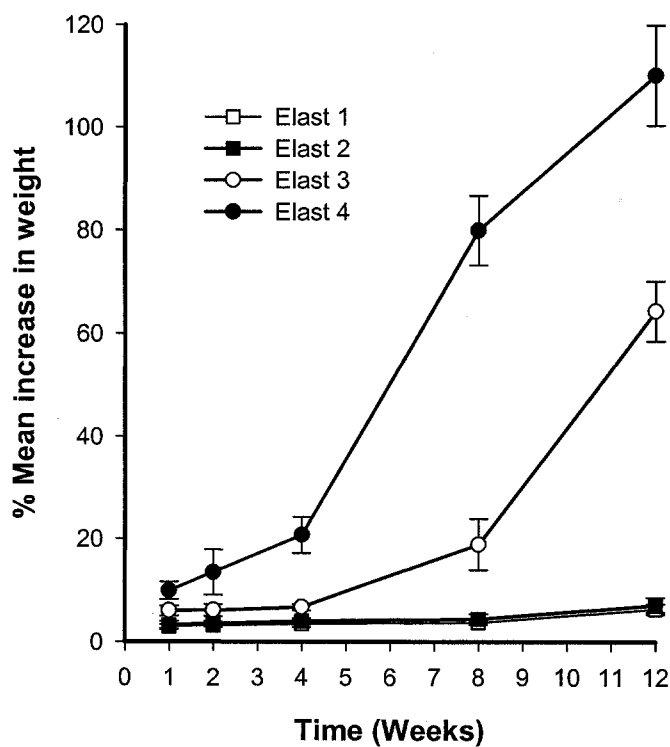


Figure 2.8 Percentage increase in weight of the tested slabs of the corresponding elastomers

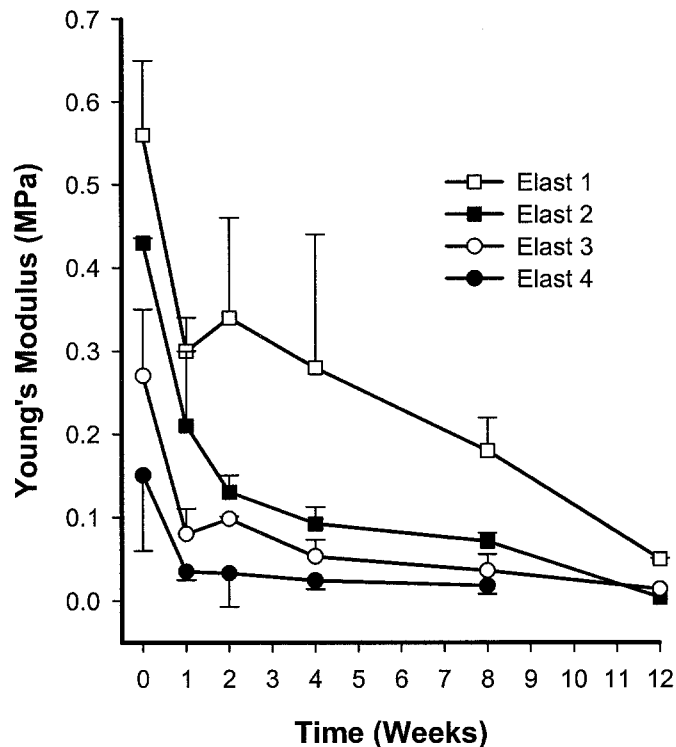


Figure 2.9 Change in Young's modulus with time.

During the degradation studies, the decrease in the modulus values with respect to time for all the prepared elastomers showed a logarithmic relationship (Figure 2.9) as has been observed with other elastomers.^{4,14} Such behaviour is indicative of a bulk hydrolysis mechanism in which random chain scission of ester groups along the backbone occurs.^{4,14} Such a pattern of degradation would result in the accumulation of the acidic monomers inside the bulk of the polymer contributing to further autocatalytic acidic degradation. The fact that no significant weight loss of the dried tested specimens for all the elastomers were observed after 4 weeks as shown in Figure 2.10 excluded the occurrence of any major surface erosion. Although some reports indicate that an increase in Young's modulus with time is possible due to an increase in the crystallinity of the degrading

amorphous polymer,^{7,21} this was not observed with this material indicating that crystal formation did not occur.

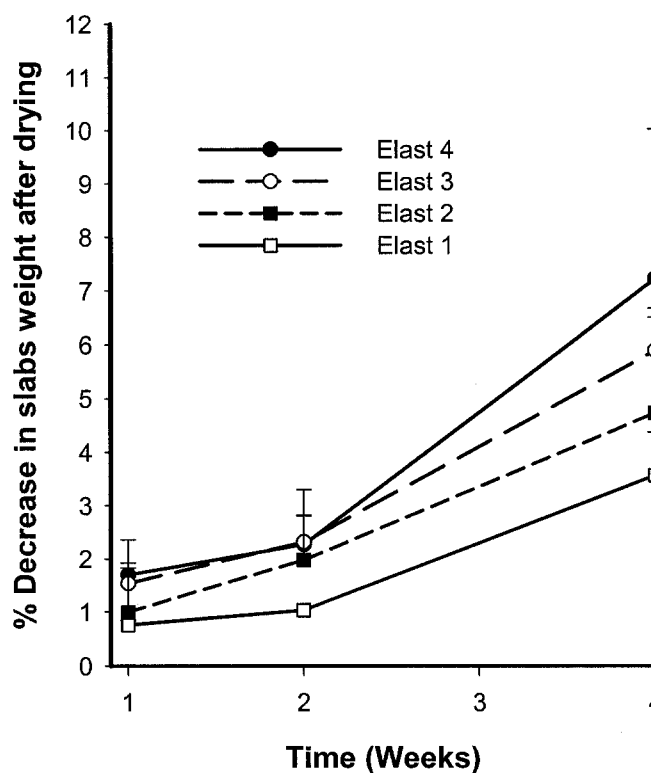


Figure 2.10 Change in weight of the tested elastomers with time after drying

As shown in Figure 2.11, the drop in the pH of the degradation media for the control samples in which the medium was kept unchanged over the experiment length was not significant in the first two weeks. This can be explained by less water penetration into the bulk of the slabs and less dissolution of the acidic monomer and/or oligomer degradation products to the surrounding medium. This explanation is supported by the minor increase in weight during that period for all the tested slabs as previously shown in Figure 2.8. By the fourth and eighth week of the degradation study, water penetration into the bulk of the

slabs resulted in major dissolution of the acidic hydrolysis products into the degradation medium with a subsequent drop in its pH. This drop was very significant with Elast 4 and Elast 3, since both have less crosslinking density which allows greater water penetration and accelerated autocatalytic hydrolysis within their bulk.

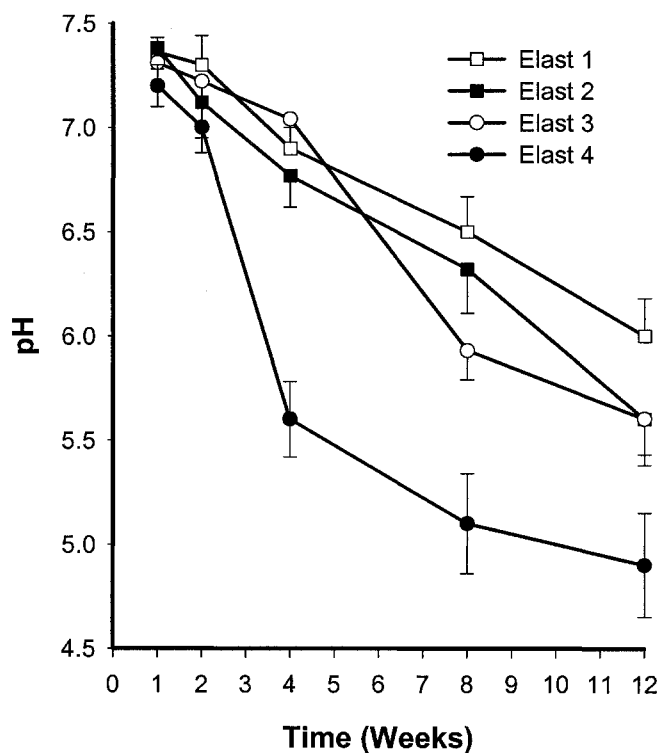


Figure 2.11 Change in pH of the degradation media with time.

The change in the ultimate tensile stress, σ_u , with time is shown in Figure 2.12. Similarly to the decrease in the Young's modulus with time for all the tested samples, a logarithmic decrease in the ultimate tensile stress was also observed. The decrease in σ_u was most significant after one week of the degradation study and then declined in a slower fashion. This pattern was followed regardless of the crosslinking density and the initial σ_u of the

tested elastomer. By the end of the 12 weeks, all the elastomers regardless of crosslinking ratio, showed ultimate tensile stress values approaching zero.

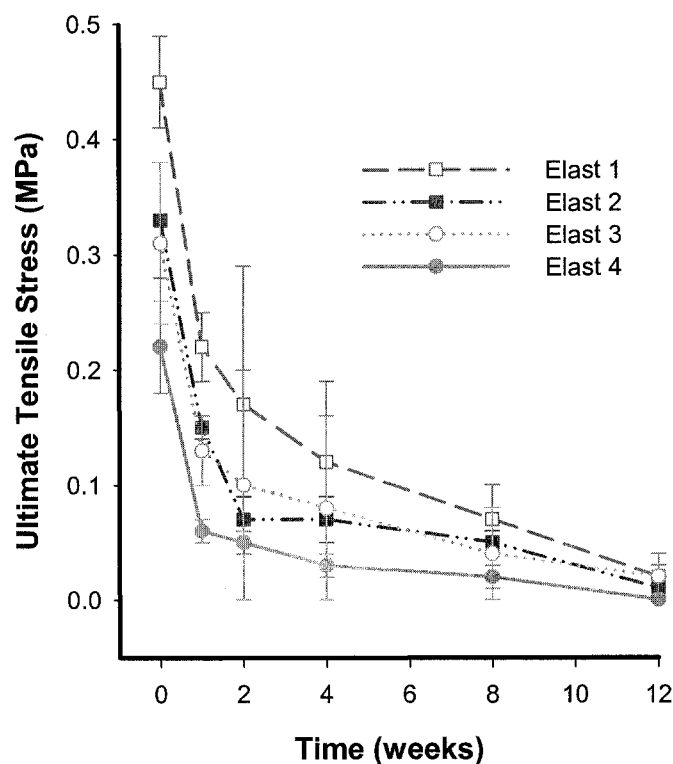


Figure 2.12 Change in ultimate tensile stress with time.

The changes in the extension ratio (λ_b) for the tested specimens with time are reported in Table 2.5. As would be expected, a decrease in the λ_b values accompanied the use of higher amounts of BCP in crosslinking SCP prepolymers reflecting the increased crosslink density. As a result, Elast 4 has higher λ_b compared to Elast 1 which demonstrated less strain values as reported in Table 2.4. Table 2.5 reports the changes in λ_b values for all the prepared elastomers over time. It is shown here that as a result of the decrease in the elastomer crosslink density with time due to degradation, an increase in their λ_b values occurred. This increase in the λ_b values for all the tested elastomers were

most significant after the first week of degradation and thereafter increased in a logarithmic fashion.

Table 2.4 Summary of the mechanical properties of the elastomers. Values are means (standard deviation).

Elastomer	Young's Modulus (MPa)	Extension Ratio (λ_b)	Max Stress (MPa) (σ)	% Strain at Max Load
Elast 1	0.56 (0.09)	1.57	0.45 (0.04)	56.7 (5.32)
Elast 2	0.43 (0.06)	1.78	0.33 (0.05)	78.6 (7.40)
Elast 3	0.27 (0.08)	2.14	0.32 (0.07)	113.6 (6.19)
Elast 4	0.14 (0.09)	2.34	0.22 (0.04)	134 (37.13)

Table 2.5 Summary of the changes in the extension ratio values with time for the tested slabs. Values are mean (standard deviation).

Time (Weeks)	Elastomer Tested			
	Elast 4	Elast 3	Elast 2	Elast 1
0	2.34 (0.38)	2.14 (0.06)	1.79 (0.08)	1.57 (0.13)
1	3.28 (0.16)	3.13 (0.32)	--	1.73 (0.09)
2	3.58 (0.95)	2.56 (0.58)	1.74 (0.07)	1.83 (0.12)
4	3.45 (0.83)	3.02 (0.36)	1.94 (0.23)	1.47 (0.26)
8	3.36 (0.60)	2.61 (0.47)	1.86 (0.18)	1.73 (0.23)
12	--	3.72 (0.62)	2.01 (0.23)	1.94 (0.31)

2.4. Conclusions

Ring opening polymerization of ϵ -CL with DL-LA using glycerol as initiator and SnOct as a catalyst resulted in a star copolymer that was further reacted with different ratios of the crosslinking monomer, 2,2-bis(ϵ -caprolactone-4-yl)-propane (BCP). Higher amounts of the BCP used in crosslinking the star copolymer prepolymer resulted in an increase in glass transition temperature, Young's modulus, and ultimate tensile strength. Upon degradation in phosphate buffered saline, the elastomers showed a logarithmic decrease in their Young's modulus with time as an indication of a bulk hydrolysis mechanism that was also accompanied by an increase in water absorption and a decrease in their ultimate tensile strength. In addition, the extension ratio of the tested elastomers increased with time accompanied by a decrease in their Young's modulus and ultimate tensile strength.

2.5. References

- (1) Sodian, R.; Sperling, J. S.; Martin, D. P.; Egozy, A.; Stock, U.; Mayer, J. E., Jr.; Vacanti, J. P. *Tissue Eng.* **2000**, *6*, 183.
- (2) Alberti, C. *Minerva Urol. Nefrol.* **2000**, *52*, 219.
- (3) Mulder, M. M.; Hitchcock, R. W.; Tresco, P. A. *J. Biomat. Sci.-Polym. Ed.* **1998**, *9*, 731.
- (4) Pitt, C. G.; Hendren, R. W.; Schindler, A. *J. Control. Rel.* **1984**, *1*, 3.
- (5) Pitt, C. G. and Schindler, A. E. US Patent 4146871, 1979.
- (6) Kylma, J.; Seppala, J. *Macromolecules* **1997**, *30*, 2876.
- (7) Hiljanen-Vainio, M.; Karjalainen, T.; Seppala, J. *J. Appl. Polym. Sci.* **1996**, *59*, 1281.

- (8) Leong, K. W.; Zhao, Z.; Dahiyat, B. I. In *Elastomeric Poly(Phosphoesterurethane)s*; Park, K., Ed.; American Chemical Society: 1997; p 469.
- (9) Storey, R. F.; Hickey, T. P. *Polymer* **1994**, *35*, 830.
- (10) Storey, R. F.; Warren, S. C.; Allison, C. J.; Puckett, A. D. *Polymer* **1997**, *38*, 6295.
- (11) Kim, S. H.; Han, Y.-K.; Kim, Y. H.; Hong, S. I. *Makromol. Chem.* **1992**, *193*, 1623.
- (12) Kim, S. H.; Han, Y.-K.; Ahn, K.-D.; Kim, Y. H.; Chang, T. *Makromol. Chem.* **1993**, *194*, 3229.
- (13) Bruin, P.; Veenstra, G. J.; Nijenhuis, A. J.; Pennings, A. J. *Makromol. Chem., Rapid Commun.* **1988**, *9*, 589.
- (14) Hiljanen-Vainio, M. P.; Orava, P. A.; Seppala, J. V. *J. Biomed. Mater. Res.* **1997**, *34*, 39.
- (15) Joziase, C. A. P.; Veenstra, H.; Top, M. D. C.; Grijpma, D. W.; Pennings, A. J. *Polymer* **1998**, *39*, 467.
- (16) Li, Y.; Kissel, T. *Polymer* **1998**, *39*, 4421.
- (17) Schindler, A.; Hibionada, Y. M.; Pitt, C. G. *J. Polym. Sci., Part A: Polym. Chem.* **1982**, *20*, 319.
- (18) Palmgren, R.; Karlsson, S.; Albertsson, A.-C. *J. Polym. Sci., Part A: Polym. Chem.* **1997**, *35*, 1635.
- (19) Hassal, C. H. *Org. Reactions* **1957**, *9*, 73.
- (20) Friess, S. L. *J. Am. Chem. Soc.* **1949**, *71*, 2571.
- (21) Karjalainen, T.; Hiljanen-Vainio, M.; Malin, M.; Seppala, J. *J. Appl. Polym. Sci.* **1996**, *59*, 1299.

CHAPTER 3

SYNTHESIS, CHARACTERIZATION AND IN VITRO DEGRADATION OF PHOTO-CROSSLINKED BIODEGRADABLE ELASTOMERS

Husam M. Younes¹ and Brian G. Amsden^{1,2}

A version of this chapter has been submitted to *Biomacromolecules*

1. Faculty of Pharmacy and Pharmaceutical Science, University of Alberta,
Edmonton, Alberta, Canada T6G 2N8
2. Department of Chemical Engineering, Queens University, Kingston, Ontario,
Canada, K7L 3N6

3.1. Introduction

Biodegradable elastomers have several possible applications in both the pharmaceutical and biomedical fields. Such applications include their use in localized and sustained drug delivery systems¹⁻³ and the manufacturing of scaffolds for tissue engineering⁴ of bioartificial organs⁵ and skeletal substrates.⁶ Biodegradable elastomers intended for use in such applications are preferably required to exhibit an homogenous degradation profile and to demonstrate the ability to maintain their dimensional stability during the drug release or implantation period. For this purpose, the preparation of biodegradable thermoset elastomers⁷⁻⁹ are preferable over thermoplastics^{10,11} which do not demonstrate such linearity in degradation although they are easier to handle and formulate.

A common methodology for preparing thermoset elastomers involves the preparation of amorphous star-shaped copolymer prepolymers which are further crosslinked using different approaches to form the elastomeric network. Such approaches include crosslinking with diisocyanate linkages,⁸ or methacrylate groups on the termini⁹ and the use of a bis- ϵ -caprolactone (BCP) crosslinker.^{2,12}

Although these approaches proved to be successful in preparing thermoset elastomers, they possess some disadvantages. Depending on the diisocyanate used, the final degradation product of the prepared elastomer might be mutagenic and the method involves the use of carcinogenic solvents to disperse the crosslinker into the polymer which affect the biocompatibility of the final product.⁸ In addition, even with the use of

the more compatible cyclo-aliphatic diisocyanates, the final preparation step involves a thermal post-curing process that restricts it from being used for controlled delivery of thermo-sensitive therapeutics like proteins and hormones.¹³ Methacrylate end-capped star copolymers have also been thermally cured to form elastomers; however, the network formation involved the use of cobalt naphthenate as a catalyst dissolved in 2-butanone peroxide solution which also raises the issues of biocompatibility.⁹ In our previous attempt to prepare a thermoset elastomer as a potential biomaterial for surgical applications and drug delivery for proteins and cytokines, bis- ϵ -caprolactone, a biocompatible lactone crosslinker was used to crosslink an amorphous star copolymer prepolymer prepared by polymerizing ϵ -caprolactone (ϵ -CL) with DL-lactide (DL-LA) using glycerol as initiator and stannous 2-ethylhexanoate as a catalyst. Although this approach resulted in a biocompatible biodegradable elastomer, polymerization temperatures of 120 or 180 °C were required in the curing step. This has restricted the use of the prepared biocompatible elastomer from delivering heat sensitive drugs including proteins and hormones that degrade and /or denature at such high temperatures.¹²

Photopolymerization techniques which have been used to prepare biodegradable hydrogels as drug delivery carriers¹⁴ and for various biomedical applications^{15,16} have also been utilised to prepare biodegradable photoset elastomers.^{17,18} This approach involved the preparation of prepolymers with various photosensitive termini which in the presence of the proper photoinitiator can undergo free radical polymerization once exposed to ultraviolet (UV) or laser light. This photopolymerization approach would offer a number of advantages over the conventional thermal or solution techniques in

preparing biodegradable elastomers. First, the process excludes the use of thermal energy, in other words, the polymers can be formulated at temperatures near the physiological range even once loaded with biologically thermo-sensitive therapeutics like proteins and other heat-sensitive drugs. Second, the process proceeds rapidly, on the order of minutes. Finally, the degree of crosslinking, and the mechanical properties of the photocured elastomer can be tailored by changing the density of the photosensitive termini in the prepolymer.

In this paper, we report on the synthesis, photocuring, characterisation, mechanical properties and *in vitro* degradation of a newly synthesized biodegradable elastomer that has potential as an implantable matrix for the delivery of peptide and protein drugs. This elastomer was prepared in three stages. The first involved the preparation of a star copolymer prepolymer (SCP) utilizing ring opening polymerization of ϵ -CL with DL-LA using glycerol as initiator and 2-ethylhexanoate as a catalyst. The second stage involved the conversion of the terminal hydroxyl groups into vinyl groups by an acrylation process. The final stage included photocuring which resulted in the elastomeric product which was characterized for its structure, purity and mechanical properties.

3.2. Experimental Section

3.2.1. Materials

D,L-lactide was obtained from Purac (The Netherlands) while ϵ -caprolactone was obtained from Lancaster and then dried over CaH_2 (Aldrich). Other chemicals used in the

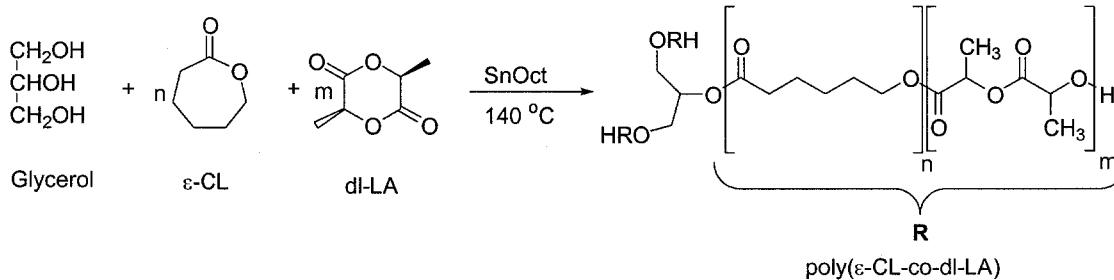
synthesis of the SCP were stannous 2-ethylhexanoate (Aldrich), and glycerol (BDH). The chemicals used in the synthesis of the acrylated SCP include acryloyl chloride, triethylamine, and 4-dimethylaminopyridine, which were all obtained from Aldrich. Other chemicals used include dichloromethane (Fisher), and hexane and ethyl acetate which were obtained from BDH. The long-wave UV (LWUV) initiator 2,2-dimethoxy-2-phenyl-acetophenone was obtained from Aldrich.

3.2.2. Preparation of poly (ϵ -caprolactone-co-D,L-lactide) (ϵ -CL/DLLA) Star Copolymer (SCP)

The detailed method of preparation was reported elsewhere.¹² In summary, solvent free polymerization was carried out in sealed silanized 20 ml ampoules. Different molar ratios of the monomers and initiators were used to prepare star copolymers of different molecular weights and arm lengths. The quantities and ratios used to prepare each are reported in Table 3.1. The following is a representative procedure that describes the preparation of a SCP. Into a dry silanized ampoule, 0.005 mol of glycerol and 0.05 mol of ϵ -CL were transferred and mixed till homogeneous. An amount equivalent to 0.05 mol of DL-LA was then transferred to the ampoule, the ampoule filled with nitrogen, then placed in an oven at 120 °C for 10 minutes allowing the DL-LA to melt. The mix was then stirred using a vortex mixer and 2-ethylhexanoate was added in an amount equivalent to 1.4×10^{-4} mol for each 1 mol of the monomer. The ampoule was filled with nitrogen, flame sealed under vacuum, and left in an oven at 140 °C for 18 hours. The prepared SCP was then purified by precipitation from dichloromethane (DCM) solution into cold

methanol. The thermal behaviour and the composition of the prepared SCP were characterized using Differential Scanning Calorimetry (DSC), Nuclear Magnetic Resonance (NMR) and Gel Permeation Chromatography (GPC). Scheme 3.1 shows a representation of the synthesis of the poly (ϵ -CL-co-DL-LA) SCP.

Scheme 3.1



3.2.3. Preparation of Acrylated SCP

One mole of acryloyl chloride was used to react with one mole of each OH in the prepolymers reported in Table 3.1. The following describes the methodology to prepare SCP-1A and a representation of the process is shown in scheme 3.2. In summary, in a round bottom flask, 20 g of SCP ($2.56 (10)^{-3}$ mole) was dissolved in 200 ml of dichloromethane (DCM) on a magnetic stirrer using a magnetic bar. The flask was sealed using a rubber septum and flushed with argon. This step was repeated every hour. The flask was then immersed in a $0\text{ }^\circ\text{C}$ ice bath, after which 10 mg of 4-dimethyl aminopyridine (DMAP) was added as a catalyst. A stepwise addition of $7.66 (10)^{-3}$ mol of each of acryloyl chloride (ACRL) and triethylamine (TEA) was performed over a period of 12 hours at $0\text{ }^\circ\text{C}$. The reaction was later continued at room temperature for

another 12 hours. The reaction completion was detected using TLC and the final solution was filtered to remove triethylamine hydrochloride salt formed during the reaction. The polymer solution was concentrated using a rotary evaporator and further purified by precipitation in ethyl acetate. FT-IR, $^1\text{H-NMR}$ and $^{13}\text{C-NMR}$ were used to characterize the purity of the final product and the disappearance of OH groups as a result of the formation of the terminal vinyl groups.

Table 3.1 List of the star copolymers and their corresponding molecular weights prepared using different monomer/initiator molar ratios.

Prepolymer	$\epsilon\text{CL/}$ DL-LA	Monomer/ Initiator *	Molecular Weight (Da)	Acrylated Prepolymer	% OH Conversion
SCP-0	50/50	10/1	2671	SCP-0A	94
SCP-1	50/50	29/1	7829	SCP-1A	96
SCP-2	70/30	14/1	2552	SCP-2A	94
SCP-3	50/50	45/1	11950	SCP-3A	93

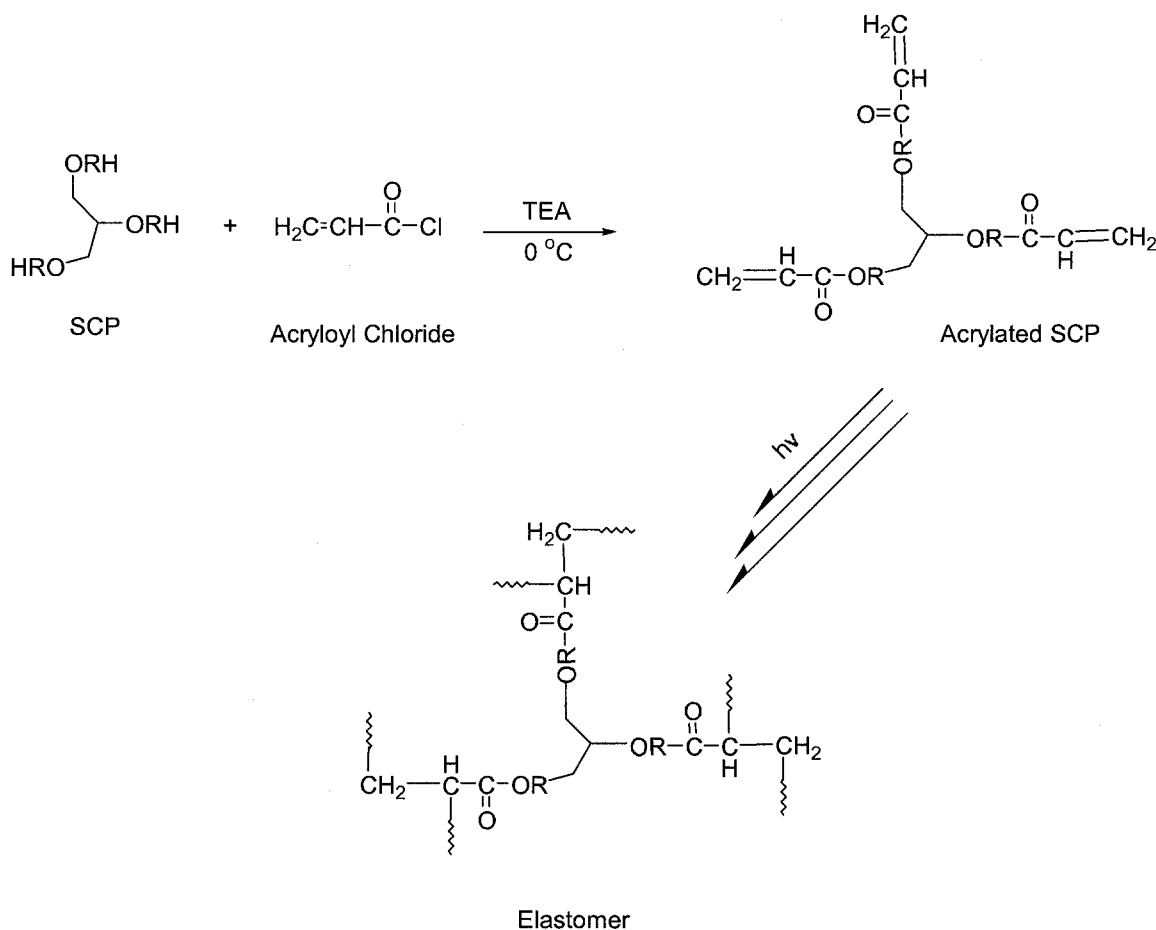
* $1.4 (10)^{-4}$ mol of SnOct was used as a catalyst for each 1 mol of monomer in preparing the corresponding star copolymer

3.2.4. UV-Crosslinking of Acrylated SCP

In a test tube, 50 μl of the UV initiator solution (30% w/v of 2,2-dimethoxy-2-phenylacetophenone (DMPA) in DCM) was added to 1 ml of the acrylated SCP solution (1 g acrylated SCP in 1 ml DCM). The thick solution was mixed using a vortex mixer and poured into a Teflon mould (80 x 6 x 2 mm). The sample was then exposed to UV light at a distance of 10 cm at room temperature for 5-10 minutes using a Black Ray model B-100AP UVP high-intensity long wave lamp of $21,700 \mu\text{w}/\text{cm}^2$ relative intensity. The

elastomer formed was then removed from the mould and characterized for its thermal properties using DSC and for its mechanical properties before and during the degradation study using an Instron 4443 tensile tester (ASTM 412). Scheme 3.2 demonstrates the UV crosslinking process of the corresponding acrylated SCP.

Scheme 3.2



3.2.5. Polymer Characterization

^1H and ^{13}C NMR were run in CDCl_3 using a Varian VXR 500 MHz Spectrometer with an Oxford Instruments superconducting magnet. The FT-IR experiments were acquired on a

Nicolet Magna 550 FT-IR spectrometer using NaCl cells. Polymer samples were prepared by casting thin films of the semisolid SCP's and their acrylated forms onto the NaCl cells. The data analysis of the spectra and the determination of the area under the peaks (AUP) were carried out using an Omnic series IR software package. The DSC experiments were carried out using a Seiko SII SSC/6200 DSC with a cooling system. The samples were run at a heating rate of 10 °C/min and the DSC was calibrated using indium and gallium standards. The enthalpies, glass transitions temperatures, and melting endotherms were determined using the internal DSC analysis program. The GPC experiments for molecular weight determinations were conducted using a Hewlett-Packard 1100 system connected to a Precision Detectors PD 2000 DLS light scattering detector supplied with a Waters 410 Differential Refractometer. The mobile phase consisted of THF at a flow rate of 2 ml/min with the system at 35 °C. The concentration of the polymers used for the GPC measurements were 2 mg/ml and the injection volume was 20 µl. The column configuration consisted of an HP guard column attached to a Phenogel linear (2) 5 µ GPC column. Monodisperse polystyrene standards (Aldrich) were used for initial system calibration. The mechanical properties of the elastomer were carried out on slabs (80 x 6 x 2 mm) using an Instron tensile tester model 4443 equipped with an extensometer. The extensometer gauge length was set to 25 mm while the specimen gauge length was set to 40 mm. The crosshead speed was set at 500 mm/min (ASTM D412). All specimens were tested at room temperature. Data analysis was carried out using a Merlin 4.11 Series IX software package.

3.2.6. In Vitro Degradation Study

Slab specimens of recorded weights of the elastomer prepared from SCP-1A prepolymers reported in Table 3.3 were subjected to an *in vitro* degradation study. Each specimen was put into a 15 ml tissue culture tube which was filled with 12 ml Phosphate Buffer Saline (PBS) of pH 7.4. The tubes were attached to a Glas-Col rugged culture rotator. The rotator was set at 30% rotation speed and placed in an oven at 37 °C. The buffer was replaced frequently to ensure a constant pH of 7.4 during the whole period of the study. One set of samples representing each ratio was left without changing its buffer to monitor the change in the medium's pH with respect to time. The specimens were then dried, weighed and subjected to tensile testing at time periods of 0, 1, 2, and 4 weeks.

4.3. Results and Discussion

Three arm star copolymer prepolymers (SCP) that have hydroxyl groups at their terminals were prepared using ring opening polymerization of ϵ -CL and DL-LA at 140 °C using glycerol as initiator and 2-ethylhexanoate as a catalyst (Scheme 3.1). The molecular weight of the prepared SCPs was tailored by using different monomer/initiator ratios. Table 3.1 reports the ratios of ϵ -CL, DL-LA and glycerol used in preparing prepolymers of different molecular weights. The prepared prepolymer SCPs were previously characterized using DSC and different spectroscopic methods.¹² The purpose of preparing this range of SCPs was to evaluate the effect of the arm length and the molar

ratio content of ϵ -CL and DL-LA on the mechanical properties of the photoset elastomers prepared by photo-crosslinking the corresponding prepolymers.

Although different photopolymerizable end groups have previously been incorporated into the chain ends of polymers for the purpose of UV photo-crosslinking (for example cinnamate and coumarin)^{19,20} acrylates were chosen here because they possess greater reactivity and can undergo very rapid photopolymerization.²¹ In addition, they eventually undergo degradation to acrylic acid which is extensively metabolized to water soluble components that are rapidly and safely excreted by the kidney with no possibility of bioaccumulation.²² For this reason, the terminal hydroxyl groups in the SCPs prepared were subjected to an acrylation process as per Hubbell and co-workers²³ using acryloyl chloride for the purpose of introducing unsaturated vinyl terminals that can be crosslinked using UV or laser photopolymerization technology in the presence of the proper photoinitiator.

To determine the effect of using different molar ratios of acryloyl chloride to SCP in the acrylation reaction, and for the goal of determining the optimum amounts required of acryloyl chloride to undergo a complete acrylation for the terminal hydroxyl groups, different acryloyl chloride to SCP molar ratios were used. Table 3.2 reports the different amounts of acryloyl chloride used to react with the SCP-0 prepolymer. The stacked IR spectra for the acrylated prepolymers reported in Table 3.2 are shown in Figure 3.1. It is clear that as the acryloyl chloride to SCP molar ratio increases, the intensity of the corresponding OH stretching at around 3500 cm^{-1} decreases with a concomitant increase

in the formation of the terminal vinyl groups indicated by the appearance of the new C=C stretching peak at around 1620 cm^{-1} .

Table 3.2 List of the acrylated prepolymers prepared using different amounts of acryloyl chloride to react with the SCP prepolymer.

Acrylated SCP-0A codes	Acryloyl chloride (mol)/SCP OH (mol)
SCP-0A1	1.0/1.0
SCP-0A2	0.8/1.0
SCP-0A3	0.4/1.0
SCP-0A4	0.167/1.0

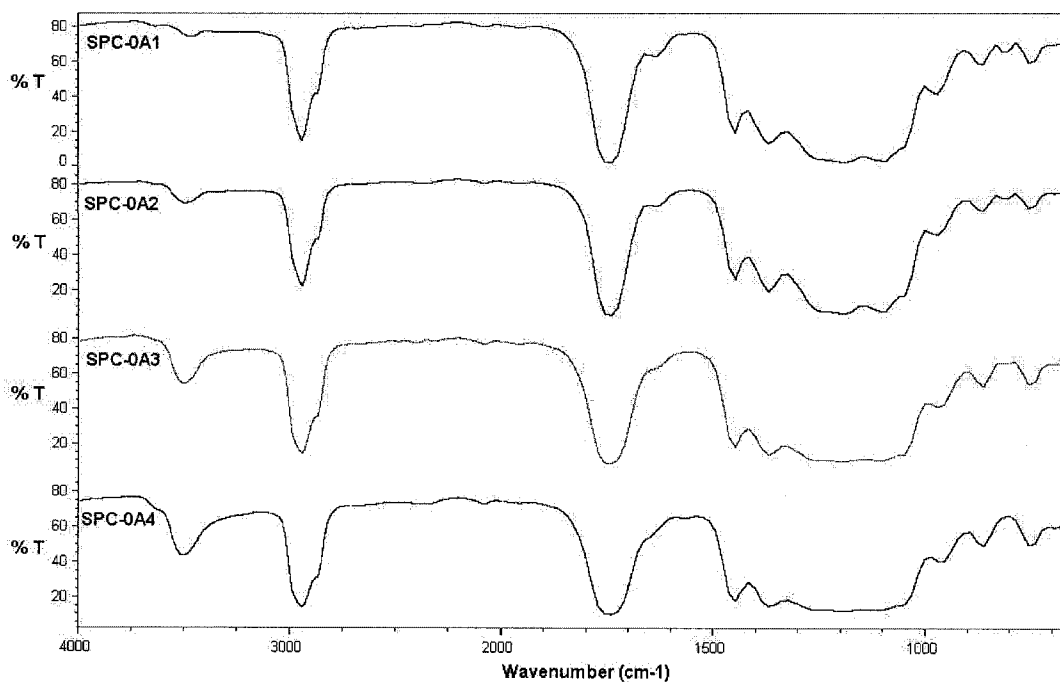


Figure 3.1 Stacked FT-IR Spectra of the acrylated star copolymers reacted with different amounts of acryloyl chloride.

A nearly complete disappearance of the OH stretching takes place with SCP-0A1 compared to minor changes with OH stretching peak in case of SCP-0A4. This result can

be seen more clearly in Figure 3.2 which shows the overlaid IR spectra of both SCP-0 and SCP-0A1. This analysis was further confirmed using $^1\text{H-NMR}$ spectroscopy in which the vinyl group's presence is illustrated by the peaks in the region between 5.9 and 6.1 ppm as shown in Figure 3.3. It is clear here that there were no interfering peaks of any kind in the $^1\text{H-NMR}$ of the purified SCP-0A1 compared to the non-acrylated SCP-0.

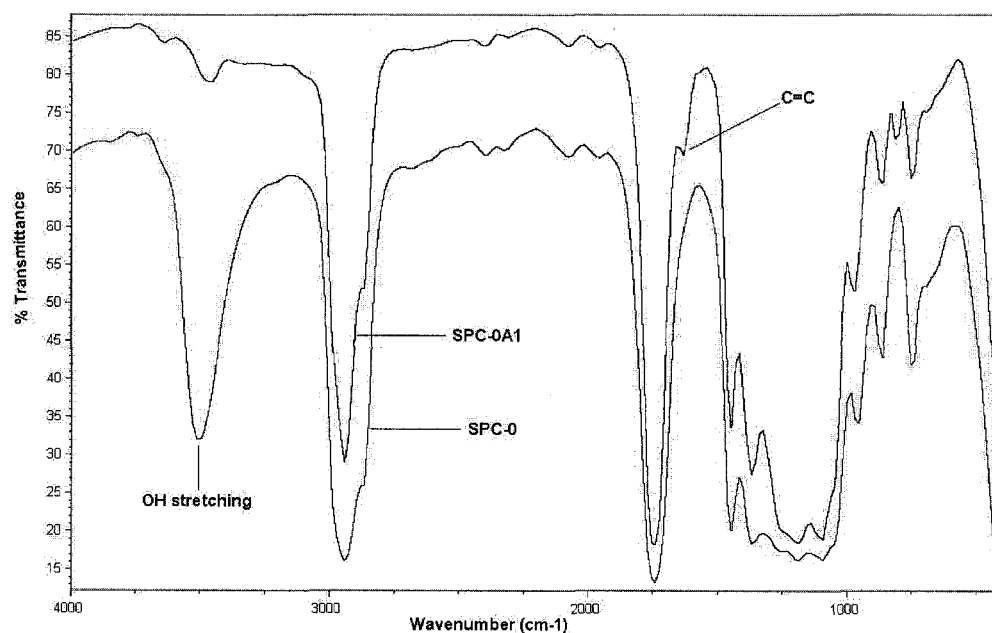


Figure 3.2 Overlapped FT-IR spectra of SCP before and after the acrylation process showing the corresponding peaks.

The approximate percent conversion of the hydroxyl groups to the corresponding vinyl groups, which are reported in Table 3.3, were calculated using equation 3.1.

$$\% \text{Conversion} = 100 - \left[\left(\frac{(AUP_{OH-Str} / AUP_{C=O})_{prepolymer}}{(AUP_{OH-Str} / AUP_{C=O})_{acrylated-polymer}} \right) * 100 \right] \quad (3.1)$$

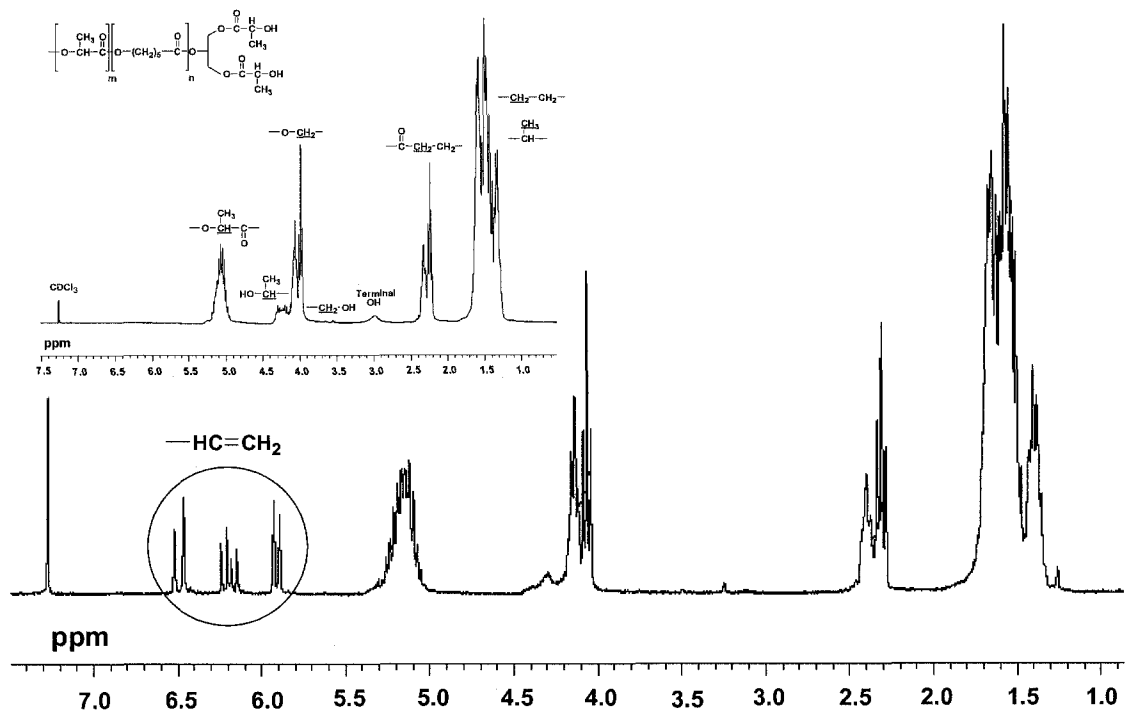


Figure 3.3 $^1\text{H-NMR}$ spectra of the SCP-0 before acrylation (upper left) and the acrylated SCP-01A (lower).

Table 3.3 The area under the peak for the OH and C=O stretching vibrations for SCP and the acrylated prepolymers and the % of conversion of the terminal hydroxyl to the vinyl groups.

Acrylated Prepolymer	AUP (OH)	AUP (C=O)	AUP OH/ AUP C=O	Measured % Conversion	Theoretical % Conversion
SCP-0	5678	7185	0.800	0	0
SCP-0A1	419	8734	0.048	94	100
SCP-0A2	1236	7758	0.172	79	80
SCP-0A3	3949	8056	0.490	39	40
SCP-0A4	4645	7663	0.606	24	16.7

In this equation AUP_{OH-str} is the area under the peak for the OH stretching vibration at 3500 cm^{-1} and $AUP_{C=O}$ is the area under the peak for the carbonyl group stretching vibration at 1730 cm^{-1} . There was no significant difference between the measured percentage of conversion compared to the theoretical values calculated except for SCP-0A4 in which the experimental conversion was a little higher than the theoretical. This could be attributed to lack of accuracy upon measuring 0.16 moles of acryloyl chloride using a regular 1 ml syringe.

Based on the above discussion, it is important to mention here that all the prepolymers reported in Table 3.1 were reacted with the optimum amount of acryloyl chloride *i.e.* 1 mol acryloyl chloride to 1 mole OH in the prepolymer and resulted in a percentage of conversion that exceeded 93% in each of them (Table 3.1). After preparing and purifying the set of acrylated SCP prepolymers reported in Table 3.1, we attempted to undergo a UV photo-initiated radical crosslinking using 2,2-dimethoxy-2-phenyl-acetophenone (DMPA) as a photoinitiator. The latter possesses some advantages that make it preferable to use over other photoinitiators. First, it possesses high photoinitiation reactivity which results in an accelerated crosslinking process. Second, the presence of a pendant acrylic group in its structure reduces the extractable amount of unreacted photoinitiator remaining in the UV-cured material with no significant loss of its initiation efficiency²⁴ and finally, its reported biocompatibility¹⁶ and its low toxicological burden. Furthermore, it has been reported that its oral LD_{50} in rats is in excess of 2 g/kg.²⁵ One study by Bryant et al reported cytotoxicity of this photoinitiator for chondrocytes encapsulation into photocrosslinked hydrogel²⁶. Such situation is not applicable in our study since the

procedure in which the photocrosslinked polymer prepared is taking place outside the body and therefore do not involve direct contact between the body cells and radicals. Therefore, any cell damage once this prepared device is implanted after being prepared is inherently limited in this case.

Curing was achieved after 10 minutes exposure of the sample to LWUV light at a distance of 10 cm. It was also noticed that once the photopolymerization process started, the formation of the crosslinked elastomer was rapid and accompanied by evaporation and removal of the dichloromethane solvent. That a crosslinked network was formed was confirmed by immersing the polymers into dichloromethane. The polymers swelled but did not dissolve.

To determine the effect of changing the monomer (ϵ -CL : DL-LA) and initiator (glycerol) ratios on the mechanical properties of the final photo-crosslinked products, selected photocured samples prepared from the corresponding prepolymers reported were subjected to tensile testing. A representative stress-strain curve for SCP-1A is given in Figure 3.4.

Table 3.4 reports those samples tested and a summary of their mechanical properties. It is shown here that the elastomers prepared from the SCP-0A1, SCP-0A2 and SCP-2A acrylated prepolymers were hard/tough and brittle. The samples photo-crosslinked using SCP-0A1 and SCP-0A2 were the most hard and brittle indicated by their higher Young's modulus values. This can be explained by the fact that using low monomer/initiator ratios

in preparing the acrylated prepolymers of those two samples resulted in a prepolymer of short arm length which restricted the chains mobility and their stretching ability which consequently restricted the elasticity of the final products as indicated by their low strain

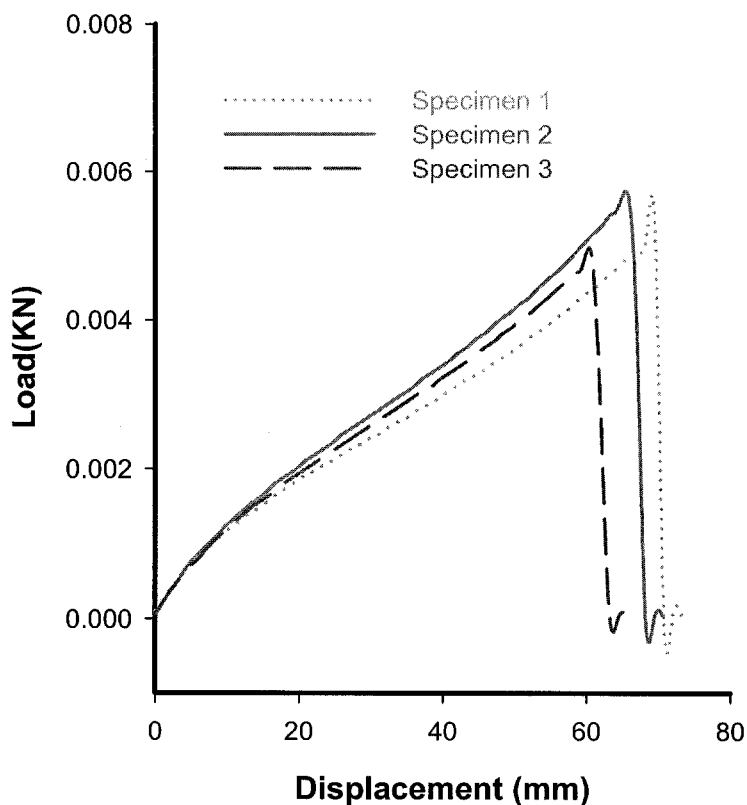


Figure 3.4 The stress-strain profile for the tested specimens of the elastomers prepared by photo-crosslinking of the SCP-1A prepolymers

values. Furthermore, increasing the degree of conversion of the hydroxyl groups to acrylate groups produced an even more brittle sample (SCP-0A1) due to an increase in crosslink density. Samples photo-crosslinked using SCP-2A acrylated prepolymers demonstrated less brittleness compared to those used SCP-0A1 since a higher ϵ -CL content was used in their preparation (*i.e* 70/30 ratio see Table 3.1).

Table 3.4 Summary of the mechanical properties of the tested slabs of the corresponding prepared elastomers. Values are mean (standard deviation).

Acrylated Prepolymer used	Young's Modulus (MPa)	Max Stress (MPa)	% Strain (ϵ)	Extension Ratio (λ_b)	Description of prepared elastomers
SCP-0A1	1.512 (0.23)	0.217 (0.07)	11.40 (3.19)	1.11	Very Hard, Brittle
SCP-0A2	1.210 (0.25)	0.19 (0.05)	16.00 (2.81)	1.16	Hard, Brittle
SCP-1A	0.268 (0.01)	0.44 (0.04)	263.7 (16.0)	3.64	Tough, Elastic
SCP-2A	0.639 (0.07)	0.11 (0.06)	18.28 (3.15)	1.18	Tough, Brittle
SCP-3A	0.041 (0.01)	0.05 (0.01)	261.1 (63.5)	3.61	Weak, Elastic

On the other hand, samples photocured using SPC-1A and SBC-3A acrylated prepolymers resulted in elastomeric samples with high extension ratios. The use of a high monomer:initiator ratio in both of them resulted in higher molecular weight and longer arm length which contributed to their stretching properties. Elastomers prepared using SPC-3A prepolymers were weaker and lacked the strength that was demonstrated upon using SCP-1A, as indicated by the lower ultimate stress, σ , values. The elastomers prepared using the SCP-1A acrylated prepolymers demonstrated the strength and elasticity that is required for the intended applications of this elastomer. Furthermore, DSC analysis of the elastomers prepared using SCP-1A acrylated prepolymers showed an amorphous pattern with a T_g of -11.5 °C. This value was in accordance to our goal to prepare an amorphous photoset elastomer that has a T_g well below body temperature. Therefore, the elastomers photocured using SCP-1A prepolymers were further characterized for the changes in their tensile properties in PBS degradation media.

To determine the changes in the mechanical properties and the degradation patterns of the elastomers prepared using SCP-1A prepolymers as a function of time, slab specimens of recorded weights were subjected to an *in vitro* degradation. Table 3.5 summarizes those changes over 0, 1, 2, and 4 weeks. It is shown from the data in Table 3.5 that there were no significant changes in the mean values of percent weight increase of the prepared slabs over the first 2 weeks of the study. Significant changes were only recorded by the end of the fourth week. This result gives an indication of a low rate of water absorption into the bulk of the slabs and consequently a low degradation rate within the first 2-4 weeks.

Table 3.5 Summary of the changes in the mechanical properties during *in vitro* degradation of elastomers prepared by photo-crosslinking of SCP-1A prepolymers. Values are mean (standard deviation).

Week	Young's Modulus (MPa)	Max Stress (MPa)	% Strain (ϵ)	Extension Ratio (λ_b)	% increase in weight
0	0.268 (0.01)	0.44 (0.04)	263.7 (16.0)	3.64 (0.15)	-----
1	0.248 (0.05)	0.48 (0.12)	362.6 (60.6)	4.62 (0.26)	3.92 (0.02)
2	0.262 (0.03)	0.48 (0.07)	364.7 (17.7)	4.65 (0.62)	4.05 (0.05)
4	0.23 (0.04)	0.39 (0.04)	374.1 (19.4)	4.74 (0.32)	10.82 (1.79)

This was also evident by the minor changes in the mechanical properties reported within the first 4 weeks of the degradation study. Such observations and results can be explained by the fact that this photoset elastomer possesses a high crosslink density which makes it more resistant to water penetration. Nevertheless, this minute amount of water succeeded in penetrating into the bulk of the samples will start to hydrolyse part of the polymer's chains resulting in decreasing the crosslink density of this polymer with time. As a result

of this degradation an increase in its strain and extension ratio took place reaching most significant values by the end of 4 weeks period.

3.4. Conclusions

Ring opening polymerization of ϵ -CL with DL-LA using glycerol as initiator and SnOct as a catalyst resulted in a star copolymer that was further reacted with different ratios of the ACRL to convert the terminal OH groups in to photosensitive vinyl termini. Higher amounts of the ACRL used in the reaction resulted in an increase in % of conversion with a nearly complete conversion achieved once 3 moles of ACRL are used to react with 1 mole of SCP. The UV photopolymerization process resulted in a variety of photoset polymers whose elasticity is dependent on the monomers and initiator ratios used in the preparation of the prepolymers. The analysis of the changes in the mechanical properties in PBS degradation medium for the elastomers prepared by photo-crosslinking the SCP-1A acrylated showed minor changes in Young's modulus, ultimate stress, and extension ratio within the first 2 weeks of the study. Significant changes were only observed by the fourth week of the degradation period. This analysis was supported by the insignificant mean changes in percent weight of the tested slabs over the first two weeks. The above conclusion was drawn based on the high crosslink density the tested elastomer demonstrated upon running the swelling studies. A longer period of degradation study is a future plan to determine the exact changes in the tensile properties after the 1 month of degradation in PBS.

3.5. References and Notes

- (1) Pitt, C. G. and Schindler, A. E. US Patent 4,146,871, 1979.
- (2) Pitt, C. G.; Hendren, R. W.; Schindler, A. *J. Control. Rel.* **1984**, *1*, 3-14.
- (3) Wada, R.; Hyon, S. H.; Nakamura, T.; Ikada, Y. *Pharm. Res.* **1991**, *8*, 1292-1296.
- (4) Sodian, R.; Sperling, J. S.; Martin, D. P.; Egozy, A.; Stock, U.; Mayer, J. E., Jr.; Vacanti, J. P. *Tissue. Eng.* **2000**, *6*, 183-188.
- (5) Alberti, C. *Minerva Urol. Nefrol.* **2000**, *52*, 219-222.
- (6) Mulder, M. M.; Hitchcock, R. W.; Tresco, P. A. *J. Biomater. Sci. Polym. Ed.* **1998**, *9*, 731-748.
- (7) Joziase, C. A. P.; Veenstra, H.; Top, M. D. C.; Grijpma, D. W.; Pennings, A. J. *Polymer* **1998**, *39*, 467-473.
- (8) Storey, R. F.; Hickey, T. P. *Polymer* **1994**, *35*, 830-838.
- (9) Storey, R. F.; Warren, S. C.; Allison, C. J.; Puckett, A. D. *Polymer* **1997**, *38*, 6295-6301.
- (10) Kylma, J.; Seppala, J. *Macromolecules* **1997**, *30*, 2876-2882.
- (11) Lofgren, A.; Renstad, R.; Albertsson, A. C. *J. Appl. Polym. Sci.* **1995**, 1589-1600.
- (12) Younes, H. M.; Amsden, B. G. *Biomacromolecules* **2002**, submitted.

- (13) Bruin, P.; Veenstra, G. J.; Nijenhuis, A. J.; Pennings, A. J. *Makromol. Chem., Rapid Commun.* **1988**, *9*, 589-594.
- (14) West, J. L.; Hubbell, J. A. *React. Polym.* **1995**, *25*, 139-147.
- (15) Elisseeff, J.; McIntosh, W.; Anseth, K.; Riley, S.; Ragan, P.; Langer, R. *J. Biomed. Mater. Res.* **2000**, *51*, 164-171.
- (16) Sawhney, A. S.; Pathak, C. P.; Van Rensburg, J. J.; Dunn, R. C.; Hubbell, J. A. *J. Biomed. Mater. Res.* **1994**, *28*, 831-838.
- (17) Regula, D. W.; Bregen, M. F.; Cooper, S. L.; Jamilolkowski, D. D.; Bezwada, R. S. US Patent 5,674,921, 1997.
- (18) Sakurai, F.; Kidokoro, H.; Tamura, M. US Patent 4,980,260, 1990.
- (19) Matsuda, T.; Mizutani, M. *Macromolecules* **2000**, *33*, 791-794.
- (20) Ichimura, K.; Akita, Y.; Akiyama, H.; Kudo, K.; Hayashi, Y. *Macromolecules* **1997**, *30*, 903-911
- (21) Decker, C. *Pigm. Resin Tech.* **2001**, *30*, 278-286.
- (22) World health organization: health and safety guide number 104. *I. P. C. S.* 1997.
- (23) Hubbell, J. A.; Pathak, C. P.; Sawhney, A. S.; Desai, N. P.; Hill, J. L. US Patent 5410016, 1995.
- (24) Decker, C. *J. Coating Technol.* **1987**, *59*, 97-106.

- (25) Ciba Corporation: *Material Safety Data Sheet for Irgacure 651* **2002**, 1-5.
- (26) Bryant, S. J.; Nuttelman, C. R.; Anseth, K. S. *J. Biomater. Sc. Polymer Ed.* **2000**, *11*, 439-457.

CHAPTER 4

OSMOTICALLY CONTROLLED DRUG DELIVERY FROM A NEW PHOTO-CURED BIODEGRADABLE ELASTOMER

Husam M. Younes¹ and Brian G. Amsden^{1,2}

A version of this chapter has been submitted to *Journal of Controlled Release*

1. Faculty of Pharmacy and Pharmaceutical Science, University of Alberta, Edmonton, Alberta, Canada T6G 2N8
2. Department of Chemical Engineering, Queens University, Kingston, Ontario, Canada, K7L 3N6

4.1. Introduction

Osmotically driven delivery of water soluble drugs from elastomeric polymers has been the focus of many previous studies [1-5]. Several reports have investigated the different factors that affect the rate and mode of release from those systems [2,4,6,7]. Others have focused on the development of different mathematical models that describe the release profiles from such systems [8-10].

Some studies reported those systems to release the drugs following $t^{1/2}$ kinetics [11,14,15] while others reported them to follow pseudo-zero order kinetics [4,10,16]. However, in more recent studies, it has been demonstrated that the mechanism governing the release of agents from elastomeric monoliths depended on the volumetric loading. When the matrix system is loaded above a critical volume fraction called the percolation threshold, most of the agent particles dispersed in the polymer matrix are interconnected with one another. In this case, the active agent is predominantly released by diffusion through the water-filled pores that are formed as water imbibed from the surface of the device replaces the active agent that leaches out. As the volumetric loading of the drug increases and its particle size decreases, the rate of drug release increases [8]. For osmotic release to dominate, the drug loading must be below this critical volume fraction, which is approximately 30 to 35 % [6,8,17]. In addition, it was reported that the main parameters affecting the release were the osmotic activity of the loaded drug and/or excipient, saturation concentration and density of the dispersed drug, the tensile strength, Young's modulus and the hydraulic permeability of the polymer and the fraction of particles

released by dissolution and diffusion [2,4,8].

A description for the release of drugs via an osmotic mechanism is illustrated in Figure 4.1. The Figure has been divided into three temporal regions which typify the kinetics of drug delivery. The first region (region A) illustrates the initially high drug release rate due to drug particles dissolving from the system surface and the apparently facilitated rupture of drug-containing capsules nearest to the surface. This accounts for between 5 to 15 % of the initially loaded drug. After this first burst period, a steady state release of the drug is observed for a certain period of time (region B). Release in this region occurs by water vapor contacting the solid particles and dissolving the solid at the solid/polymer interface, generating a solution either at saturation or very near to saturation. The particle is now referred to as a capsule. The gradient in water activity between the release medium and the capsule draws water into the capsule, and the capsule swells. At some point, if the capsule wall is thin enough, the capsule ruptures, and its contents are pumped out of the capsule into the porous network (region C). This process continues serially throughout the matrix.

Ethylene vinyl acetate copolymers (EVA) and poly(dimethylsiloxane) (PDMS) were among the most extensively studied hydrophobic non-degradable elastomers used as monolithic devices for this purpose [4,7,9,11-13]. The general approach that was utilized was to create fractures and interconnected pores inside the polymers leading to the surface by either relying on the osmotic activity of the drug itself or co-formulating the loaded drugs with highly osmotically active electrolytes like sodium chloride, which act

as pore forming agents.

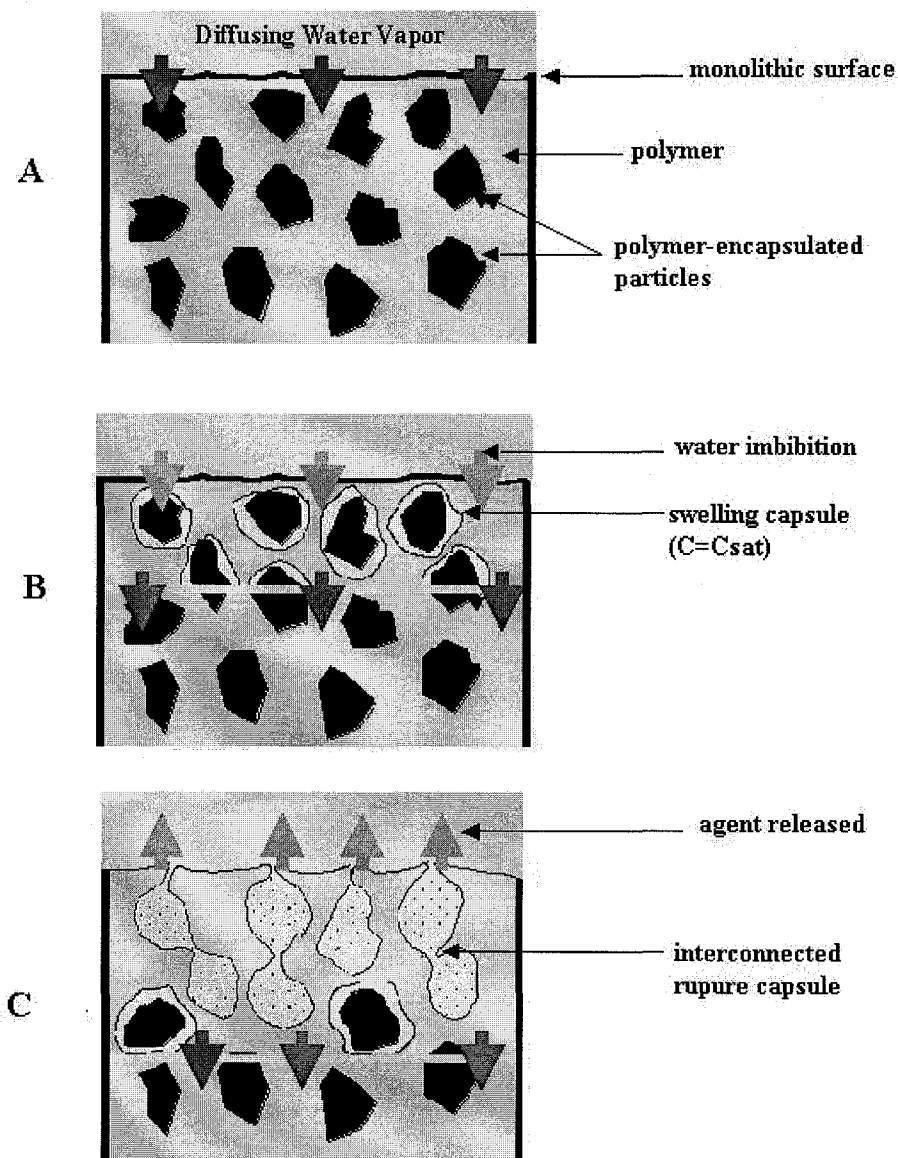


Figure 4.1 Osmotic release mechanism. (a) water diffusion through polymer to first layer of agent particles; (b) swelling of particle capsules due to water imbibition under an osmotic activity gradient; (c) interconnected pore network formation and agent release as a result of capsule rupturing; (d) the elastomer eventually start significant degradation which overlaps with stage C. (Reproduced from reference 8 with permission)

In our recent study on the preparation of a polymeric carrier for proteins and peptides, we succeeded in synthesizing a new biodegradable photoset elastomer in a three-step procedure. The first step involved the preparation of a star copolymer prepolymer utilizing ring opening polymerization of ϵ -caprolactone with D,L-lactide using glycerol as initiator and 2-ethylhexanoate as a catalyst. The second stage involved the conversion of the terminal hydroxyl groups into vinyl groups by an acrylation process. The final stage was a photopolymerization process which resulted in an elastomeric product which was further characterized for its structure, purity and mechanical properties [18].

This newly synthesized elastomer would offer some advantages over EVA and PDMS elastomers. First, it is biodegradable which waives the need for its removal after being implanted. Second, the mechanical properties of this elastomer can be easily modified by varying comonomer ratios, the monomer/initiator ratio and the degree of its acrylation. Third, the dispersion of the drug and the UV photo-crosslinking of the prepolymers can be carried out at temperatures near the physiological range even once loaded with biologically thermo-sensitive therapeutics like proteins and other heat-sensitive drugs. Finally, the curing process proceeds rapidly, on the order of minutes.

The purpose of the present study, therefore, is to demonstrate the release mechanism from this newly synthesised hydrophobic photo-cured biodegradable elastomer. Pilocarpine nitrate was used as a model of a drug with a reasonably high osmotic activity. Pilocarpine nitrate was also co-formulated with another, more osmotically active agent (i.e. trehalose) to examine means of enhancing the release of a water soluble agent from an elastomeric,

degradable, monolithic system.

4.2. Materials and Methods

4.2.1. Materials

D, L-lactide was obtained from Purac, The Netherlands, while ϵ -caprolactone was purchased from Lancaster and then dried over CaH_2 (Aldrich). Other chemicals used in the synthesis of the star copolymer prepolymer were 2-ethylhexanoate (Aldrich), and glycerol (BDH). The chemicals used in the synthesis of the acrylated star copolymer prepolymer include acryloyl chloride, triethylamine, and 4-dimethyl aminopyridine, which were all obtained from Aldrich. Other chemicals used include dichloromethane (Fisher), hexane and ethyl acetate which were obtained from BDH. The long-wave UV (LWUV) initiator 2, 2-dimethoxy-2-phenyl-acetophenone was obtained from Aldrich. D (+) trehalose and pilocarpine nitrate salt were obtained from Sigma. The osmolality standards of 100, 290 and 1000 mmol/kg were all purchased from Wescor Company.

4.2.2. Preparation of poly (ϵ -caprolactone-co-D,L-lactide) (ϵ -CL/DLLA) Star Copolymer (SCP)

The detailed method of preparation and the full structural characterization of the SCP prepolymer were reported elsewhere [19]. In summary, into a dry silanized ampoule, 1.7×10^{-3} mol of glycerol and 0.05 mol of ϵ -CL were transferred and mixed till

homogeneous. An amount equivalent to 0.05 mol of DL-LA was then transferred to the ampoule, the ampoule filled with nitrogen, then placed in an oven at 120 °C for 10 minutes allowing the DL-LA to melt. The mix was then stirred using a vortex mixer and 2-ethylhexanoate (SnOct) was added in an amount equivalent to $1.4 (10)^{-4}$ mol for each 1 mol of the monomer. The ampoule was filled with nitrogen, flame sealed under vacuum, and left in an oven at 140 °C for 18 hours. The prepared SCP was then purified by precipitation from dichloromethane (DCM) solution into cold methanol. The final polymer number average molecular weight was 7800 g/mol.

4.2.3. Preparation of Acrylated SCP

The method of Hubbell, with minor adaptation, was used here [20]. In summary, in a round bottom flask, 20 g of SCP ($2.56 (10)^{-3}$ mole) was dissolved in 200 ml of DCM on a magnetic stirrer using a magnetic bar. The flask was sealed using a rubber septum and flushed with argon. This step was repeated every hour. The flask was then immersed in a 0 °C ice bath, after which 10 mg of 4-dimethyl aminopyridine (DMAP) was added as a catalyst. A stepwise addition of $7.66 (10)^{-3}$ mol of each of acryloyl chloride (ACRL) and triethylamine (TEA) was followed over a period of 12 hours at 0 °C. The reaction was later continued at room temperature for another 12 hours. The reaction completion was detected using TLC and the final solution was filtered to remove triethylamine hydrochloride salt formed during the reaction. The polymer solution was concentrated using a rotary evaporator and further purified by precipitation in ethyl acetate. FT-IR, ^1H -NMR and ^{13}C -NMR were used to characterize the purity of the final product and the

disappearance of OH groups as a result of the formation of the terminal vinyl groups. The degree of conversion of the terminal hydroxyl groups was calculated to be 94% [18].

4.2.4. Preparation of pilocarpine nitrate (PCN) loaded cylinders

In a test tube, 0.6 ml of the UV initiator solution (30% w/v of 2,2-dimethoxy-2-phenylacetophenone (DMPA) in DCM) was added to 12 ml of the acrylated SCP solution (12 g acrylated SCP in 12 ml DCM). The resulting thick solution was further mixed till homogenous. A 5% v/v of PCN load was achieved by adding 0.65 g of its micronized powder (sieved through 45 μm mesh) to the mix. The viscous suspension was then mixed using vortex for 30 seconds. The product poured into the bottom of sealed cylindrical glass moulds of either 1 or 2 cm in length and 0.5 cm in diameter. The moulds were then exposed to UV light at a distance of 5 cm at room temperature for 10 minutes using a Black Ray model B-100AP UVP high-intensity long wave inspection lamp of 21,700 $\mu\text{w}/\text{cm}^2$ relative intensity. The photo-crosslinked elastomers were then removed from the mould by breaking and peeling the glass to get the final cylinders loaded with 5% v/v PCN. Each cylinder was then weighed. The amount of PCN loaded in each cylinder was calculated on a weight and volume basis. When a 1:1 mix of PCN and trehalose were used to load the elastomeric monolithic systems, both were dissolved in water and re-crystallized to get intimately mixed particles. Water was then evaporated under vacuum and then powder was passed through of 45 μm mesh sieves to obtain the final micronized mix. Figure 4.2 illustrates the experimental protocol used in preparing the elastomeric monoliths.

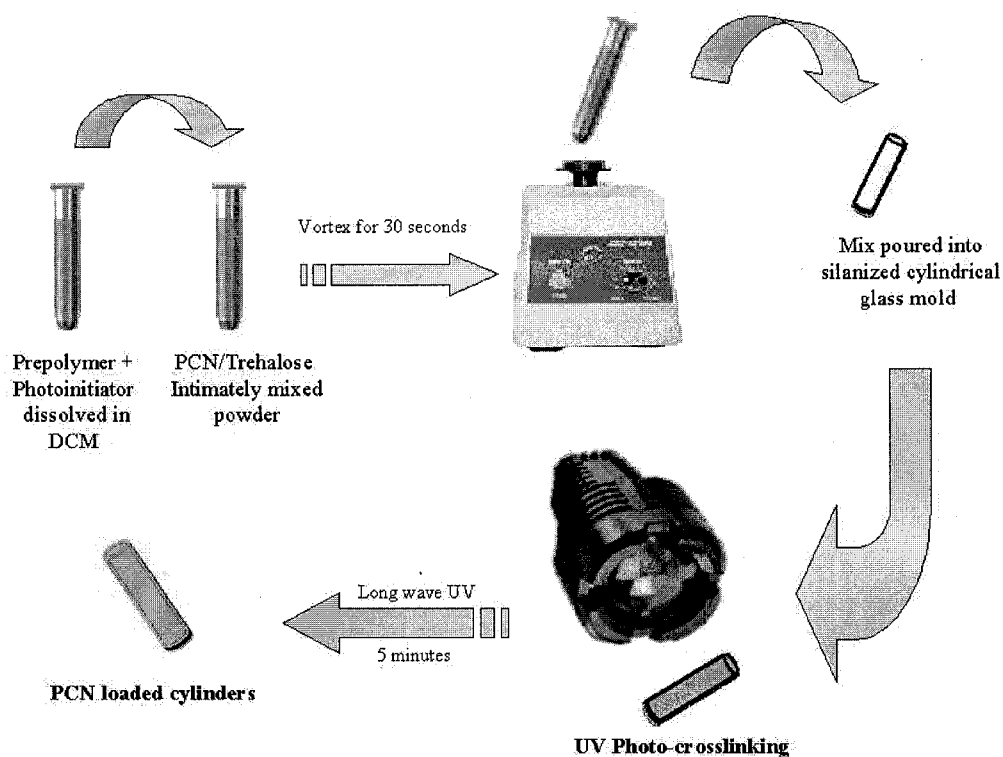


Figure 4.2 Method of loading PCN into the photoset elastomer.

4.2.5. Osmotic activity measurements

The osmolality of 10 μ l of triplicate samples of saturated solutions of PCN, distilled water (DW), 3% w/v NaCl and 1/15 M phosphate buffer saline (PBS) of pH 7.4 was measured using a Wescor vapour pressure osmometer which was previously calibrated using 100, 290 and 1000 mmol/kg (NaCl) standards at 37 °C.

4.2.6. In Vitro release study and UV analysis

The prepared monolith cylinders of 1 and 2 cm length loaded with 5% PCN with or

without trehalose were subjected to *in vitro* release studies using DW, 1/15 M PBS and 3% NaCl as release media. Four samples of each cylinder were put into 40 ml scintillation vials filled with 30 ml of a dissolution medium. The vials were attached to a Glas-Col rugged culture rotator. The rotator was set at 30% rotation speed and placed in an oven at 37 °C. The receptor release medium was replaced with fresh medium over a period of three months or until 100 % cumulative release was achieved. The receptor release medium was replaced with a fresh medium to ensure sink conditions and constant osmotic pressure driving force. This was done on a daily basis during the first two weeks and on a weekly basis thereafter. Solutions withdrawn were filtered and their concentrations were determined using an UV method of analysis at a maximum wavelength of 208 nm using a Philips PU 8740 UV/VIS Scanning spectrophotometer.

4.3. Results and Discussion

Our primary intention was to formulate PCN at a volumetric loading of 15-20 % v/v, which is still below the percolation threshold, to achieve a prolonged steady-state drug release as has been described in previous reports [4,6]. Nevertheless, our final decision to use loadings of 5-10 % v/v was based on two reasons. First, 5% v/v loads of PCN were enough to simulate our original goal to use this system for the release of highly potent water-soluble therapeutics like cytokines and proteins which need only to be loaded in very low doses in order to elicit the required effect. Second, our experimental findings showed that 5% v/v loadings were the optimums which still enable the UV light to crosslink the system. Any loadings exceeding that limit retarded this process and

produced an uncrosslinked matrix.

In an attempt to demonstrate the osmotic release mechanism of water soluble agents from this newly synthesized photoseal biodegradable elastomer, PCN was used as a model compound because of its moderate osmotic activity (Table 4.1) and the ease of determining its concentration in the release media using UV method of analysis. It is important to report here that before running the release studies, the stability of PCN in the three release media used was tested by monitoring the changes in the concentration of a prepared stock solution of PCN in each of them over a period of one week. The study showed no significant changes from its initial concentration over the tested period.

Table 4.1 Osmolality of pilocarpine nitrate solutions and the release media.

Solution	Osmolality (mmol/Kg)
saturated pilocarpine nitrate	791
distilled water	20
PBS of pH=7.4	280
3% NaCl	919
trehalose	1524

The release profiles for 5% v/v load of PCN from cylinders of 2 cm and 1 cm length are illustrated in Figures 4.3 and 4.4 respectively. As shown in the Figures, the release profiles can be divided into three distinct regions. The first, which extends up to about 5-7 days and accounts for 10-15% of the loaded drug, represents the initial burst resulting

from those particles located on the surface of the biodegradable elastomer. The burst amount in the two Figures was essentially the same in both cases regardless of the cylinder length. The second stage of release following the initial burst proceeds more slowly, approaches linearity in both situations, and extends up to 42 days, after which a dramatic increase in the release rate takes place.

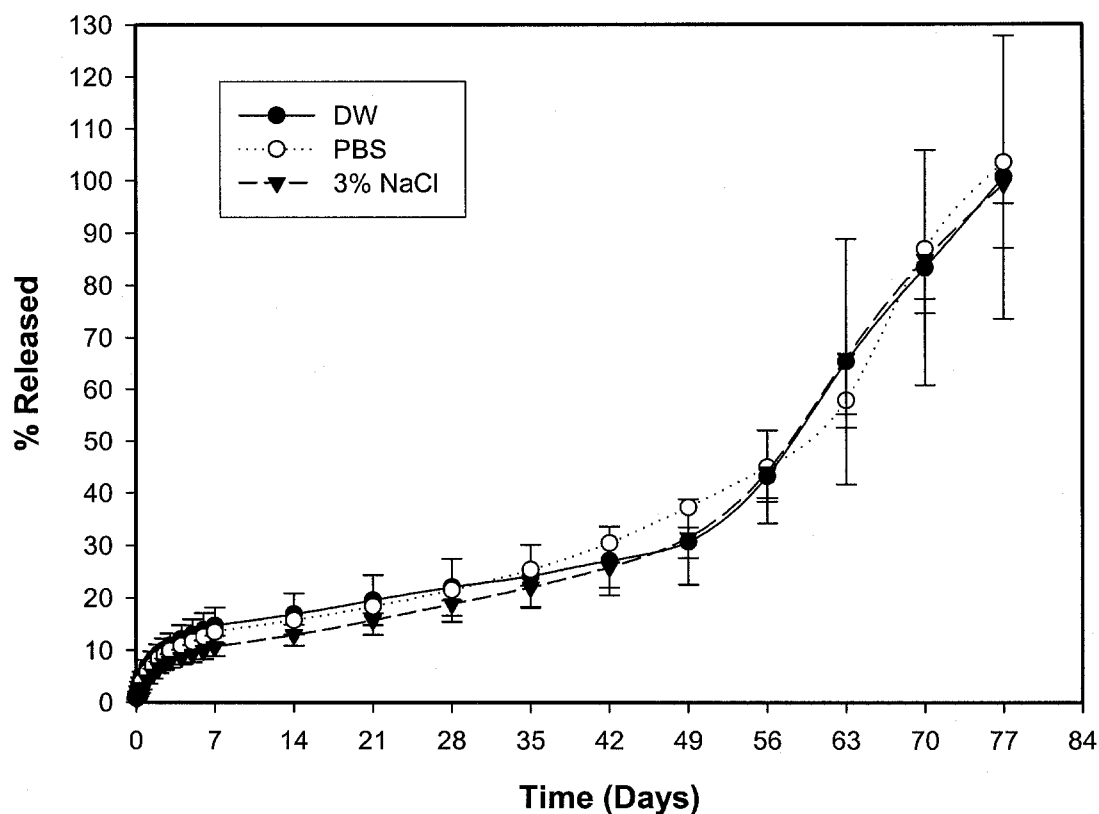


Figure 4.3 Cumulative percent PCN released from 5% v/v loaded cylinders (2 cm length) using distilled water, PBS and 3% NaCl as release media. Values are means of 4 samples \pm standard deviation.

The initial burst amount reported for the two cylinder lengths agrees with the values typically found for diffusional release from non-degradable matrix systems [21,22]. The slopes in the second linear stage of release for Figures 4.3 and 4.4 are reported in Table

4.2 and their regression plots are shown in Figures 4.5 and 4.6 respectively.

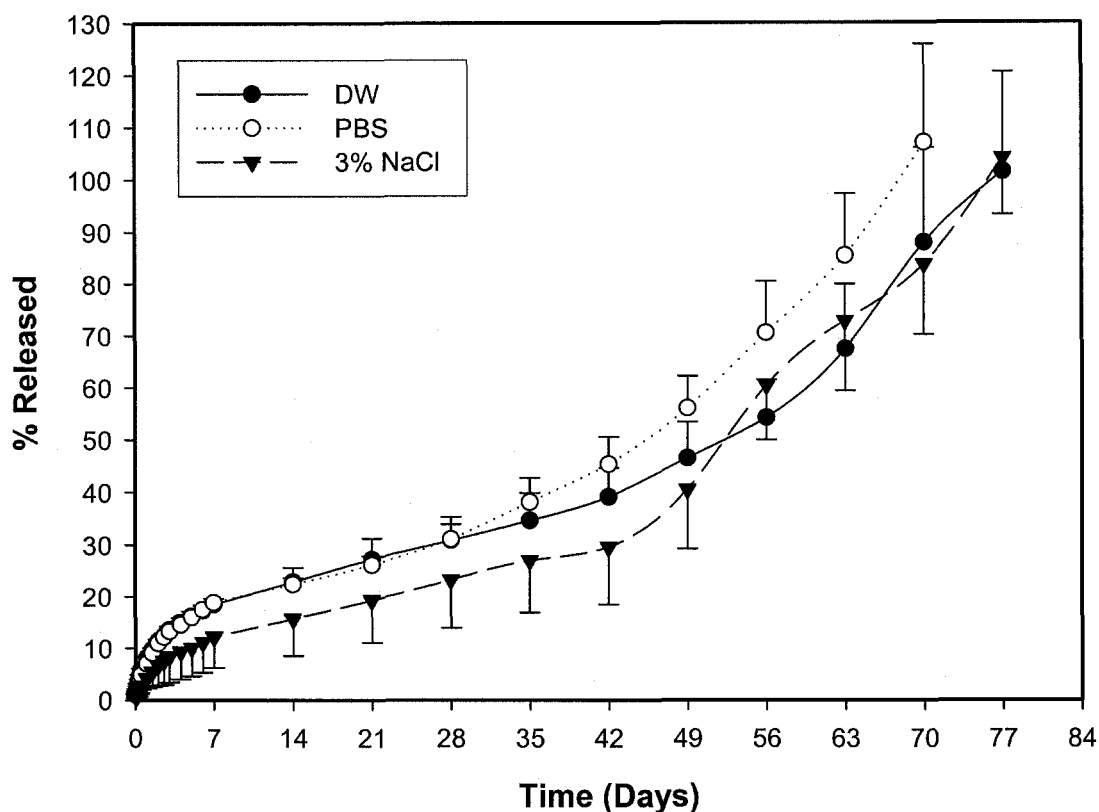


Figure 4.4 Cumulative percent PCN released from 5 % v/v loaded cylinders (1 cm length) using distilled water, PBS and 3% NaCl as release media. Values are means of 4 samples \pm standard deviation.

Table 4.2 Slopes of the linear phase of release shown in Figures 4.5 and 4.6 Values are mean \pm SD.

Release Medium	5% load PCN with 2 cm length	5% v/v PCN with 1 cm length	5% v/v PCN: trehalose
DW	0.350 ± 0.007	0.578 ± 0.011	N/A
PBS	0.419 ± 0.03	0.583 ± 0.032	1.61 ± 0.04
3% NaCl	0.431 ± 0.017	0.506 ± 0.013	N/A

As seen from Figure 4.5, the slopes of the linear release phase from the 2 cm cylinders in the three dissolution media are within the same range. The same behaviour is also applicable in the 1 cm cylinders as shown in Figure 4.6. The greater slope values the 1 cm cylinders have in all the dissolution media when compared to those of the 2 cm length cylinders is attributed to the fact that a higher proportion of the incorporated drug is released from the ends of the shorter cylinders compared to the fraction released from the sides of longer cylinders. The fact that the rate of release during this linear phase is statistically equivalent for each of the cylindrical sizes indicates that one release mechanism is controlling the release of PCN from the two systems, regardless of the release medium used.

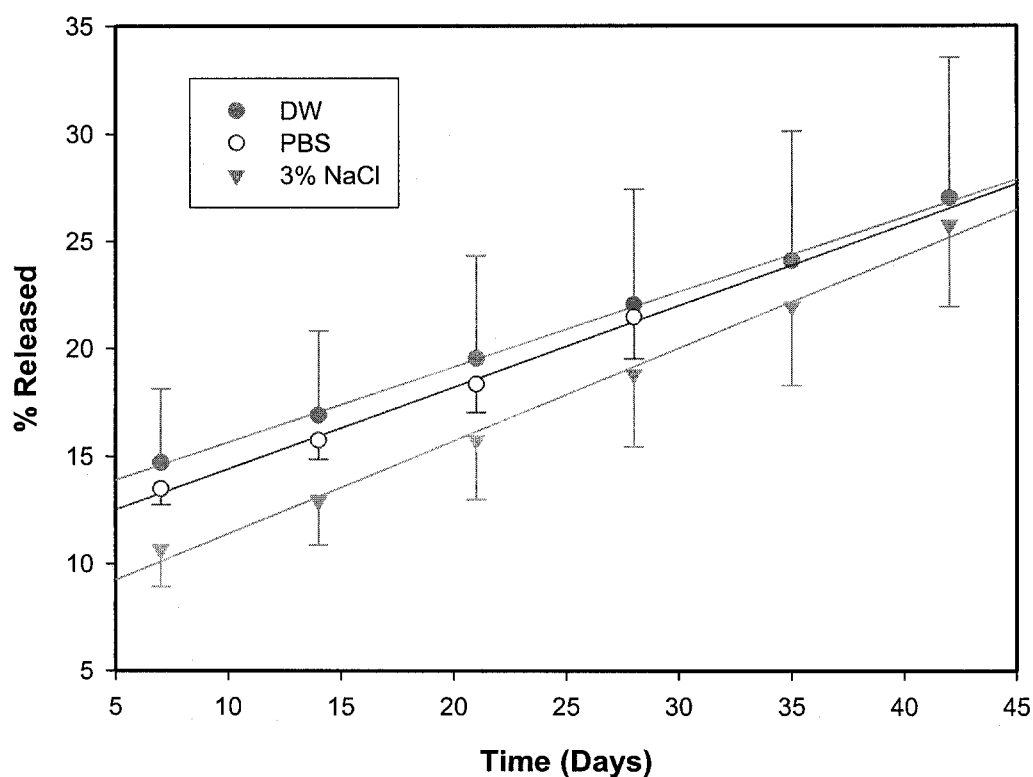


Figure 4.5 Regression of the data obtained during the linear release phase (7-42 days) from 5% v/v cylinders of 2 cm length.

Since we hypothesized that the release of PCN dispersed in this biodegradable elastomer during the constant release period was of an osmotic nature, the release mode during that period was anticipated to be dependent on the difference in osmotic pressure between the external release medium and the saturated solution of PCN inside the capsules formed in the elastomer. However, the release rate during this linear release phase (between 5-42 days) is not osmotically dominated. Otherwise, the use of the 3 % NaCl as a release medium, which possesses a higher osmotic pressure than the saturated PCN solution, would have resulted in prevention of its release during that linear stage rather than just decreasing it compared to those in which DW and PBS were used. Another release mechanism is governing the rate of drug release, which is most likely polymer degradation releasing particles which have relatively thin walls of polymer surrounding them.

The steady state portion of the release rate profile was approximately 8 weeks, during which time approximately 15 % of the PCN contained in the system was released. Within this period, a dynamic balance between the osmotic imbibition of water and the release of drug from the system is achieved. After the steady state region, a sudden increase in release rate takes place as a result of significant degradation in the polymer matrix which will overlap with the proposed serial osmotic mechanism.

The degradation rate of the polymer was greatest upon using PBS as the release medium, as indicated by the faster onset of accelerated drug release for monoliths immersed in this buffer (35 days versus 42 days). This could be attributed to the accelerated base-catalyzed

degradation caused by its higher pH compared to that of DW and NaCl, each of which possesses a pH of around 6.8. This hydrolytic effect of PBS on the elastomeric structure was distinguished by observing more swelling and turbidity in the vials which contain PBS compared to those containing DW and 3 % NaCl. However, the slopes of the linear phases in each of the two tested cylindrical sizes were almost the same regardless of the release medium used. PBS only played a role in speeding up the next stage of release, which is the accelerated release section.

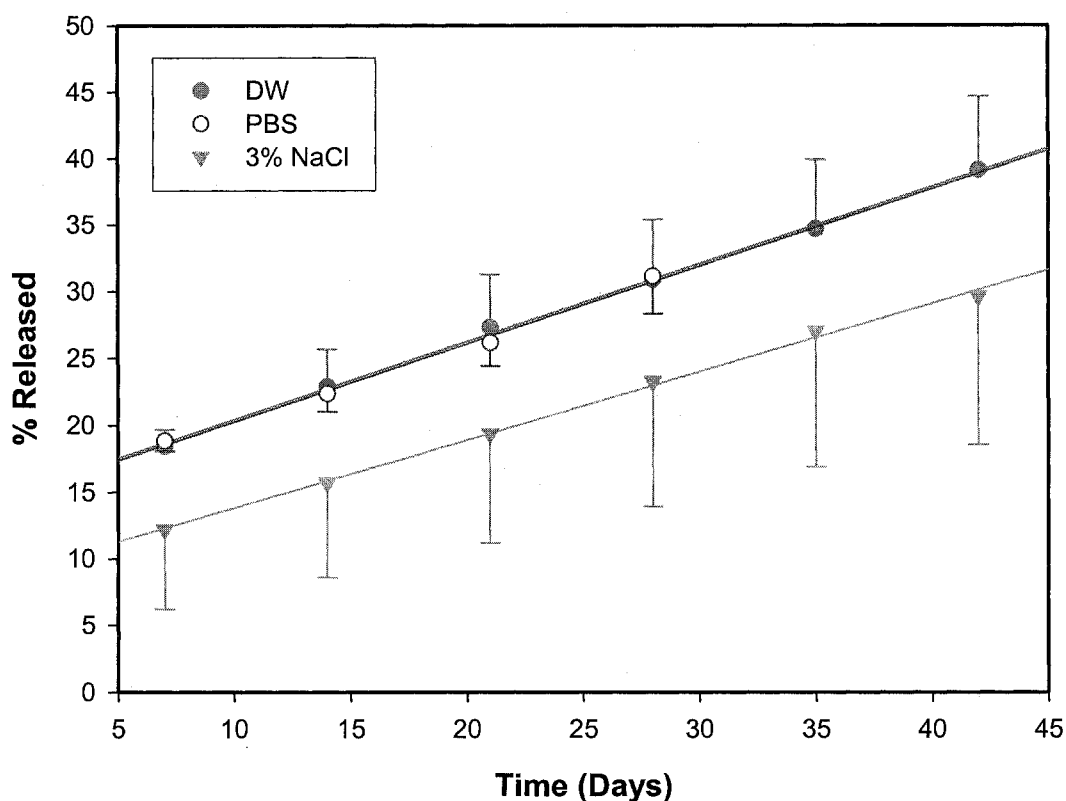


Figure 4.6 Regression of the data obtained during the linear release phase (7-42 days) from 5% v/v cylinders of 1 cm length.

One goal of the development of this system was the delivery of protein drugs. Since most proteins cannot be loaded at high volume fractions, pore-forming agents of high osmotic

activity have been used in many cases when the protein does not have enough osmotic activity to elicit the required capsule fracture or when a complete release of the loaded fraction was needed.[2,6,8] In addition, in order to be incorporated as solid particles most proteins need to be lyophilized with stabilizing agents like sugars (e.g. mannitol, trehalose) which also possess high osmotic activity. For this reason it was decided to load the cylinders with 1:1 intimately mixed PCN and trehalose particles at a total volume fraction of 5% v/v.

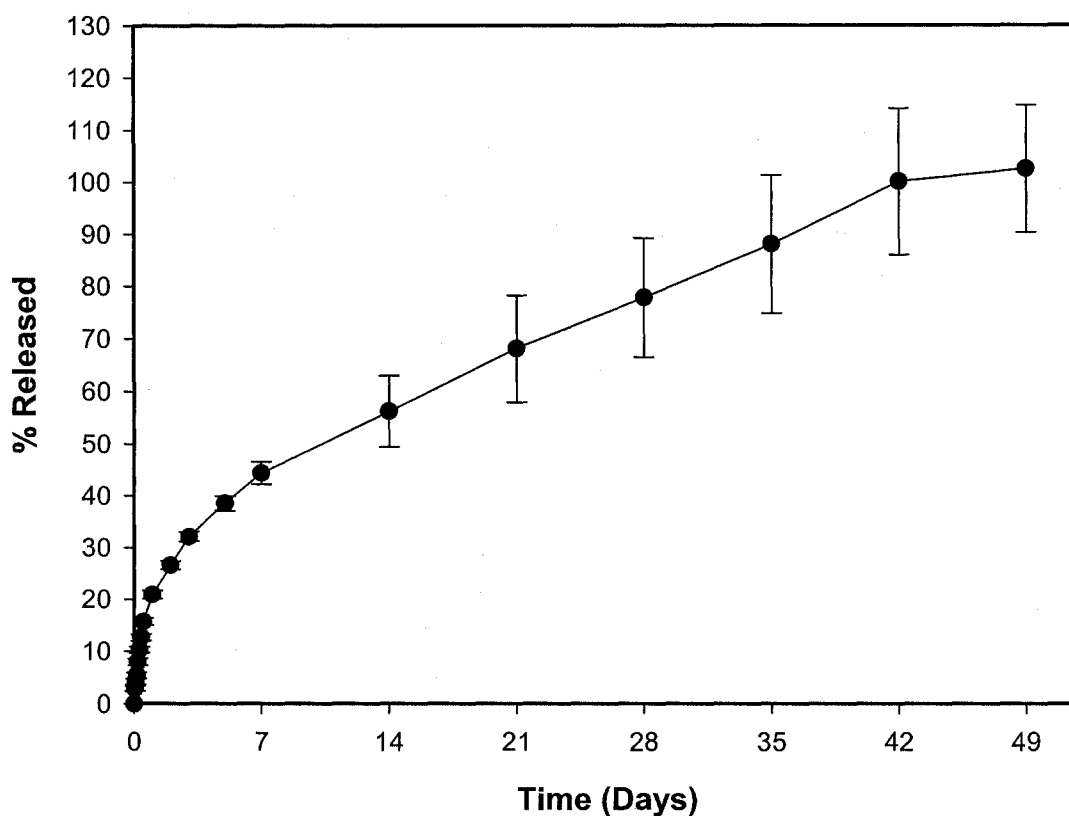


Figure 4.7 Cumulative percent PCN released for 5% v/v of 1:1 intimately mixed PCN and trehalose in PBS of pH=7.4.(1 cm length). Values are means of 4 samples \pm standard deviation.

Figure 4.7 shows the release profile for this system in PBS at pH 7.4. The addition of the

more osmotic trehalose produced a much faster release in all phases with a disappearance of the third, degradation controlled, phase of release. The fact that a percent released above 100 was detected for some samples could be attributed to a minor interference of trehalose with the UV detection of PCN. A larger fraction of PCN (30-40%) is released during the initially rapid release phase after which the release becomes constant and slower in rate until essentially complete release of PCN is achieved. Based on this result, it is evident that the osmotic release mechanism is now playing a dominant role in the release mechanism since the incorporation of the more osmotic trehalose enhanced the release rate in the initial period and a constant release was observed until all the PCN loaded was released. The release rate during this linear phase was approximately two-three times faster in this system compared to the release profiles when PCN alone was incorporated as indicated by its higher slope value in PBS, 1.61 versus 0.58 percent released per day (Figure 4.8 and Table 4.2).

The release behaviour of PCN from this degradable elastomer appears to be more complex than just osmotically controlled. The geometry of the delivery device must also play a role, because one would expect to find more particles near the surface of the cylinder than near the centre, and so release should slow down with time, yet the release becomes linear. This must be due to polymer degradation taking place during the release process.

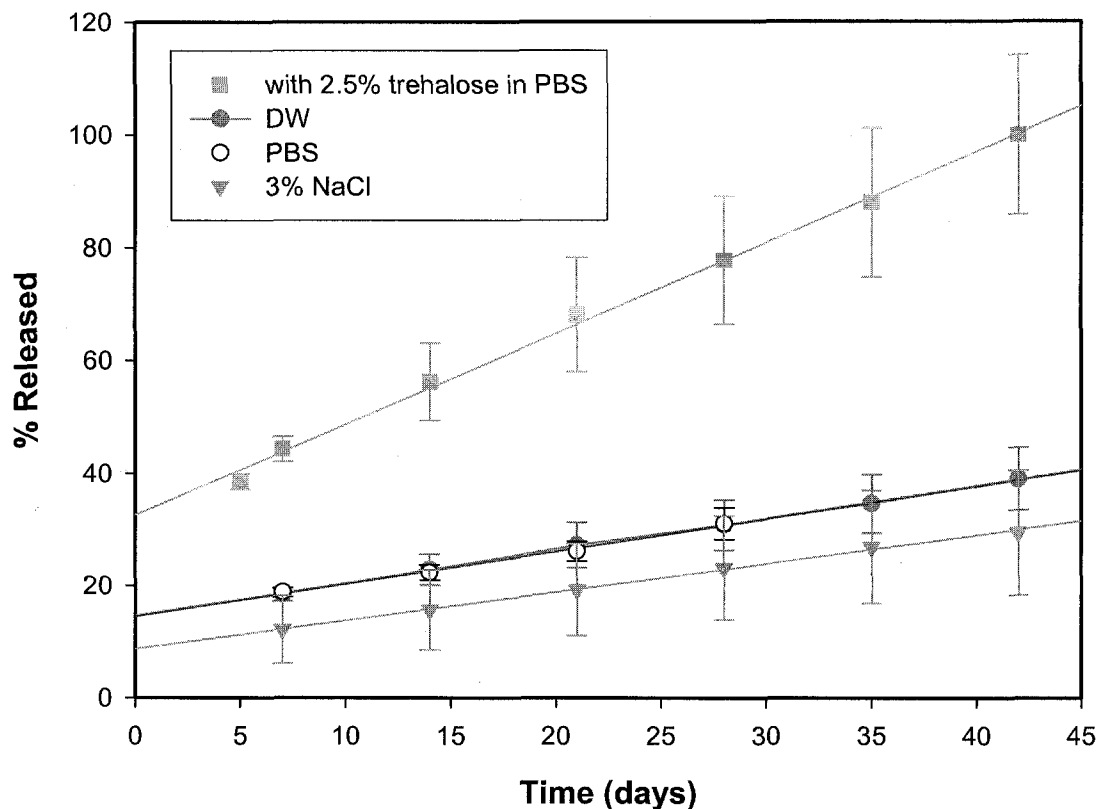


Figure 4.8 Regression fitting for the data obtained during the linear release phase (7-42 days) from 5% v/v cylinders of 1 cm length in comparison with the linear phase (5-42 days) from 5% v/v loaded cylinders of 1 cm length of 1:1 intimately mixed PCN and trehalose.

4.4. Conclusions

The release mechanism of pilocarpine nitrate of 5% v/v loadings from monolithic cylinders of a newly synthesised elastomer was demonstrated. The release rate was distinguished by three release stages in which the second linear release phase was mainly dominated by a non-osmotic mechanism. This linear phase of release was extended while its degradation related release was eliminated by co-formulating the drug with the high

osmotically active agent, trehalose. Upon using this excipient, a large fraction of pilocarpine nitrate was released during the initially rapid release phase after which the release becoming linear and slower in rate until essentially complete release of pilocarpine nitrate. In this situation, osmotic release mechanism was the dominant mechanism that contributed to that enhancement in the drug release.

4.5. References

- [1] B. G. Amsden, Osmotically activated agent release from electrostatically generated polymer microbeads, *AIChE J.* 42 (1996) 3253-3266.
- [2] V. Carelli, G. Di Colo, C. Guerrini, E. Nannipieri, Drug release from silicone elastomer through controlled polymer cracking: an extension to macromolecular drugs., *Int. J. Pharm.* 50 (1989) 181-188.
- [3] R. F. Fedors, Osmotic effects in water absorption by polymers, *Polymer* 21 (1980) 207-212.
- [4] R. Gale, S. K. Chandrasekaran, D. Swanson, J. Wright, Use of osmotically active therapeutic agents in monolithic systems., *J. Memb. Sci* 7 (1980) 319-331.
- [5] A. S. Michaels, S. Guillod, Osmotic bursting drug delivery device, U.S. Patent 4,177,256
- [6] B. Amsden, Y-L. Cheng, A generic protein delivery system based on osmotically rupturable monoliths, *J. Control. Rel.* 33 (1995) 99-105.

- [7] N. F. Sheppard, M. Y. Madrid, R. Langer, Polymer matrix controlled release systems: Influence of polymer carrier and temperature on water uptake and protein release., *J. Appl. Polym. Sci.* 46 (1992) 19-26.
- [8] B. G. Amsden, Y-L. Cheng, M. F. A. Goosen, A mechanistic study of the release of osmotic agents from polymeric monoliths., *J. Control. Rel.* 30 (1994) 45-56.
- [9] R. Schirrer, P. Thepin, Water absorption, swelling, rupture and salt release in salt-silicone rubber compounds, *J. Mater. Sci.* 27 (1992) 3424-3434.
- [10] J. Wright, S. K. Chandrasekaran, R. Gale, D. Swanson, A Model for the release of osmotically active agents from monolithic polymeric matrices., *AIChE Symp. Ser.* 77 (1981) 62-68.
- [11] D. S. T. Hsieh, Y. W. Chien, Enhanced release of drugs from silicone elastomers. Part 2. Induction of swelling and changes in microstructure, *Drug Dev. Ind. Pharm.* 11 (1985) 1411-1432.
- [12] M. Kajihara, T. Sugie, M. Mizuno, N. Tamura, A. Sano, K. Fujioka, Y. Kashiwazaki, T. Yamaoka, S. Sugawara, Y. Urabe, Development of new drug delivery system for protein drugs using silicone (I), *J. Control. Rel.* 66 (2000) 49-61.
- [13] M. Kajihara, T. Sugie, T. Hojo, H. Maeda, A. Sano, Fujioka, K, S. Sugawara, Y. Urabe, Development of a new drug delivery system for protein drugs using silicone (II), *J. Control. Rel.* 73 (2001) 279-291.

- [14] V. Carelli, G. Di Colo, E. Nannipieri, Effect of water-soluble additives on drug release from silicone-rubber matrices. III. A study of release mechanism by differential scanning calorimetry, *Int. J. Pharm.* 30 (1986) 9-16.
- [15] G. Di Colo, V. Carelli, E. Nannipieri, M. F. Serafini, D. Vitale, Effect of water-soluble additives on drug release from silicone rubber matrices. II. Sustained release of prednisolone from non-swelling devices., *Int. J. Pharm.* 30 (1986) 1-7.
- [16] V. Carelli, G. DiColo, E. Nannipieri, Factors in zero-order release of clonidine hydrochloride from monolithic polydimethylsiloxane matrices, *Int. J. Pharm.* 35 (1987) 21-28.
- [17] B. G. Amsden, Y-L. Cheng, Enhanced fraction releasable above percolation threshold from monoliths containing osmotic excipients, *J. Control. Rel.* 31 (1994) 21-32.
- [18] H. M. Younes, B. G. Amsden, Synthesis, characterization, and in vitro degradation of photo-crosslinked biodegradable elastomers, *Biomacromolecules* (2002) submitted.
- [19] H. M. Younes, B. G. Amsden, Synthesis, characterization and in vitro degradation of a biodegradable elastomer, *Biomacromolecules* (2002) submitted.
- [20] J. A. Hubbell, C. P. Pathak, A. S. Sawhney, N. P. Desai, J. L. Hill, Photopolymerizable biodegradable hydrogels as tissue contacting materials and controlled-release carriers, U.S. Patent 5,410,016, April 25, 1995

- [21] W. M. Saltzman, R. Langer, Transport rates of proteins in porous materials with known microgeometry., *Biophys. J.* 55 (1989) 163-171.
- [22] R. A. Siegel, R. Langer, Mechanistic studies of macromolecular drug release from macroporous polymers.2. models for the slow kinetics of drug release., *J. Control. Rel.* 14 (1990) 153-167.

CHAPTER 5

OSMOTIC RELEASE DELIVERY AND ACTIVITY ASSESSEMENT OF INTERFERON- γ FROM A NEW BIODEGRADABLE ELASTOMER

Husam M. Younes ¹, Ayman O. El-Kadi ¹ and Brian G. Amsden ^{1,2}

A version of this chapter has been submitted to *Pharmaceutical Research*

1. Faculty of Pharmacy and Pharmaceutical Science, University of Alberta, Edmonton, Alberta, Canada T6G 2N8
2. Department of Chemical Engineering, Queens University, Kingston, Ontario, Canada, K7L 3N6

5.1. Introduction

Interferon- γ (IFN- γ) which is also known as immune or type II interferon has several applications in the treatment of a number of immunological, viral and neoplastic diseases (1-3). It is currently FDA approved for reducing the frequency and severity of serious infections associated with chronic granulomatous disease and for delaying time to disease progression in patients with severe, malignant osteopetrosis (4,5).

Although IFN- γ has been extensively investigated for this broad range of indications, it possesses properties which have limited its clinical use. Systemic delivery, which is the major route used to administer this interferon, of high concentrations yields significant side effects and toxicities. Some of those side effects but not all include fever, fatigue, nausea, vomiting, neurotoxicity, and leucopenia (6,7). Recently, we demonstrated that in certain instances, such as in cancer immunotherapy, it is desirable to have a localized and continuous delivery of a cytokine to maintain safer and more efficient clinical outcome (8). For this reason, different strategies have been explored to formulate and deliver IFN- γ while at the same time trying to achieve two major goals. The first is to deliver and target IFNs specifically and safely to their site of action to maximize their therapeutic efficacy while minimizing their toxicity. The other is to overcome stability issues during the preparation of dosage forms containing these cytokines, and to help in maintaining this stability during storage of the dosage form and after administration to the body.

Various means of achieving localized delivery of IFN- γ have been investigated and

include the use of liposomes and biodegradable microspheres (9-11). Liposomes have the distinct advantage of easy administration by injection. However, they also have distinct disadvantages. They produce relatively short drug release durations necessitating additional painful injections, and release rates are neither sustained nor controllable. Thus, they do not appear to be optimal for sustained, local delivery. A detailed description of IFN- γ liposomal drug delivery systems and their merits and demerits are reported elsewhere (8).

Polymeric microspheres have also been developed which are capable of delivering a virtually constant amount of an encapsulated protein. These formulations typically consist of a biodegradable polymer, poly (lactide-co-glycolide) (PLG), throughout which the protein is distributed as discrete solid particles. The protein is released in three phases: an initial burst; diffusion controlled release; and erosion controlled release. The initial burst is due to surface resident protein particles, while the diffusion controlled release is a result of dissolved protein diffusing through the water-filled pores and channels within the microspheres (10,11).

The problems of using the PLG microspheres formulation involve both acidic protein degradation, and denaturation at an organic solvent-water interface. When polymers such as PLG degrade, they liberate oligomers and monomers carrying carboxylic acid end groups. The presence of these oligomers and monomers has been found to decrease the local pH at the surface of the polymer and in the pores and channels of the device (12,13). In fact, a recent work has measured the pH at the centre of PLG microspheres to be as

low as 1.5 (14). At this pH, IFN- γ is certain to undergo cleavage and deactivation. This reduction in the pH of the inner environment of the microspheres has been linked to inactivation and denaturation of other proteins within PLG microspheres prior to being released (14). In addition, the protein-loaded microspheres are typically prepared using a water-in oil-in water (w/o/w) emulsification procedure in which the protein is dissolved in the aqueous phase. This preparation procedure has also been found to result in protein denaturation due to contact of the protein with the polymer solvent at the solvent-water interface (15).

There is one report in which rhIFN- γ has been incorporated into PLG microspheres and its stability after release studied (16). These researchers examined the effects of microsphere preparation by w/o/w emulsion, buffer pH and buffer system on the release of IFN- γ . Using this emulsion procedure they successfully incorporated 100 % of the rhIFN- γ in the PLG microspheres. The stability of the cytokine was maintained during the fabrication procedure through the use of trehalose in the aqueous phase. However, they found that, although rhIFN- γ was stable after microspheres preparation and it was released for up to 50 days, after 7 days the released rhIFN- γ only had an activity of 30-38 %. Thus, maintaining stability of IFN- γ within PLG microspheres is still a problem.

In an attempt to solve these stability problems with IFN- γ , an elastomeric drug delivery vehicle has been developed which utilizes osmotic activity as the drug delivery driving force (17). The biodegradable elastomeric system was designed in a way that no significant changes in its mechanical properties would take place until the majority of the

dispersed drug had been released. IFN- γ was incorporated into a polymer solution as solid particles as an intimate mixture with trehalose, and the system solidified into an elastomeric drug matrix by photocuring using ultra-violet light. IFN- γ was intimately mixed with trehalose by lyophilization to achieve two goals. First, trehalose will act as a stabilizing agent for IFN- γ (18). Second, its intimate presence with IFN- γ as dispersed powder would extend the steady-state release period in the delivery system as has been reported previously.(17)

5.2. Materials and Methods

5.2.1. Materials

D, L-lactide was obtained from Purac (The Netherlands) while ϵ -caprolactone was purchased from Lancaster and then dried over CaH_2 (Aldrich). Other chemicals used in the synthesis of the star copolymer prepolymer were 2-ethylhexanoate (Aldrich), and glycerol (BDH). The chemicals used in the synthesis of the acrylated star copolymer prepolymer include acryloyl chloride, triethylamine, and 4-dimethyl aminopyridine, which were all obtained from Aldrich. Other chemicals used include dichloromethane (Fisher), hexane and ethyl acetate which were obtained from BDH. The long-wave UV (LWUV) initiator 2, 2-dimethoxy-2-phenyl-acetophenone was obtained from Aldrich. D (+) trehalose and pilocarpine nitrate salt were obtained from Sigma. The osmolality standards of 100, 290 and 1000 mmol/kg were all purchased from Wescor Company. Recombinant murine interferon-gamma (greater than 98% purity) was purchased from

Peptotech Canada Inc. Fetal bovine albumin, Dulbecco's phosphate buffer saline, Dulbecco's modified eagle medium, non-essential amino acids, penicillin, streptomycin, gentamycin, and trypsin were obtained from Invitrogen Canada Inc. Sodium bicarbonate was obtained from BDH while glucose, HEPES, pyruvate solution, lipoic acid, L-Glutamine, vitamin B12 solution and Lipopolysaccharide (LPS) was purchased from sigma. Vitamin supplement solution and amphotericin B were obtained from ICN Canada. Zinc sulphate was obtained from Anachemica. Recombinant murine IFN- γ ELISA kit was purchased from Amersham Pharmacia Biotech. Materials used in preparing Griess reagent include N-(1-Naphthyl) ethylenediamine dihydrochloride, sulphanilamide, 85 % phosphoric acid and sodium nitrite were obtained from Aldrich. Materials used in protein content analysis include copper sulphate purchased from ICN. Sodium potassium tartarate and anhydrous sodium carbonate were purchased from Fisher. Folin-phenol reagent was purchased from sigma.

5.2.2. Preparation of poly (ϵ -caprolactone-co-D, L-lactide) (ϵ -CL/DLLA) Star Copolymer (SCP)

The detailed method of preparation and the full structural characterization of the SCP prepolymer were reported elsewhere (19). In summary, into a dry silanized ampoule, 1.7×10^{-3} mol of glycerol and 0.05 mol of ϵ -CL were transferred and mixed till homogeneous. An amount equivalent to 0.05 mol of DL-LA was then transferred to the ampoule, the ampoule filled with nitrogen, then placed in an oven at 120 °C for 10 minutes allowing the DL-LA to melt. The mix was then stirred using a vortex mixer and

2-ethylhexanoate (SnOct) was added in an amount equivalent to $1.4 (10)^{-4}$ mol for each 1 mol of the monomer. The ampoule was filled with nitrogen, flame sealed under vacuum, and left in an oven at 140 °C for 18 hours. The prepared SCP was then purified by precipitation from dichloromethane (DCM) solution into cold methanol

5.2.3. Preparation of Acrylated SCP

The method of Hubbell, with minor modification was used (20). In summary, in a round bottom flask, 20 g of SCP ($2.56 (10)^{-3}$ mole) was dissolved in 200 ml of DCM on a magnetic stirrer using a magnetic bar. The flask was sealed using a rubber septum and flushed with argon. This step was repeated every hour. The flask was then immersed in a 0 °C ice bath, after which 10 mg of 4-dimethyl aminopyridine was added as a catalyst. A stepwise addition of $7.66 (10)^{-3}$ mol of each of acryloyl chloride and triethylamine was followed over a period of 12 hours at 0 °C. The reaction was later continued at room temperature for another 12 hours. The reaction completion was detected using TLC and the final solution was filtered to remove triethylamine hydrochloride salt formed during the reaction. The polymer solution was concentrated using a rotary evaporator and further purified by precipitation in ethyl acetate. FT-IR, $^1\text{H-NMR}$ and $^{13}\text{C-NMR}$ were used to characterize the purity of the final product and the disappearance of OH groups as a result of the formation of the terminal vinyl groups.

5.2.4. Lyophilization of Protein with Excipient

Trehalose was lyophilized with interferon at a ratio of 1:1 w/w trehalose: interferon using 5 mM succinate buffer adjusted at pH of 5.5. To prepare the lyophilized protein, the excipient was added as a solid to aliquots of the protein solution and stirred gently at room temperature until dissolved. The solution was then filtered with a 0.22 μm low protein binding filter to remove any particulates. The filtered solution was subjected to a cycle of freezing to $-55\text{ }^{\circ}\text{C}$ in dry ice, primary drying at $-10\text{ }^{\circ}\text{C}$ and 120 mTorr for 24 hours, followed by secondary drying at $5\text{ }^{\circ}\text{C}$ and 120 mTorr for 12 hours to obtain the dried lyophilized product.

5.2.5. Preparation of Drug Loaded Elastomer

To provide good encapsulation efficiencies, a suspension of the lyophilized protein/excipient solids, which had been sieved to $< 20\text{ }\mu\text{m}$, was prepared in a solution of polymer and dichloromethane containing the photo-initiator (0.25 g of SCP + 250 μl of DCM + 12.5 μl of 30% w/v of 2,2-dimethoxy-2-phenyl-acetophenone in DCM). This suspension was poured into glass cylindrical moulds of 1mm diameter and 10 mm length capped at each end, and then exposed to UV radiation for 1-2 minutes, to crosslink the elastomer. After crosslinking, the glass cylinder was broken and the drug-loaded cylinder removed. To avoid any settling of the protein particles, the amount of dichloromethane added was kept to the minimal amount required. The small size of the protein particles also assisted in retarding the settling rate. The protein content in each elastomeric cylinder was calculated based on % v/v and further confirmed using weight calculations.

5.2.6. In Vitro release study

The prepared monolith cylinders loaded with lyophilized rmIFN- γ were subjected to *in vitro* release studies using PBS of pH 7.4 as release medium. Each of the triplicate samples was put into a 4 ml scintillation vials filled with 3 ml of the dissolution medium. The vials were attached to a Glas-Col rugged culture rotator. The rotator was set at 30% rotation speed and placed in an oven at 37 °C. The receptor release medium was replaced with fresh medium every sampling time to ensure sink conditions and constant osmotic pressure driving force. Solutions collected were divided into aliquots, frozen at -80 °C for subsequent cytokine activity using cell cultures of BV-2 cells and concentration analysis using a rmIFN- γ ELISA system.

5.2.7. Cell lines and culture

BV-2 immortalized murine Microglial cell line was provided by Dr. J. Madrenas, University of Western Ontario, London, Ontario, Canada. Using sterile cell culture flasks, the cells were cultured in Dulbecco's modified eagle medium (DMEM) supplemented with 5% fetal bovine serum (FBS), 2 mM L-glutamine, 2.5 μ g/ml amphotericin B, and 50 μ g/ml gentamycin in a humidified incubator in 5% CO₂ at 37 °C. Before culturing into 12- well sterile culture plates, they were trypsinized, washed in PBS and re-suspended in DMEM containing 5% FBS. From this stock, 1 ml was transferred into each well of the 3x4 culture plate which was incubated for 24 hours in a humidified incubator in 5% CO₂ at 37 °C. The medium in the culture plate was then discarded, each well washed with PBS and 1 ml of serum free DMEM was transferred into each well of

the plate. Each treatment was added on 6 wells while the 6 other wells were left untreated as blank. The plates were then incubated in a humidified incubator in 5% CO₂ at 37 °C for 24 hours and then analysed for their nitrite and protein content.

5.2.8. Nitrite assay and protein analysis

The amount of nitrite converted from NO released in the culture medium as a result of the stimulation of BV-2 cells was determined by Griess method. Using 96-well plates, each well was filled with 100 µl of the culture medium mixed with an equal volume of Griess reagent. After 10 minutes of incubation at room temperature, the optical density of the samples was measured using v_{max} kinetic microplate (Molecular Devices) reader at 560 nm. Culture medium processed through the same steps but with no treatment was used as the blank in all the experiments.

Protein content in the culture medium was analysed following Lowry method using folin phenol reagent (21).

5.3. Results and Discussion

The main problem with the delivery of peptides and proteins is to maintain their stability before, during and after their release. The activity of a protein molecule is determined by its conformation in solution. Proteins are susceptible to aggregation, denaturation and adsorption at interfaces, deamidation, isomerization, cleavage, oxidation, thiol disulfide

exchange, and β elimination in aqueous solutions. The major factors affecting these changes are mechanical forces such as shear, the presence of surfactants, buffers, ionic strength, the presence of oxidizers such as ions, radicals and peroxide, light, pH and temperature. Thus, protein denaturation may result in a loss of potency and the conformation changes in the protein molecule may make the protein immunogenic (22).

IFN- γ possesses a number of stability problems. Firstly, IFN- γ is a prime candidate for acid degradation. It contains an acid-labile group (Asp-Pro bond at positions 2 and 3), which is broken at pH 2.3 with subsequent loss of activity. Furthermore, IFN- γ , as are many recombinant proteins, is particularly susceptible to aggregation when present in relatively high concentration in solution. This is because that when it was produced through genetically engineered bacteria, post-translational glycosylation of the protein molecule does not take place (23). Various means of stabilizing proteins in solution have been determined. These include the addition of compounds such as polyols, inorganic salts, and amino acids (24).

In our previous work, we demonstrated the osmotic release mechanism for water soluble drugs from a new biodegradable photo-crosslinked elastomer. It has also been found that many protein drugs require only very low doses to elicit therapeutic effects. For example, only few picograms per day of epidermal growth factor are required to induce tissue regeneration (25). Therefore, such proteins were often co-formulated with other water soluble excipients to increase the fraction releasable of the drug without significantly increasing the release rate (26). For this reason, trehalose was lyophilized with rmIFN- γ

at a ratio of 1:1 w/w trehalose: interferon using succinate buffer adjusted at pH of 5.5. The use of trehalose with IFN- γ in this study would offer the maximum stabilizing effect offered by this sugar (18) and it also acts as an osmotically active pore-forming agent that helps in extending the steady-state release period before any significant degradation to the polymer takes place, as has been previously reported (8). The loading of IFN- γ incorporated into the elastomeric cylinders was calculated to be 0.5 % v/v which was equivalent to 55 μ g of rmIFN- γ per each cylinder.

In an attempt to determine the activity of IFN- γ , it was cultured with BV-2 Microglial cells. The stimulatory effect of IFN- γ on these cells results in the induction of nitric oxide synthase (iNOS) enzyme with a subsequent release of NO which is converted to nitrites that can be detected and analysed (27-29). Figure 5.1 shows a plot of the molar concentration of NO released per mg of protein in the treated culture medium. Lipopolysaccharide (LPS) was used as a positive control that is well known to stimulate NO production in BV-2 cells (29). As for the rmIFN- γ induction effect, the Figure shows a highly significant NO stimulatory activity on BV-2 cells with all the used concentrations compared to the control. The reason that there was no significant difference in the activity of between those treated with a 100 ng/ml and 20 ng/ml is that IFN- γ effect is dose-dependent. In other words, after a certain dose, a maximal IFN- γ -induced production of NO is reached after which no further significant increase will take place (28). It is also shown in Figure 5.1 that the lowest concentration of rmIFN- γ used (2 ng/ml) showed a significant activity (4 fold higher) when compared to the control.

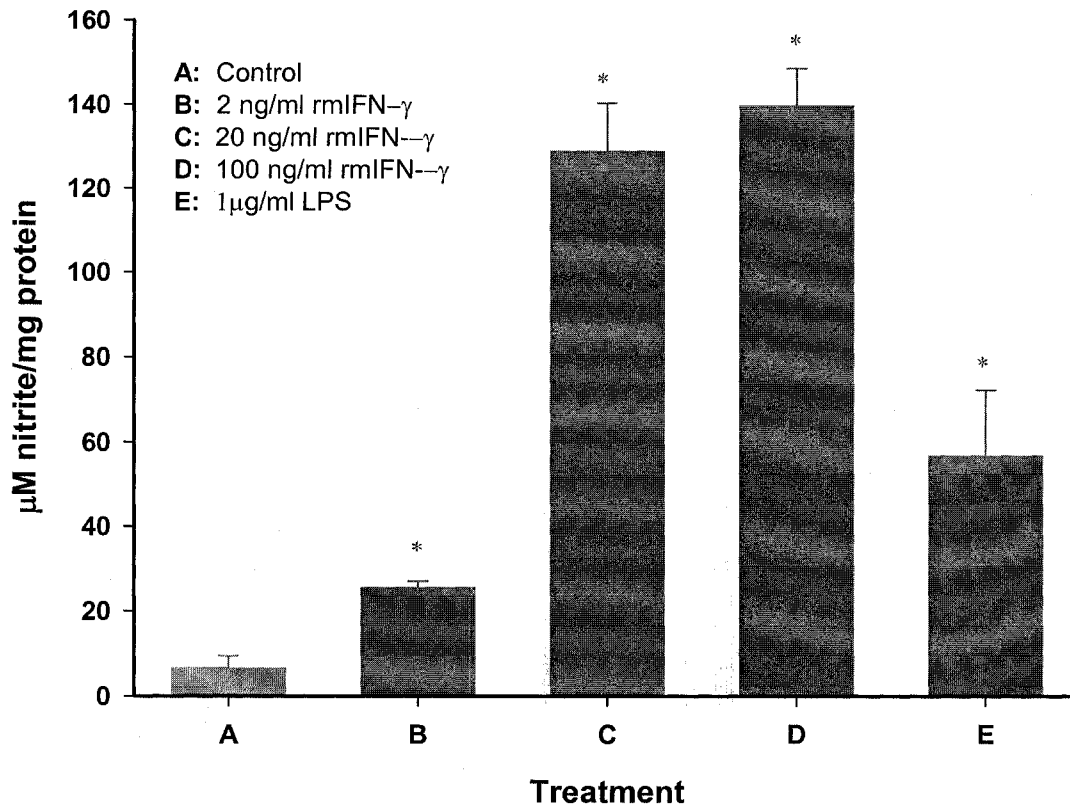


Figure 5.1 Nitrite concentration detected in culture medium of BV-2 Microglial cell. Cultures were incubated for 24 hours with various concentrations of rmIFN- γ , or LPS. Data are means \pm SEM from 6 cell cultures. * $p < 0.05$ compared to control

The demonstrated sensitivity of the BV-2 Microglial cells to the stimulatory effect resulting from using different concentrations of rmIFN- γ was further used as a tool to determine whether any changes in the activity of this cytokine were taking place during the preparation steps involved in loading the drug into the delivery system. As shown in Figure 5.2, there was a significant difference between the activities of rmIFN- γ in all the preparation steps and the control. This result indicates that rmIFN- γ maintained its activity before and after its lyophilization with trehalose in 5 mM succinate buffer of pH

5.5. It was also noted that this lyophilization process of rmIFN- γ with trehalose resulted in a more stable formulation compared to the non-lyophilized batch. Trehalose contributed in maintaining the biological activity of the lyophilized rmIFN- γ even after storing aliquots of the cytokine frozen at -80 °C for 3 days.

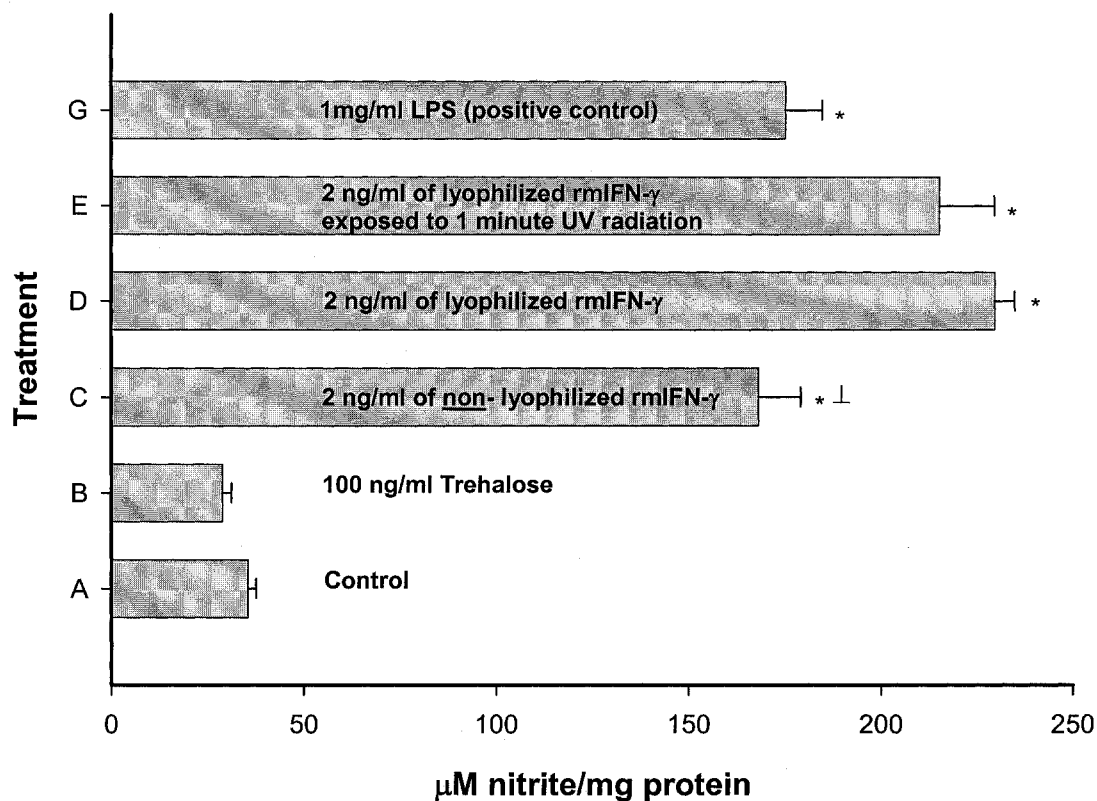


Figure 5.2 Nitrite concentration detected in culture medium of BV-2 Microglial cell. Cultures were incubated for 24 hours with 2 ng/ml rmIFN- γ during different preparation steps. LPS was used as a positive control. Data are means \pm SEM from 6 cell cultures. * $p < 0.05$ compared to control. *⊥ $p < 0.05$ compared to lyophilized rmIFN- γ .

As a means of simulating the conditions to which rmIFN- γ will be exposed upon being loaded into the biodegradable elastomer, a lyophilized sample of the rmIFN- γ was used as a treatment after being exposed to UV rays for 1-2 minutes and its activity in BV-2 cell

cultures was tested. As shown in Figure 5.2, there was no significant difference between the activity before and after exposure to UV light. This indicates that the rmIFN- γ is stable and active even after its suspension into the prepared cylinders of the biodegradable elastomer.

The release of rmIFN- γ from the cylinders was determined by a release study in PBS at 37 °C. The samples collected at different time intervals were divided into aliquots and stored at -80 °C for later activity and concentration analysis. It is important to mention here that a pilot stability study for a known concentration of rmIFN- γ was undertaken to see if any changes in its activity would take place in PBS at 37 °C over a period of 24 hours. The results showed no significant change in its measured activity in BV-2 culture over that period for all the samples collected.

Figure 5.3 illustrates the activity of the released rmIFN- γ for samples collected over a period of 23 days. The released rmIFN- γ maintained its activity for up to 15 days after which a loss of its activity took place. This loss in activity is most likely attributable to aggregation of the cytokine after this period of time. The freezing-thawing cycle might also have a role in the process since the sample collected was kept for almost one month before analysis. A parallel test of the amount of rmIFN- γ released was also carried out in the release medium. Figure 5.4 shows the release profile for rmIFN- γ detected in PBS using ELISA method of analysis.

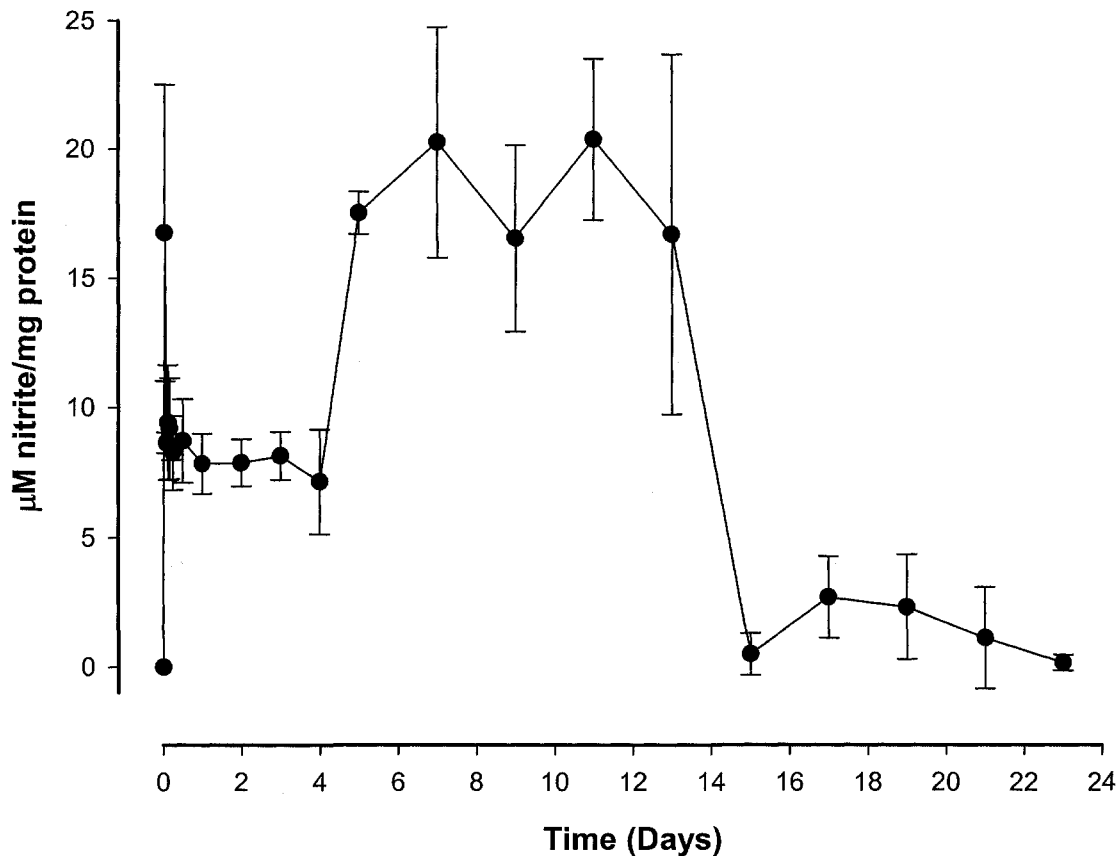


Figure 5.3 Nitrite concentration detected in culture medium of BV-2 Microglial cell. Cultures were incubated for 24 hours with the released rmIFN- γ at different time intervals.

The data indicates that a constant sustained release of IFN was achieved. However, the release rate was quite low, and slower compared to what has been shown earlier with our studies using pilocarpine nitrate (17). This result is attributed to the fact that the loading of the protein in this case (0.5% v/v) was very low and therefore the particles of protein dispersed in the matrix were less interconnected with each other when compared to the case of the more highly loaded pilocarpine nitrate. Other factors that might also contribute to this observation is denaturation and/or aggregation of the cytokine which

render it insoluble and therefore slows down the osmotic release mechanism and results in blockage of the formed interconnected pores (30). Since the activity of the protein was nearly eliminated after 15 days of its release, it was decided to stop the activity study at this point.

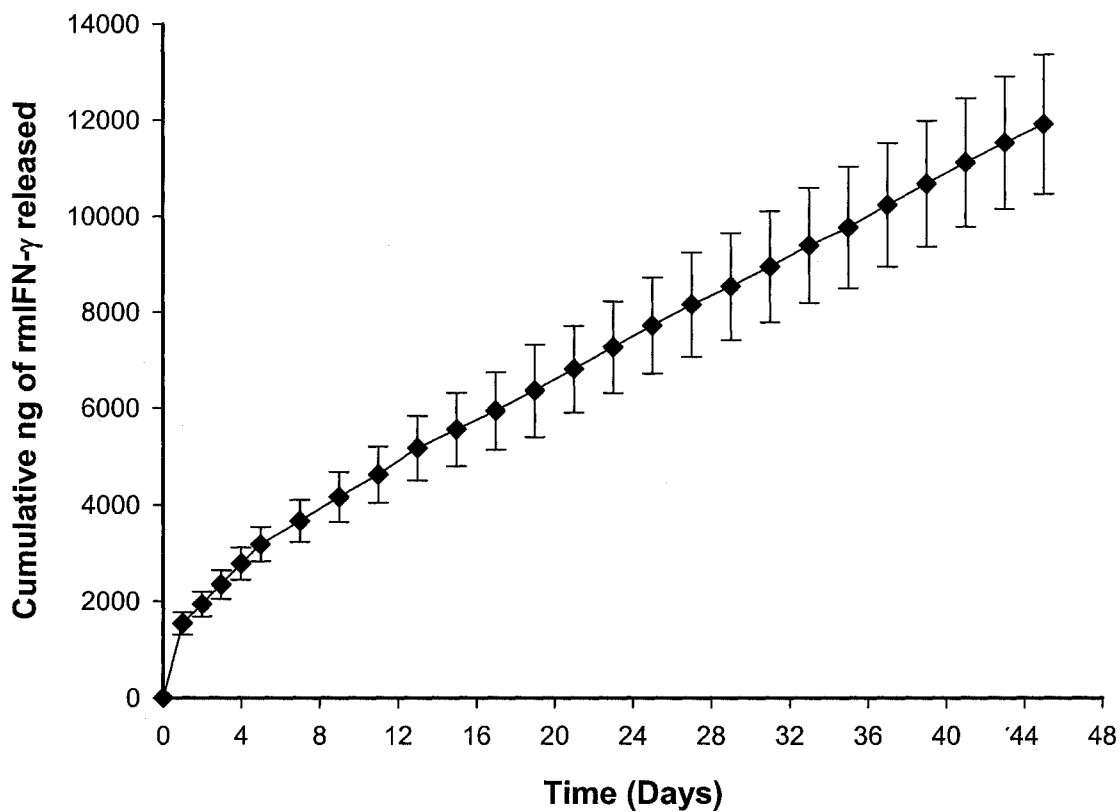


Figure 5.4 Cumulative amount of rmIFN- γ released in PBS medium at 37 °C detected using ELISA assay from stored frozen aliquots. Cylinders are of 1 mm diameter and 10 mm length with 0.5 % v/v rmIFN- γ loading. Values are mean \pm SD of cumulative data.

Figure 5.5 demonstrates that a good correlation was established between the percent of rmIFN- γ released and its corresponding stimulatory effect on the BV-2 cells represented by the cumulative nitrite detected in the cell cultures. This correlation was almost linear

for up to 15 days after which a loss of the cytokine activity was observed. This result demonstrates that the amount released during the first two weeks was active and in its activity was directly proportional to the amount released. A future study for the conformational changes and possible aggregates formation of rmIFN- γ in the frozen samples is required which would clarify this issue.

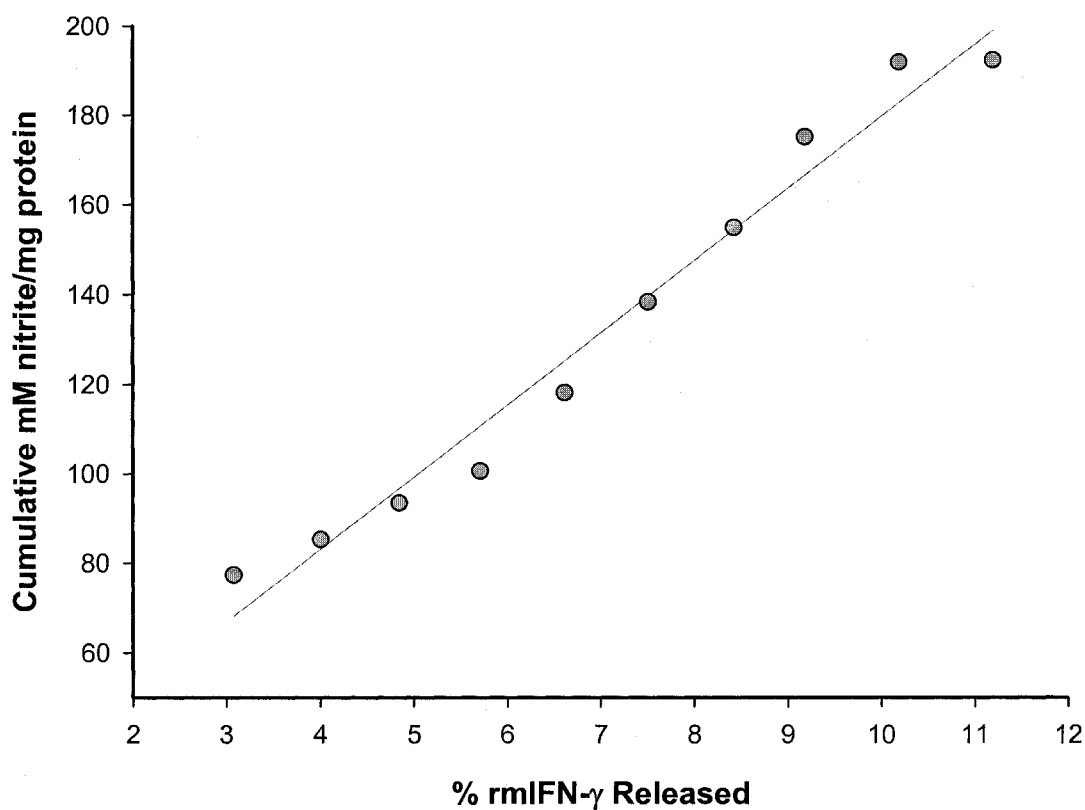


Figure 5.5 Correlation between the percentage cumulative amount released of rmIFN- γ and the cumulative activity detected between 1 to 15 days period of release ($r^2=0.974$).

5.4. Conclusions

A new delivery vehicle composed of a biodegradable elastomer was developed for protein delivery and demonstrated to be effective in delivering active IFN- γ for in a

constant and sustained release fashion. More work needs to be done to determine if the loss of stability of IFN- γ after a two week delivery period was due to the storage conditions, or from degradation in the device. A future study of the conformational changes of rmIFN- γ and its subsequent aggregates using circular dichroism and gel permeation chromatography is a future work. This sort of investigation for the structural changes would give a clearer picture of how and what made this cytokine lose its activity after this period of time.

5.5. References

1. R. M. Stone, D. R. Spriggs, K. A. Arthur, R. J. Mayer, J. Griffin, and D. W. Kufe. Recombinant human gamma interferon administered by continuous intravenous infusion in acute myelogenous leukemia and myelodysplastic syndromes, *Am. J. Clin. Oncol.* **16**: 159-163 (1993).
2. V. H. Gressler, R. E. Weinkauff, W. A. Franklin, and H. M. Golomb. Is there a direct differentiation-inducing effect of human recombinant interferon on hairy cell leukemia in vitro?, *Cancer* **64**: 374-378 (1989).
3. C. F. Nathan, G. Kaplan, W. R. Levis, A. Nusrat, M. D. Witmer, S. A. Sherwin, C. K. Job, C. R. Horowitz, R. M. Steinman, and Z. A. Cohn. Local and systemic effects of intradermal recombinant interferon-gamma in patients with lepromatous leprosy, *N. Engl. J. Med.* **315**: 6-15 (1986).

4. D. Conte, M. Fraquelli, F. Capsoni, M. Giacca, L. Zentilin, and M. T. Bardella. Effectiveness of IFN-gamma for liver abscesses in chronic granulomatous disease, *J. Interferon Cytokine Res.* **19**: 705-710 (1999).
5. L. Shankar, E. J. A. Gerritsen, and L. L. Key. Osteopetrosis: pathogenesis and rationale for the use of interferon-gamma-1b, *Biodrugs* **7**: 23-29 (1997).
6. A. K. Thom, D. L. Fraker, J. K. Taubenberger, and J. A. Norton. Effective regional therapy of experimental cancer with paralesional administration of tumour necrosis factor-alpha + interferon-gamma, *Surg. Oncol.* **1**: 291-298 (1992).
7. J. R. Quesada, M. Talpaz, A. Rios, R. Kurzrock, and J. U. Gutterman. Clinical toxicity of interferons in cancer patients: a review, *J. Clin. Oncol.* **4**: 234-243 (1986).
8. H. M. Younes and B. G. Amsden. Interferon-gamma therapy: Evaluation of routes of administration and delivery systems, *J. Pharm. Sci.* **91**: 2-17 (2002).
9. M. L. Van Slooten, G. Storm, A. Zoepfel, Z. Kupcu, O. Boerman, D. J. A. Crommelin, E. Wagner, and R. Kircheis. Liposomes containing interferon-gamma as adjuvant in tumor cell vaccines, *Pharm. Res.* **17**: 42-48 (2000).
10. G. Spenlehauer, M. Vert, J.-P. Benoit, F. Chabot, and M. Veillard. Biodegradable cisplatin microspheres prepared by the solvent evaporation method: Morphology and release characteristics, *J. Control. Rel.* **7**: 217-229 (1988).

11. R. C. Mehta, B. C. Thanoo, and P. P. DeLuca. Peptide containing microspheres from low molecular weight and hydrophilic poly(d,l-lactide-co-glycolide), *J. Control. Rel.* **41**: 249-257 (1996).
12. A. Gopferich, R. Gref, Y. Minamitake, L. Shieh, M. J. Alonzo, Y. Tabata, and R. Langer. Drug delivery from bioerodable polymers: systemic and intravenous administration. In J.L.Cleland and R.Langer (eds), *Formulation and Delivery of Proteins and Peptides*, ACS, Washington, 1994, pp. 242-277.
13. A. Shenderova, T. G. Burke, and S. P. Schwendeman. Evidence for an acidic microclimate in PLGA microspheres, *Proc. Control. Rel. Soc.* **Issue 25**: (1998).
14. K. Fu, D. W. Pack, A. Laverdiere, S. Son, and R. Langer. Visualization of pH in degrading polymer microspheres, *Proc. Control. Rel. Soc.* **Issue 25**: (1998).
15. M. S. Hora, R. K. Rana, J. H. Nunberg, T. R. Tice, R. M. Gilley, and M. E. Hudson. Release of human serum albumin from poly(lactide-co-glycolide) microspheres, *Pharm. Res.* **7**: 1190-1194 (1990).
16. J. Yang and J. L. Cleland. Factors affecting the in vitro release of recombinant human interferon- gamma (rhIFN-gamma) from PLGA microspheres, *J. Pharm. Sci.* **86**: 908-914 (1997).
17. H. M. Younes and B. G. Amsden. Osmotically controlled drug delivery from a new phot-cured biodegradable elastomer, *J. Control. Rel.*, submitted (2002)

18. J. L. Cleland and A. J. S. Jones. Stable formulations of recombinant human growth hormone and interferon-gamma for microencapsulation in biodegradable microspheres, *Pharm. Res.* **13**: 1464-1475 (1996).
19. H. M. Younes and B. G. Amsden. Synthesis, characterization and in vitro degradation of a biodegradable elastomer. *Biomacromolecules*, submitted (2002).
20. J. A. Hubbell, C. P. Pathak, A. S. Sawhney, N. P. Desai, and J. L. Hill. Photopolymerizable biodegradable hydrogels as tissue contacting materials and controlled-release carriers, U.S. Patent 5,410,016. 1995.
21. O. H. Lowry, N. J. Rosebrough, A. L. Farr, and R. J. Randall. Protein measurement with the folin-phenol reagent, *J. Biol. Chem.* **193**: 265-275 (1951).
22. V. H. L. Lee. Changing needs in drug delivery in the era of peptide and protein drugs. In V. H. L. Lee (eds), *Peptide and Protein Drug Delivery*, Marcel Dekker, New York, 1991, pp. 1-56.
23. Z. Estrov, R. Kurzrock, and M. Talpaz, *Interferons, basic principles and clinical applications*, R.G. Landes Co, Austin, 1993.
24. N. Oeswein and S. J. Shire. Physical biochemistry of protein drugs. In V. H. L. Lee (eds), *Peptide and Protein Drug Delivery*, Marcel Dekker, New York, 1991, pp. 167-202.
25. T. G. Park, W. Lu, and G. Crotts. Importance of in vitro experimental conditions on protein release kinetics, stability and polymer degradation in protein encapsulated

- poly (D,L-lactic acid-co-glycolic acid) microspheres, *J. Control. Rel.* **33**: 211-222 (1995).
26. B. Amsden and Y-L. Cheng. A generic protein delivery system based on osmotically rupturable monoliths, *J. Control. Rel.* **33**: 99-105 (1995).
27. J. Kang, M. Yang, I. Jou, and E. Joe. Identification of protein kinase C isoforms involved in interferon- gamma-induced expression of inducible nitric oxide synthase in murine BV2 microglia, *Neurosci. Lett.* **299**: 205-208 (2001).
28. M. Jana, X. Liu, S. Koka, S. Ghosh, T. M. Petro, and K. Pahan. Ligation of CD40 stimulates the induction of nitric-oxide synthase in microglial cells, *J. Biol. Chem.* **276**: 44527-44533 (2001).
29. H. Possel, H. Noack, J. Putzke, G. Wolf, and H. Sies. Selective upregulation of inducible nitric oxide synthase (iNOS) by lipopolysaccharide (LPS) and cytokines in microglia: in vitro and in vivo studies, *Glia* **32**: 51-59 (2000).
30. N. F. Sheppard, M. Y. Madrid, and R. Langer. Polymer matrix controlled release systems: Influence of polymer carrier and temperature on water uptake and protein release., *J. Appl. Polym. Sci.* **46**: 19-26 (1992).

CHAPTER 6

GENERAL DISCUSSION AND CONCLUSIONS

6.1 General Discussion

In our introductory discussion, it was shown that in certain instances, such as in cancer immunotherapy, it is desirable to have a localized and continuous delivery of Interferon- γ . Polymeric delivery systems have been extensively investigated for this purpose, however, the conventional degradable polymers, such as poly (lactide-co-glycolide), have been demonstrated to denature protein drugs before they are released from the delivery system, rendering them inactive. To solve this problem, an elastomeric drug delivery vehicle has been designed which utilizes osmotic activity as the drug delivery driving force. This system was designed to enable the protein drug to be released before any major degradation takes place and therefore prevent the cytokine from being exposed to the acidic medium of the accumulated monomers.

To achieve this goal, we attempted to prepare an amorphous elastomer that would have a T_g well below body temperature, and that would maintain its form stability for the intended time period of release. To accomplish this, a trifunctional alcoholic initiator (glycerol) was reacted with a 1:1 molar ratio of both DL-LA and ϵ -CL using SnOct as catalyst. A monomer: initiator molar ratio of 10:1 was used to prepare this star copolymer. The purified SCP prepared was then crosslinked in different ratios with a bis-caprolactone (BCP) monomer (Scheme 2.3).

The mechanical tensile testing for the tested slabs of the differently crosslinked elastomers reflected behaviour typical of amorphous elastomers tested above their T_g . In

addition, as expected, incorporating higher amounts of the BCP crosslinker resulted in a highly crosslinked tough elastomer indicated by higher Young's modulus (E) values and lower ultimate strain (ϵ). On the contrary, samples with less crosslinker amount used, were soft, weak elastomeric polymer with a low E and high ϵ .

During the degradation studies, the decrease in the modulus values with respect to time for all the elastomers showed a logarithmic relationship as has been observed with other elastomers [1,2]. Such behaviour was indicative of a bulk hydrolysis mechanism in which random chain scission of ester groups along the backbone occurs [1-3]. Such a pattern of degradation would result in the accumulation of the acidic monomers inside the bulk of the polymer contributing to further autocatalytic acidic degradation. The fact that no significant weight loss of the dried tested specimens for all the elastomers were observed after 4 weeks excluded the occurrence of any major surface erosion. Although some reports indicated that an increase in Young's modulus with time is possible due to an increase in the crystallinity of the degrading amorphous polymer [4-6], this was not observed with this material indicating that crystal formation did not occur.

Using BCP as a crosslinker to prepare the elastomers required for the cytokine delivery system showed a few limitations. First, the extent of the crosslinking process was dependent on the reactivity of BCP. Although its reactivity was supposed to be similar to ϵ -CL monomer as been reported earlier [2,7], the fact that it is in the solid form restricted its solubility in the polymer mix and therefore decreased its reactivity which rendered the end product with low degree of crosslinking. Initially, the use of a crosslinking

temperature of 180 °C was required to overcome this problem in which a substantial oxidation of the BCP occurred during the crosslinking reaction, as was noted by the discoloration of the sample. In later attempts to increase reactivity and to lower the crosslinking temperature, the pre-addition of 1 g of ϵ -CL monomer helped in minimizing the solubility problem that other researchers reported while using BCP as a crosslinking agent [7] and reduced the temperature required for crosslinking from 180 °C down to 120 °C.

Second, although the samples that were crosslinked with higher amounts of BCP resulted in a tougher material, all the ratios prepared were determined to have a low crosslinking density as indicated by the rapid drop in their mechanical properties after one week of the degradation study. These slabs, however, did maintain their integrity for 3 months. The mechanical tensile testing also indicated that the samples prepared were not acting completely elastomeric but rather showed rubbery behaviour. The crosslinking density of the prepared samples should be further explored by undergoing swelling study to determine the sol-gel content and by running cyclic tensile testing as well to have the exact idea about the mechanical behaviour of the material under cycles of stress.

Third, the use of heat in the crosslinking process has limited its use as a delivery system for heat sensitive drugs such as hormones and proteins. It is important to mention here that attempts to undergo the crosslinking process using solution polymerization were not successful in solving that problem. Finally, the preparation of star copolymer prepolymers prepared using different monomer ratios other than 1:1 DL-LA: ϵ -CL would

also give a broader understanding of the behaviour of the final elastomeric product and the effect of changing the monomer and initiator ratios on their mechanical properties and crosslinking density.

Polymers prepared from D,L-lactide and ϵ -caprolactone and copolymers of these monomers have been demonstrated to be biocompatible and are used in FDA approved devices, but little information exists for the toxicity of the BCP crosslinker used in this work. The BCP molecule was first proposed for use in preparing elastomers of biodegradable polycaprolactone by Pitt et al. [2]. These researchers focused on the mechanism of biodegradation of these elastomers *in vivo*, and followed this degradation for up to 107 weeks in rabbits and rats. However, aside from noting that at 14 and 28 days post-implantation in a rat host reaction to the elastomers was minimal, little toxicity information was provided. It was the objective of Appendix 1 to report on some initial biocompatibility studies of this elastomer.

The main results that can be highlighted from this study are that, under the conditions examined, the leachate of the elastomer material does not exhibit any cytotoxicity, is not locally irritating, and does not exhibit any signs of systemic toxicity. These findings mean that the method used to prepare the material does not leave any toxic compounds within the material. The two week implantation study shows that the material is not toxic after this time period in the body. However, as shown in the *in vitro* studies the material does not significantly degrade until about 3 months in PBS buffer, although degradation products are released from the material during the first two weeks and so possible

bioreactivity as a result of degradation products has not been completely assessed. Nevertheless, previous work by Pitt and co-workers using the same crosslinking compound, demonstrated no adverse long-term tissue response [2]. This new elastomer thus showed promise as a biomaterial.

For the above reasons, photo-crosslinking was used as an alternative way of achieving the crosslinking of the elastomer without the necessity of using heat. In Chapter 3, we reported on the synthesis, photocuring, characterisation, mechanical properties and *in vitro* degradation of a newly synthesized biodegradable elastomer that has potential as an implantable matrix for the delivery of peptide and protein drugs.

The use of this approach as a way of crosslinking the prepared acrylated prepolymer offers a number of advantages over the thermal crosslinking method. First, the process waived the use of thermal energy, which enabled us to crosslink the polymer at room temperatures and therefore having no problem in loading biologically thermo-sensitive therapeutics like proteins and other heat-sensitive drugs into this prepared elastomer. Second, the process proceeded rapidly. Finally, the degree of crosslinking, and the mechanical properties of the photocured elastomer could be tailored by changing the density of the photosensitive termini in the prepolymer.

The mechanical testing of the prepared photo-crosslinked elastomers indicated that they possessed high crosslink densities which made them more resistant to water penetration. This was also evident by immersing the polymers into dichloromethane. The polymers

swelled but did not dissolve. It was evident therefore that a tough elastomeric material was prepared and the detailed investigation of its mechanical properties (Chapter 3) showed that it maintained its integrity for the tested period of the degradation study. More important, it was evident that only minor changes in the mechanical properties reported within the 4 weeks of the degradation study. This has offered major advantage over the BCP crosslinked elastomer in the fact that it showed slower bulk hydrolysis rate as a result of which less exposure of the loaded protein to the accumulated acidic monomers would be achieved. Therefore, this approach possessed significant advantages over the BCP crosslinked polymers. As has been reported earlier for the BCP crosslinked elastomers, a long term biocompatibility study is also required to be done on this photo-crosslinked elastomer as a future plan.

After preparing the new elastomer, it was necessary to demonstrate the release mechanism from this newly synthesised hydrophobic photo-cured biodegradable elastomer. Pilocarpine nitrate was used as a model of a drug with a reasonably high osmotic activity. Pilocarpine nitrate was also co-formulated with another, more osmotically active agent (i.e. trehalose) to examine means of enhancing the release of a water soluble agent from an elastomeric, degradable, monolithic system.

One of the limitations faced in loading the drug into the UV-crosslinked elastomeric device was the restriction of not exceeding 5% v/v loadings. This was attributable to the fact that the drug was suspended into the matrix and acted as an obstacle against the penetration of UV rays above that loading threshold. Nevertheless, this was not a major

restriction for our main intention to load proteins and cytokines into the delivery device. It has been found that many protein drugs require only very low doses to elicit therapeutic effects. For example, only few picograms per day of epidermal growth factor are required to induce tissue regeneration [8].

The release studies performed indicated the ability of our system to achieve a linear release profile in PBS once PCN and trehalose were intimately mixed and loaded within the delivery system. The use of trehalose helped in boosting up the osmotic activity of the loaded drug which also simulates the situation of loading proteins previously lyophilized with such stabilizing sugars. In addition, the use of trehalose in our study helped in achieving a linear and complete release in PBS before any major degradation of the elastomer takes place as has been shown previously in the reported degradation studies. Further study of the release behaviour of the PCN from this system should be undertaken in both 3% NaCl and DW to confirm the osmotic release mechanism. In addition, a longer term study of the degradation kinetics of this elastomer should be a future study to correlate it to the release behaviour from this elastomer.

In the last chapter, the study of the activities of IFN- γ in BV-2 cells during the preparation steps and after being released in PBS was reported. The study demonstrated that IFN- γ was stable up to the point when it was loaded into the delivery system. The method of loading this protein into the UV-crosslinked elastomer involved the load of the solid lyophilized protein into the prepolymer which was further crosslinked under UV

exposure. This process used in the preparation steps of the presented work has contributed in many aspects when compared to the current available polymeric delivery systems for IFN- γ . First, the use of the UV crosslinking methodology shortened the process required to prepare the delivery system to become in the order of minutes and avoided the need for using heat to formulate the polymer. Second, this process proved to retain the activity and the stability of the loaded protein during the preparation steps as being discussed in chapter 5 of this thesis. Third, the prepared delivery system demonstrated a low burst effect when compared to that achieved by liposomes as delivery systems [9]. In addition, a zero order release pattern was achieved during the whole release period.

On the other hand, this delivery system managed to reserve almost 70-80% of the activity of the released protein indicated by the good correlation achieved between the cumulative concentration released of IFN- γ and the corresponding cumulative activity reported. This was a significant contribution in retaining the activity of IFN- γ for the 14 days period when compared to 30% retained activity over a period of 7 days reported previously using PLG microspheres [10].

Future studies regarding the reason of why IFN- γ lost its activity after the two weeks period should be conducted. Such studies should involve the determination of its conformational changes using circular dichroism studies and the use of light scattering technology to determine if any aggregation has taken place during the loading process especially upon the use of DCM and after exposure to UV. Future work should also be

done to determine the effect of altering the mechanical properties of the prepared elastomers on the stability and activity of the loaded protein. It could be that the decrease in the rate of degradation of the elastomeric device would help in releasing the loaded protein before any major exposure to the acidic microenvironment takes place. This accumulation of the acidic monomers after 14 days might have resulted in the denaturation of IFN- γ and therefore rendered it inactive.

6.2. General Conclusions

The conclusions can be summarized as follows:

1. Ring opening polymerization of ϵ -CL with DL-LA using glycerol as initiator and SnOct as a catalyst resulted in a star copolymer that was further reacted with different ratios of the crosslinking monomer, 2,2-bis(ϵ -caprolactone-4-yl)-propane (BCP). Higher amounts of the BCP used in crosslinking the star copolymer prepolymer resulted in an increase in glass transition temperature, Young's modulus, and ultimate tensile strength. Upon degradation in phosphate buffered saline, the elastomers showed a logarithmic decrease in their Young's modulus with time as an indication of a bulk hydrolysis mechanism that was also accompanied by an increase in water absorption and a decrease in their ultimate tensile strength. In addition, the extension ratio of the tested elastomers increased with time accompanied by a decrease in their Young's modulus and ultimate tensile strength.

2. Under the conditions in which the BCP crosslinked elastomer biocompatibility was examined, the leachate of the elastomer material does not exhibit any cytotoxicity, is not locally irritating, and does not exhibit any signs of systemic toxicity. This finding means that the method used to prepare the material does not leave any toxic compounds within the material. The two week implantation study shows that the material is not toxic after this time period in the body. However, in vitro studies show that the material does not significantly degrade until about 4 months in PBS buffer, although degradation products are released from the material during the first two weeks and so possible bioreactivity as a result of degradation products has not been completely assessed. Nevertheless, previous work by Pitt and co-workers [2] using the same crosslinking compound, demonstrated no adverse long-term tissue response. This new elastomer thus shows promise as a biomaterial for tissue engineering.

3. Ring opening polymerization of ϵ -CL with DL-LA using glycerol as initiator and SnOct as a catalyst resulted in a star copolymer that was further reacted with different ratios of the ACRL to convert the terminal OH groups in to photosensitive vinyl termini. Higher amounts of the ACRL used in the reaction resulted in an increase in % of conversion with a nearly complete conversion achieved once 3 moles of ACRL are used to react with 1 mole of SCP. The UV photopolymerization process resulted in a variety of photosest polymers whose elasticity is dependent on the monomers and initiator ratios used in the

preparation of the prepolymers. The analysis of the changes in the mechanical properties in PBS degradation medium for the elastomers prepared by photocrosslinking the SCP-1A acrylated showed minor changes in Young's modulus, ultimate stress, and extension ratio within the first 2 weeks of the study. Significant changes were only observed by the fourth week of the degradation period. This analysis was supported by the insignificant mean changes in percent weight of the tested slabs over the first two weeks. The above conclusion was drawn based on the high crosslink density the tested elastomer demonstrated upon running the swelling studies. A longer period of degradation study is a future plan to determine the exact changes in the tensile properties after the 1 month of degradation in PBS.

4. The release mechanism of pilocarpine nitrate of 5% v/v loadings from monolithic cylinders of a newly synthesised elastomer was demonstrated. The release rate was distinguished by three release stages in which the second linear release phase was mainly dominated by a non-osmotic mechanism. This linear phase of release was extended while its degradation related release was eliminated by co-formulating the drug with the high osmotically active agent, trehalose. Upon using this excipient, a large fraction of pilocarpine nitrate was released during the initially rapid release phase after which the release becoming linear and slower in rate until essentially complete release of pilocarpine nitrate. In this situation, osmotic release mechanism was the dominant mechanism that contributed to that enhancement in the drug release.

5. A new delivery vehicle composed of a biodegradable elastomer was developed for protein delivery and demonstrated to be effective in delivering active IFN- γ for in a constant and sustained release fashion. More work needs to be done to determine if the loss of stability of IFN- γ after a two week delivery period was due to the storage conditions, or from degradation in the device. A future study of the conformational changes of rmIFN- γ and its subsequent aggregates using circular dichroism and gel permeation chromatography is a future work. This sort of investigation for the structural changes would give a clearer picture of how and what made this cytokine lose its activity after this period of time.

6.3. References

- [1] M. P. Hiljanen-Vainio, P. A. Orava, J. V. Seppala, Properties of epsilon-caprolactone/DL-lactide (epsilon-CL/DL-LA) copolymers with a minor epsilon-CL content, *J. Biom. Mater. Res.* 34 (1997) 39-46.
- [2] C. G. Pitt, R. W. Hendren, A. Schindler, The enzymatic surface erosion of aliphatic polyesters, *J. Control. Rel.* 1 (1984) 3-14.
- [3] R. Sodian, J. S. Sperling, D. P. Martin, A. Egozy, U. Stock, J. E. Mayer, Jr., J. P. Vacanti, Fabrication of a trileaflet heart valve scaffold from a polyhydroxyalkanoate biopolyester for use in tissue engineering, *Tissue Eng.* 6 (2000) 183-188.

- [4] M. Hiljanen-Vainio, T. Karjalainen, J. Seppala, Biodegradable lactone copolymers. I. Characterization and mechanical behavior of ϵ -caprolactone and lactide copolymers, *J. Appl. Polym. Sci.* 59 (1996) 1281-1288.
- [5] T. Karjalainen, M. Hiljanen-Vainio, M. Malin, J. Seppala, Biodegradable lactone copolymers. III. Mechanical properties of epsilon -caprolactone and lactide copolymers after hydrolysis in vitro, *J. Appl. Polym. Sci.* 59 (1996) 1299-1304.
- [6] H. M. Younes, B. G. Amsden, Biodegradable elastomer as potential drug carrier: Synthesis, characterization and in vitro degradation, *Biomacromolecules* (2002) submitted.
- [7] R. Palmgren, S. Karlsson, A.-C. Albertsson, Synthesis of degradable crosslinked polymers based on 1,5-dioxepan-2-one and crosslinker of bis- ϵ -caprolactone type, *J. Polym. Sci. A: Polym. Chem.* 35 (1997) 1635-1649.
- [8] T. G. Park, W. Lu, G. Crotts, Importance of in vitro experimental conditions on protein release kinetics, stability and polymer degradation in protein encapsulated poly(D,L-lactic acid-co-glycolic acid) microspheres, *J. Control. Rel.* 33 (1995) 211-222.
- [9] M. L. Van Slooten, A. J. W. G. Visser, A. Van Hoek, G. Storm, D. J. A. Crommelin, W. Jiskoot, Conformational stability of human interferon-gamma on association with and dissociation from liposomes, *J. Pharm. Sci.* 89 (2000) 1605-1619.

- [10] J. Yang, J. L. Cleland, Factors affecting the in vitro release of recombinant human interferon- gamma (rhIFN-gamma) from PLGA microspheres, *J. Pharm. Sci.* 86 (1997) 908-914.

APPENDICES

Appendix 1

COMPATIBILITY ASSESSMENT OF A BIODEGRADABLE ELASTOMER

Brian G. Amsden ^{1,2} and Husam M. Younes ¹

A version of this chapter to be submitted to

Journal of Biomedical Materials Research

1. Faculty of Pharmacy and Pharmaceutical Science, University of Alberta,
Edmonton, Alberta, Canada T6G 2N8
2. Department of Chemical Engineering, Queens University, Kingston, Ontario,
Canada, K7L 3N6

1. Introduction

Biodegradable elastomers have a number of possible uses as biomaterials. They can be used as depots for localized drug delivery^{1, 2} and as a three dimensional matrix supporting the growth of tissue either *in vivo* or *ex vivo*.³⁻⁵ In both of these applications, the materials used to prepare the elastomers must not only be biodegradable, but must also not inhibit normal cell growth and function.

Biodegradable elastomers can be prepared in either of two ways, that is, either from thermoplastic materials,⁶⁻⁸ or as thermosets.^{9,10} Thermoplastics have the advantage of being easily fabricated by melt processing. The crosslinks which provide the elastomeric nature of these materials are composed of crystalline regions of blocks of the backbone polymer. These crystalline regions degrade much more slowly *in vivo* and produce a material which eventually becomes porous and during degradation the shape of the material does not remain constant. Although they are not as easily processed as thermoplastics, thermosets degrade more homogeneously as the crosslinks are covalent, producing an amorphous polymer. During degradation these polymers tend to hold their shape longer. Thermosets, therefore, possess certain application advantages.

We have prepared a new thermoset elastomer for use as a biomaterial. The elastomer is prepared by crosslinking a star copolymer of caprolactone and D,L-lactide with 2,2-bis(ϵ -caprolactone-4-yl)-propane (Figure 1). Details of the preparation of this polymer and its characterization are presented elsewhere.¹¹ The material is a soft, weak, elastomeric

polymer, whose physical properties and *in vitro* degradation rate can be manipulated by altering the crosslink density, and star copolymer prepolymer composition and molecular weight.

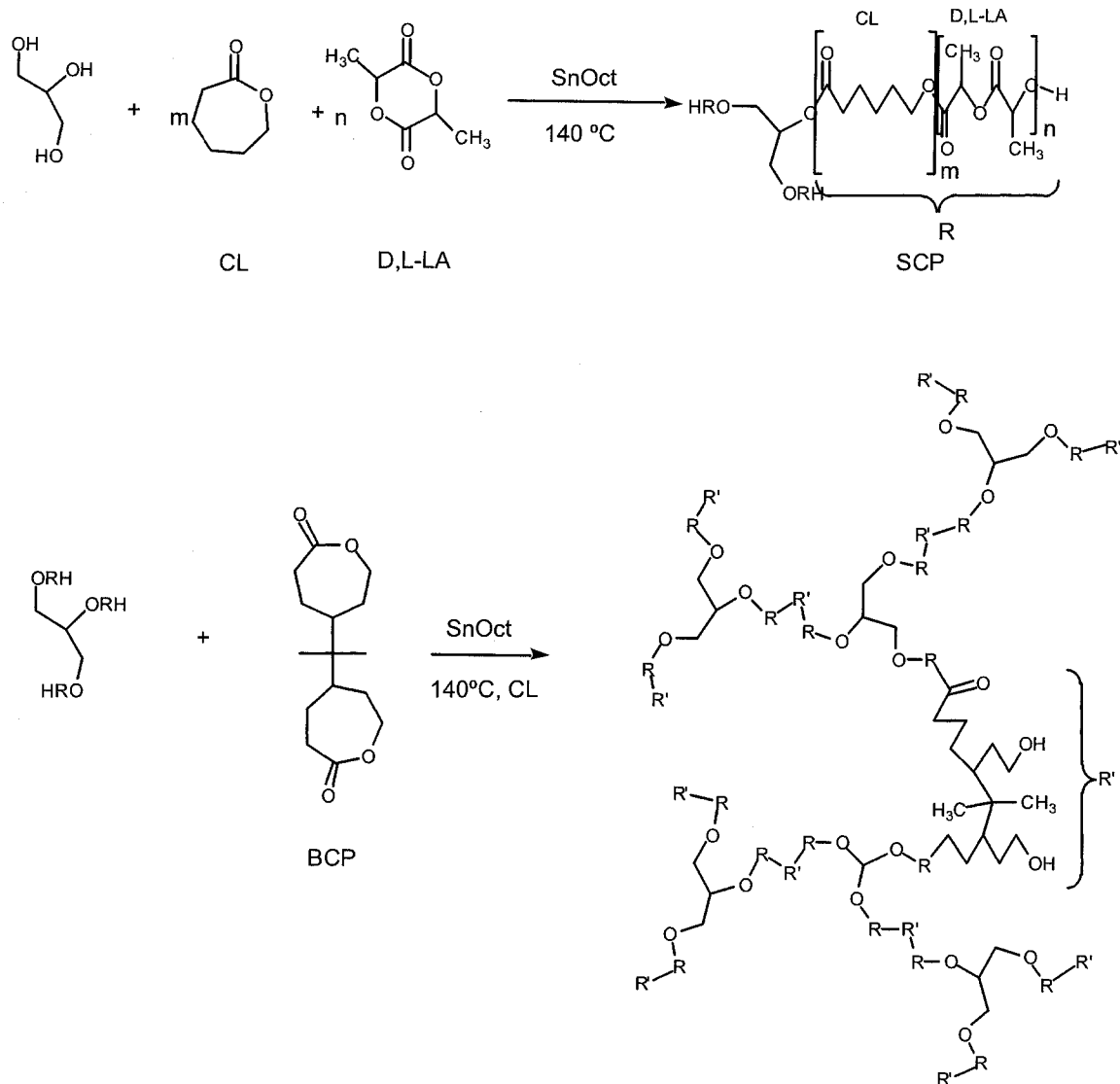


Figure 1 Scheme for production of elastomer via crosslinking star copolymer of poly(D,L-lactide – co – ϵ -caprolactone)

Our interest in preparing biodegradable elastomers is in investigating their use as scaffolds in tissue engineering. As the rate and extent of initial cell infiltration into the elastomer is considered important in determining the success of this material, short term toxicity assays of the material are necessary. Polymers prepared from D,L-lactide and ϵ -caprolactone and copolymers of these monomers have been demonstrated to be biocompatible and are used in FDA approved devices, but little information exists for the toxicity of the BCP crosslinker. The BCP molecule was first proposed for use in preparing elastomers of biodegradable polycaprolactone by Pitt et al. (1984).¹ These researchers focused on the mechanism of biodegradation of these elastomers *in vivo*, and followed this degradation for up to 107 weeks in rabbits and rats. However, aside from noting that at 14 and 28 days post-implantation in a rat host reaction to the elastomers was minimal, little toxicity information was provided. It is the objective of this paper to report on some initial biocompatibility studies of this elastomer.

2. Materials and Methods

D,L-lactide (DLLA) was obtained from Purac, the Netherlands, and ϵ -caprolactone (ϵ -CL) was obtained from Lancaster and then dried over CaH_2 (Aldrich) and purified by distillation under reduced pressure. Other chemicals used include glycerol (BDH), stannous octoate (SnOct), dichloromethane, and methanol (all from Aldrich). 2,2-bis(ϵ -caprolactone-4-yl)-propane (BCP) was prepared as outlined in Palmgren et al.¹²

2.1. Preparation of 50:50 poly (ϵ -caprolactone-dl-lactide) (ϵ -CL/DLLA) star copolymer (SCP)

Solvent-free polymerization was carried out in sealed 20 ml glass ampoules. A representative polymerization is as follows. Into a flame dried ampoule, 0.005 mol of glycerol and 0.05 mol of ϵ -CL were transferred and mixed till homogeneous. An amount equivalent to 0.05 mol of DLLA was then transferred to the ampoule, the ampoule filled with nitrogen, then placed in an oven at 120 °C for 10 minutes allowing the DLLA to melt. The molten mixture was then vortexed and SnOct was added in an amount equivalent to $1.4 (10^{-4})$ mol for each 1 mol of the monomer. The ampoule was filled with nitrogen, flame sealed under vacuum, and left in an oven at 140 °C for 24 hours. The prepared SCP was purified by precipitation from dichloromethane (DCM) solution into cold methanol.

2.2. Elastomer Synthesis

An elastomer slab was prepared by compression molding in a Teflon mold. In a flame-dried vacuum ampoule, 5 g of BCP was dissolved in 1 g of ϵ -CL monomer at 140 °C for 15 minutes under a nitrogen blanket. 15 g of molten SCP (140 °C) and an amount of SnOct equivalent to $1.4 (10^{-4})$ mol for each 1 mol of the SCP prepolymer were added to the ampoule which was then mixed by vortexing. The ampoule was replaced in the oven for 5 minutes under a mild vacuum of 10 mm Hg, to draw out entrapped air. The contents of the ampoule were then poured into a pre-heated Teflon slab mold, taking care

not to introduce air bubbles, covered with an additional sheet of Teflon, and allowed to cure for 24 hours at 140 °C. After curing, the elastomer sheet was removed using sterile surgical gloves and heat-sealed in sterile aluminum pouches for storage.

2.3. Sterilization.

The polymer was sterilized by Co⁶⁰ irradiation at a dose level of 50 kGy.

2.4. Compatibility Studies

All elastomer compatibility studies were carried out by Toxikon Inc., Bedford Massachusetts, USA.

2.4.1. In Vitro Cytotoxicity

The biological reactivity of a mammalian monolayer of L929 mouse fibroblast cells to leachate extracts of the elastomer was determined as outlined in ISO 10993-5, 1999, as follows. L929 cells were incubated in 6-well plates at 2 ml per well (seeded at $2(10^5)$ cells/well) for 24 hours at 37 ± 1 °C for 24 hours in a humidified atmosphere containing $5 \pm 1\%$ CO₂. Sterilized and clean polymer slabs (2.1 cm thick, 4.8 cm wide, and 2.9 cm long) were immersed in 10 ml Eagle's minimum essential medium, which also contained 0.25% trypsin, for 24 hours at 37 ± 1 °C for 24 hours in a humidified atmosphere containing $5 \pm 1\%$ CO₂ to prepare the test article extraction medium. After extraction,

the pH of the extraction medium was checked to determine if it had been altered from 7.2. Extraction media of a positive control (natural rubber), a negative control (negative control plastic), and a cell medium only control, were prepared in the same manner. The extracts were used to replace the maintenance medium of the cell culture. All cultures were incubated in triplicate for 48 hours for 24 hours at 37 ± 1 °C for 24 hours in a humidified atmosphere containing $5 \pm 1\%$ CO₂. At time frames of 0, 24, and 48 hours, the cultures were examined for biological reactivity, as indicated by cellular degeneration and malformation. Biological reactivity was rated on a scale from Grade 0 (no reactivity) to Grade 4 (severe reactivity).

2.4.2. Intracutaneous Extract Injection

Local response of an intracutaneous injection of a leachate extract of the elastomer in rabbits was determined by following ISO 10993-10, 1995. New Zealand White rabbits (2 male and 1 female) were acclimatized for a minimum of 5 days prior to the test. Sterilized and clean polymer slabs (2 cm thick, 5 cm wide, and 5.6 cm long) were immersed in 20 ml of either 0.9% USP sodium chloride for injection or cottonseed oil for 24 hours at 37 ± 1 °C. A volume of 0.2 ml of each test article was injected intracutaneously at 5 sites on one side of the shaved dorsal area of the three test animals. At 5 other sites on the other side of each rabbit, 0.2 ml of a control consisting of 0.9% USP sodium chloride for injection or cottonseed oil was injected (Figure 2). Prior to testing, the shaved areas of the rabbits were examined and found to be free of mechanical trauma and/or irritation. The injected sites were examined at 24, 48, and 72 hours post-

inoculation for gross evidence of tissue reaction, such as erythema, edema, and necrosis. Each site was subjectively scored, and a Primary Irritation Index was calculated by averaging the scores for each of the test article and control extracts for each of the three individual animals. This total was divided by 15 and the control score then subtracted from the test article score. The values thus obtained for each animal were then added and the sum divided by 3.

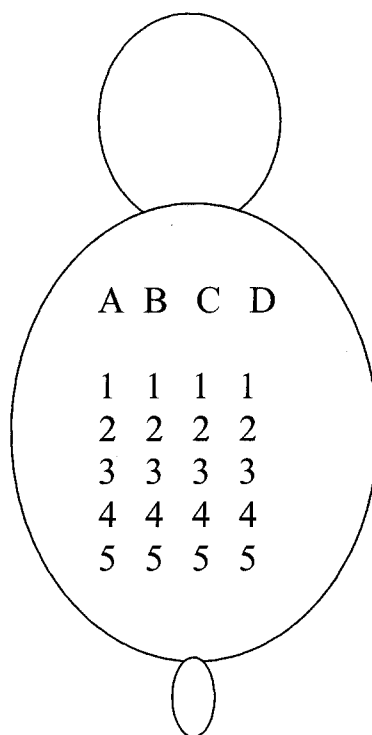


Figure 2 Injection sites for intracutaneous injection test. A = NaCl Test Article Extract B = CSO Test Article Extract, C = CSO Control and D = NaCl Control

2.4.3. Systemic Extract Injection

The systemic response of mice to leachate extracts of the elastomer was determined as outlined in ISO 10993-12, 1996. Twenty ICR male mice were acclimatized for 5 days

prior to testing. Extracts were prepared in the same manner as was done for the intracutaneous injection study. The test article extracts were injected intravenously (0.9% USP sodium chloride for injection) and intraperitoneally (cottonseed oil) at a dose of 50 ml/kg, in groups of 5 mice. Similarly, groups of 5 mice were injected with the control vehicles. The animals were observed for 72 hours post inoculation for signs of biological reactivity, such as lethargy, convulsions, hyperactivity, body weight loss, piloerection, and death.

2.4.4. Implantation Test

Tissue reaction to the presence of the solid elastomer was determined as outlined in ISO 10993-6, 1995. Three healthy New Zealand White rabbits, each weighing at least 2.5 kg, were acclimatized for 5 days prior to testing. On the day of testing, the implant sites were clipped so as to be free of fur. The animals were anaesthetized and 5 slabs of the elastomer (of dimensions 1mm x 1 mm x 10 mm) sterilized in 70 v/v % ethanol were implanted aseptically into the paravertebral muscles using a sterile hypodermic needle. Similarly, 5 strips of a Negative Control Plastic of the same dimensions were also implanted but on the opposite side of the animal. The animals were maintained for a period of 14 days, and then humanely euthanized (Figure 3). After allowing sufficient time that bleeding would not occur post-mortem, the test article sites and the control article sites were removed from the muscle tissue by carefully slicing around the implant site with a scalpel and lifting out the tissue with forceps. A macroscopic evaluation of the excised tissue was done prior to fixation, in which the sites were examined visually via a

magnifying lens for inflammation, necrosis, encapsulation, hemorrhage, and discoloration. The excised tissue was fixed in formalin, processed histologically and examined microscopically by a pathologist. The effects of the articles on the tissue were graded using the following scale: 0 = normal, 0.5 = very slight, 1 = slight, 2 = moderate and 3 = severe. Effects examined were inflammation (polymorphonuclear cells, lymphocytes, eosinophils, plasma cells, macrophages, and giant cells), fibrosis, fatty infiltrate, hemorrhage, necrosis, degeneration, foreign debris, and relative size of the involved area. A Nominal Total Score for the test and control sites for each animal was determined by dividing the mean score of all the sites for each animal (total score divided by the 13 categories of reactions) by the total number of sites examined. This average score was multiplied by 4 to yield a Nominal Total Score for four tests and four control sites. The difference between the Nominal Total Scores for the test article and the control article implant sites was used to determine the Overall Toxicity Rating of the test article.

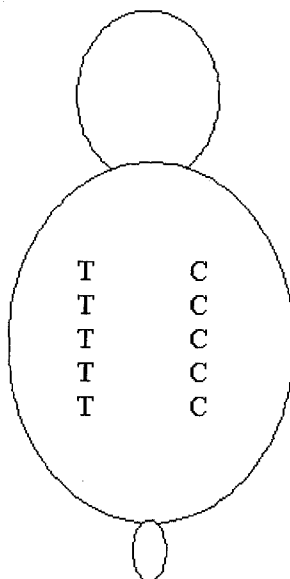


Figure 3 Injection sites for muscle implantation test. T=Test Article, C=Control

3. Results and Discussion

In the preparation of BCP a number of solvents and reactants are used.¹² These compounds include acetic acid, benzene, heptanone, dichloromethane, and m-chloroperoxybenzoic acid. Extensive efforts were taken to remove these compounds from the final product, but the presence of even trace amounts could result in toxicity of the final elastomer product. These compounds could potentially be leached out of the elastomer and be a cause of biological incompatibility.

As a first indication of possible leachate toxicity, a cytotoxicity study was done using L929 mouse fibroblast cells. This test is sensitive, relatively inexpensive and quick to conduct. The elastomer test article was immersed in the cell culture medium at 37 °C for 24 hours and the medium was then used to replace the culture medium of a monolayer of cells and the cells were monitored for 48 hours. After the leaching step, the pH of the extract medium was measured and found to be unaltered from the original pH of 7.2. Cell condition was subjectively assayed in terms of reactivity to the extract medium as either 0 for no reactivity, to 4 for a severe reactivity. Severe reactivity is the situation in which there is nearly complete destruction of the cell layers.¹³ These scores were then compared to a positive and a negative control, as well as a cell culture medium control. The results are listed in Table 1. No signs of cell reactivity to the extract medium were exhibited by the cell cultures over the 48 hour observation time frame. The same result was noted for both the medium and the negative control, while the positive control showed a severe reaction at 24 and 48 hours.

Table 1 Cytotoxicity study score results: biological reactivity to L929 mouse fibroblast cell culture.

	Controls											
	Test Article			Medium			Negative			Positive		
time (hrs)	A	B	C	A	B	C	A	B	C	A	B	C
0	0	0	0	0	0	0	0	0	0	0	0	0
24	0	0	0	0	0	0	0	0	0	4	4	4
48	0	0	0	0	0	0	0	0	0	4	4	4

The elastomer was then tested for leachate toxicity in an *in vivo* setting, by examining both intracutaneous injection for the evaluation of local skin responses and systemic injection for the evaluation of acute systemic toxicity. In these studies, the elastomer test article was extracted in both normal saline for injection and cottonseed oil, to determine if either hydrophilic or hydrophobic leachates are present that may produce a toxic response. The responses of the animals were again subjectively scored and compared to controls consisting of the injection vehicles themselves. The results of the intracutaneous test are given in Table 2 while those of the systemic test are given in Table 3. In the intracutaneous testing, none of the test rabbits exhibited any irritation response (erythema, edema, or necrosis) to the extract from the elastomer test article that was greater than that exhibited by the injection vehicles. The Primary Irritation Index for both the saline and cottonseed oil extracts was 0. In every case, the rabbits were observed to remain healthy and they all gained weight. The elastomer test article can therefore be considered a negligible intracutaneous irritant.

Table 2 Intracutaneous test skin reaction scores

Animal	Vehicle	time (hrs)	average test score	average control score
1 initial wt. 2.35 kg final wt. 2.41 kg	NaCl (0.9% USP saline for injection)	24	0	0
		48	0	0
		72	0	0
	CSO (cottonseed oil)	24	0	0
		48	0	0
		72	0	0
2 initial wt. 2.34 kg final wt. 2.38 kg	NaCl	24	0	0
		48	0	0
		72	0	0
	CSO	24	0	0
		48	0	0
		72	0	0
3 initial wt. 2.46 kg final wt. 2.49 kg	NaCl	24	0	0
		48	0	0
		72	0	0
	CSO	24	0	0
		48	0	0
		72	0	0

The results of the systemic toxicity testing indicate that none of the animals exhibited any signs of systemic toxicity to the extract injection medium over the 3 day observation period. The average score for each time period was zero, and every mouse gained weight at a comparable rate as the control animals. The elastomer test article can therefore be classed as a negligible systemic toxicity threat, for the conditions studied.

Table 3 Systemic injection test score results

Animal	Group	wt day 0 (g)	Dose (ml)	Clinical Observations					wt day 3 (g)
				I	4	24	48	72	
1	NaCl	22.6	1.1	0	0	0	0	0	24.8
2	Test	19.4	1.0	0	0	0	0	0	21.3
3	Article	20.1	1.0	0	0	0	0	0	22.2
4		21.8	1.1	0	0	0	0	0	23.9
5		22.1	1.1	0	0	0	0	0	24.2
6	CSO	18.3	0.9	0	0	0	0	0	20.6
7	Test	17.4	0.9	0	0	0	0	0	19.7
8	Article	18.6	0.9	0	0	0	0	0	20.9
9		20.9	1.0	0	0	0	0	0	22.4
10		19.1	1.0	0	0	0	0	0	21.3
11	NaCl	19.3	1.0	0	0	0	0	0	21.4
12	Control	20.1	1.0	0	0	0	0	0	22.8
13		22.4	1.1	0	0	0	0	0	24.6
14		21.8	1.1	0	0	0	0	0	23.4
15		19.4	1.0	0	0	0	0	0	21.6
16	CSO	18.2	0.9	0	0	0	0	0	20.3
17	Control	17.9	0.9	0	0	0	0	0	19.8
18		19.8	1.0	0	0	0	0	0	22.1
19		20.3	1.0	0	0	0	0	0	22.5
20		17.5	0.9	0	0	0	0	0	19.3

I = observations immediately after injection

Finally, a two week implantation study was undertaken to assess biocompatibility of the elastomer test article in contact with living tissue. After excision of the test article, the excision sites were macroscopically examined for signs of inflammation, encapsulation,

hemorrhage, necrosis and discoloration and these examinations compared to those of a negative control. It was observed that the test article and control sites had no inflammation or other signs of biological reaction. The microscopic scoring of biological reaction of the formalin fixed tissue is given in Table 4. Microscopic evaluation of the elastomer test article did not show any increase in biological reactivity as compared to the control article sites after the 14 day time period. The Toxicity Rating (average of the three animals) of the test article was 0.41, which indicates no toxicity.

Table 4 Intramuscular implantation test scores after two weeks implantation.

Animal	Observation	Test Article			Control		
		1	2	3	1	2	3
1	polymorphs	0.5	0.5	1	0.5	0.5	1
	lymphocytes	0	0	0	0	0	0
	eosinophils	0	0	0	0	0	0
	plasma cells	0	0	0	0	0	0
	macrophages	0.5	0.5	0.5	0.5	1	0.5
	giant cells	0	0	0.5	0	0	0.5
	fibrosis	0.5	0.5	0.5	0.5	0.5	0.5
	fatty infiltrate	0	0	0	0	0	0
	hemorrhage	0	0.5	0.5	0	0	0
	degeneration	0.5	0.5	0.5	0.5	0.5	0.5
	necrosis	0.5	0.5	0.5	0.5	0.5	0.5
	foreign debris	0	0	0	0	0	0
	relative size of involved area	3	3	3	3	3	3
	2	polymorphs	0.5	0.5	1	1	0.5
lymphocytes		0	0	0	0	0	0
eosinophils		0	0	0	0	0	0
plasma cells		0	0	0	0	0	0
macrophages		0.5	0.5	0.5	0.5	0.5	0.5
giant cells		0	0.5	0.5	0	0	0
fibrosis		0.5	0.5	0.5	0.5	0.5	0.5
fatty infiltrate		0	0	0	0	0	0
hemorrhage		0	0	0	0	0	0
degeneration		0.5	0.5	0.5	0.5	0.5	0.5
necrosis		0.5	0.5	0.5	0.5	0.5	0.5
foreign debris		0	3	2	0	0.5	0
relative size of involved area		3	3	3	3	3	3

3	polymorphs	0.5	2	2	0.5	0.5	0.5
	lymphocytes	0	0	0	0	0	0
	eosinophils	0	0	0	0	0	0
	plasma cells	0	0	0	0	0	0
	macrophages	0.5	0.5	0.5	0.5	0.5	0.5
	giant cells	1	0	0	0	0	0.5
	fibrosis	1	0.5	0.5	0.5	0.5	0.5
	fatty infiltrate	0	0	0	0	0	0
	hemorrhage	0	0	0.5	0	0	0
	degeneration	0.5	0.5	0.5	0.5	0.5	0.5
	necrosis	0.5	0.5	0.5	0.5	1	0.5
	foreign debris	2	0	0	0	0	0
	relative size of involved area	3	3	3	3	3	3

Grading Scale

0 = normal, no reaction

0.5 = very slight

1 = slight reaction

2 = moderate reaction

3 = severe reaction

Relative size scale (mm²)

0 = no site (0)

0.5 = very slight (>0 to 1)

1 = slight (> 1 to < 2)

2 = moderate (>2 to <3)

3 = severe (>3)

4. Conclusions

The main results are that, under the conditions examined, the leachate of the elastomer material does not exhibit any cytotoxicity, is not locally irritating, and does not exhibit any signs of systemic toxicity. This finding means that the method used to prepare the material does not leave any toxic compounds within the material. The two week implantation study shows that the material is not toxic after this time period in the body.

However, in vitro studies show that the material does not significantly degrade until

about 4 months in PBS buffer, although degradation products are released from the material during the first two weeks,¹¹ and so possible bioreactivity as a result of degradation products has not been completely assessed. Nevertheless, previous work by Pitt and co-workers¹ using the same crosslinking compound, demonstrated no adverse long-term tissue response. This new elastomer thus shows promise as a biomaterial for tissue engineering.

5. References

1. C. G. Pitt, R. W. Hendren, A. Schindler and S. C. Woodward. The enzymatic surface erosion of aliphatic polyesters. *J. Control. Rel.* 1984; 1:3-14.
2. C. G. Pitt and A. E. Schindler, Sustained Subdermal Delivery of Drugs Using Poly(epsilon-caprolactone) and its Copolymers. US Patent 4 148 871, 1979.
3. R. Sodian, J. S. Sperling, D. P. Martin, A. Egozy, U. Stock, J. E. J. Mayer and J. P. Vacanti. Fabrication of a trileaflet heart valve scaffold from a polyhydroxyalkanoate biopolyester for use in tissue engineering. *Tissue Engineering.* 2000; 6:183-188.
4. C. Alberti. From the intestinal neobladder to the bioartificial bladder: remarks on some biological implications. *Minerva Urologica e Nefrologica.* 2000; 52:219-222.
5. M. M. Mulder, R. W. Hitchcock and P. A. Tresco. Skeletal myogenesis on elastomeric substrates: implications for tissue engineering. *Journal of Biomaterials Science, Polymer Edition.* 1998; 9:731-748.
6. J. Kylma and J. Seppala. Synthesis and characterization of a biodegradable

- thermoplastic poly (ester-urethane) elastomer. *Macromolecules*. 1997; 30:2876-2882.
7. M. Hiljanen-Vainio, T. Karjalainen and J. Seppala. Biodegradable lactone copolymers. I. Characterization and mechanical behavior of epsilon -caprolactone and lactide copolymers. *J. Appl. Polym. Sci.* 1996; 59:1281-1288.
 8. K. W. Leong, Z. Zhao and B. I. Dahiyat. New biodegradable polymers for medical applications. Elastomeric Poly (phosphoesterurethane)s. In *Controlled Drug Delivery. Challenges and Strategies*: K. Park, Editor. American Chemical Society; 1997. 469-483.
 9. R. F. Storey and T. P. Hickey. Degradable polyurethane networks based on D,L-lactide, glycolide, epsilon -caprolactone, and trimethylene carbonate homopolyester and copolyester triols. *Polymer*. 1994; 35:830-838.
 10. R. F. Storey, S. C. Warren, C. J. Allison and A. D. Puckett. Methacrylate-endcapped poly(d,l-lactide-co-trimethylene carbonate) oligomers. Network formation by thermal free-radical curing. *Polymer*. 1997; 38:6295-6301.
 11. H. M. Younes and B.G. Amsden. Synthesis, characterization and in vitro degradation of a biodegradable elastomer, submitted to *Biomacromolecules*. 2002.
 12. R. Palmgren, S. Karlsson and A.-C. Albertsson. Synthesis of degradable crosslinked polymers based on 1,5-dioxepan-2-one and crosslinker of bis-epsilon-caprolactone type. *J. Polym. Sci. A: Polym Chem.* 1997; 35:1635 -1649.
 13. P. Upman. Toxicological Evaluations - Testing. In *Handbook of Biomaterials Evaluation*: A. F. von Recum, Editor. Philadelphia: Taylor and Francis; 1999. 275-289.

Appendix 2

RAW DATA

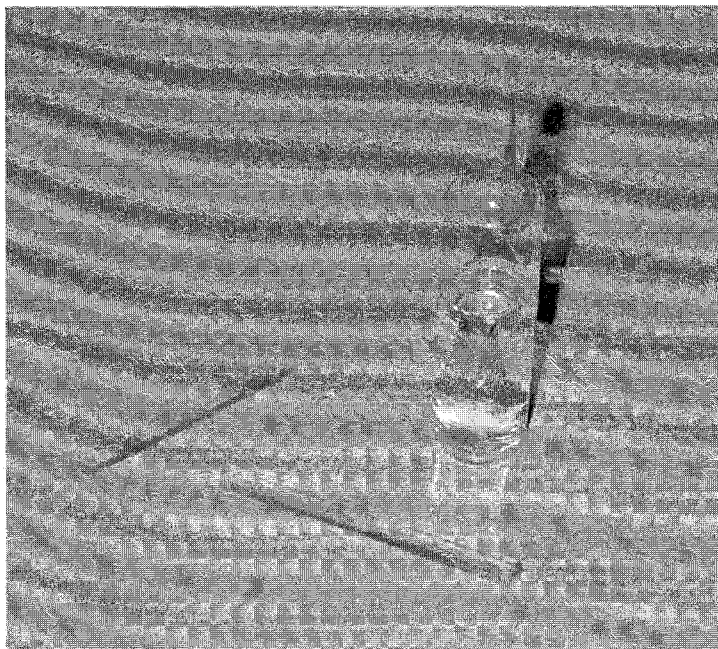


Figure 1: Picture of sealed ampoule containing the prepared star copolymer and the prepared slabs of BCP crosslinked elastomer

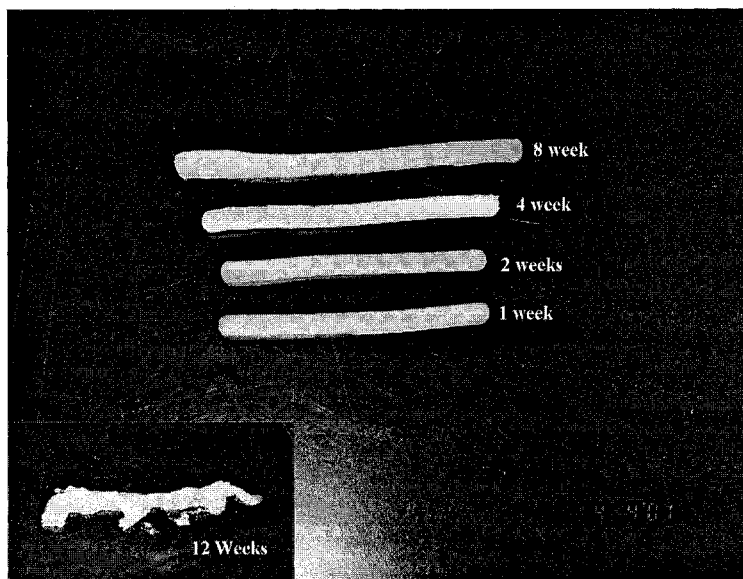


Figure 2: Picture showing the changes in the morphology and swelling behaviour of Elastomeric slabs of BCP crosslinked elastomers at different times of the degradation study

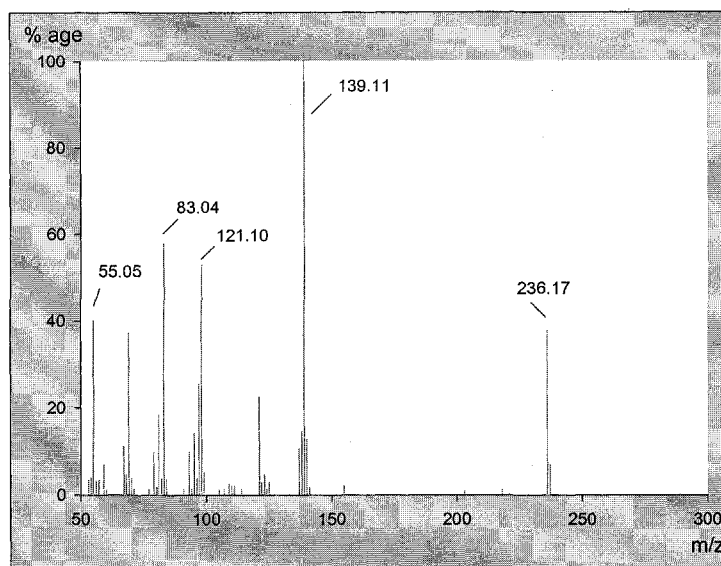


Figure 3: Mass Spectroscopy of prepared Diketone.

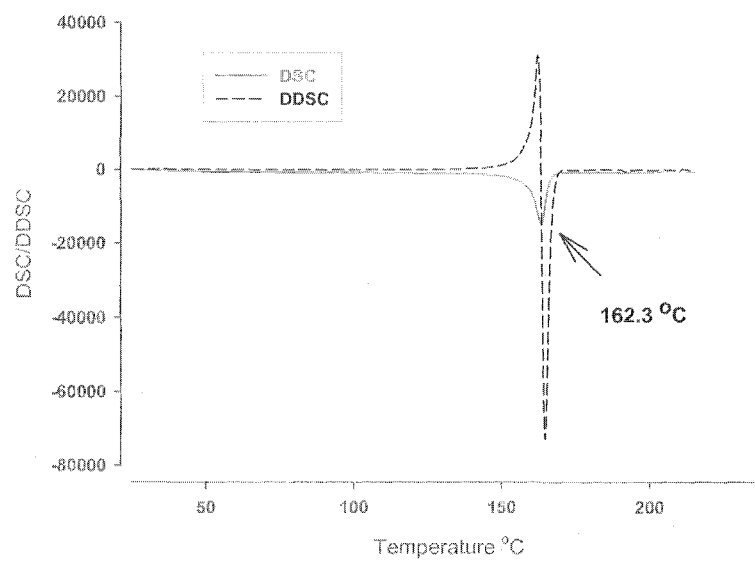


Figure 4: Differential Scanning Calorimetry of prepared Diketone.

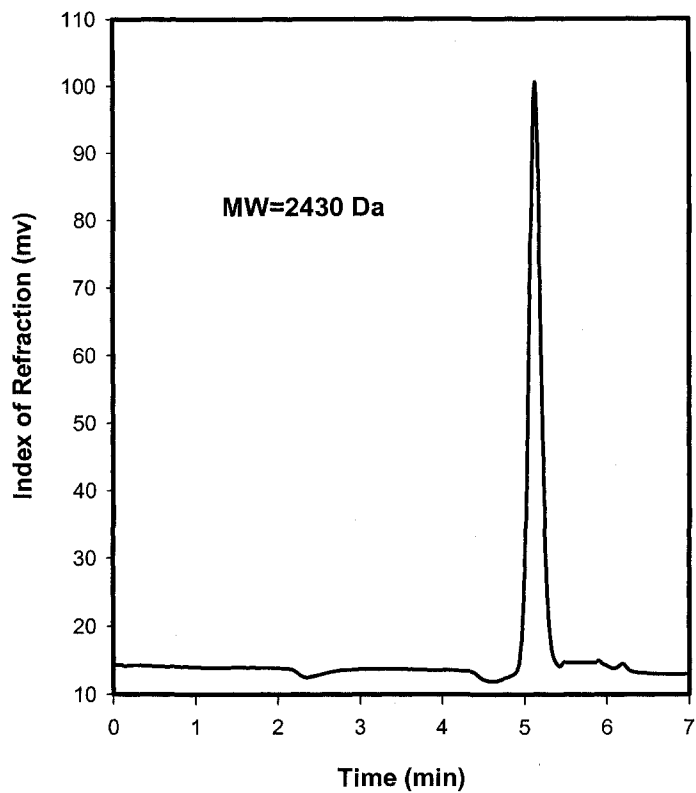


Figure 5: Gel Permeation Chromatogram of the prepared SCP.

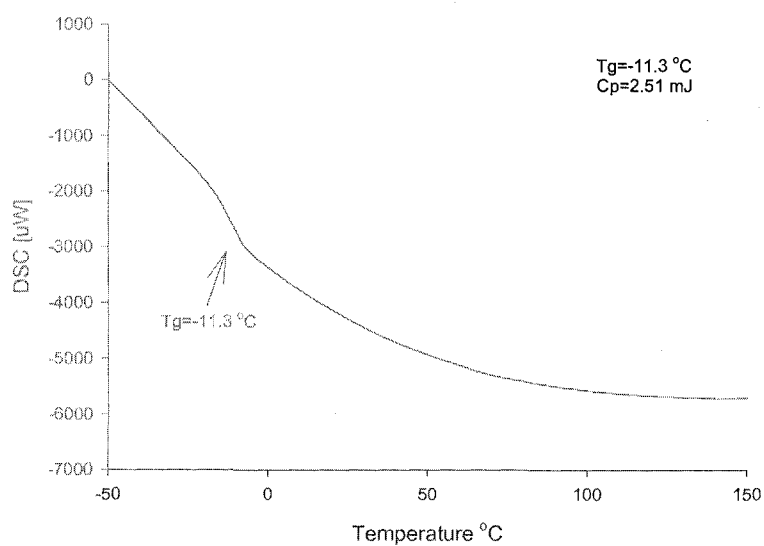


Figure 6: Differential Scanning Calorimetry of Elast 1

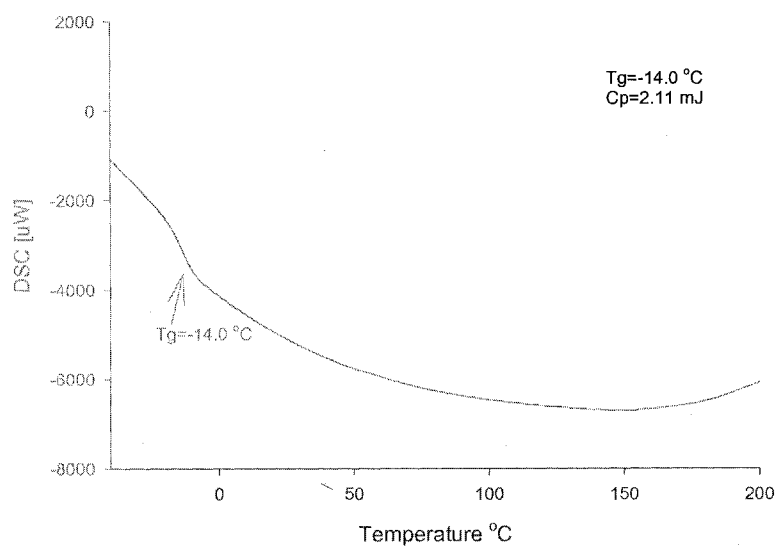


Figure 7: Differential Scanning Calorimetry of Elast 2

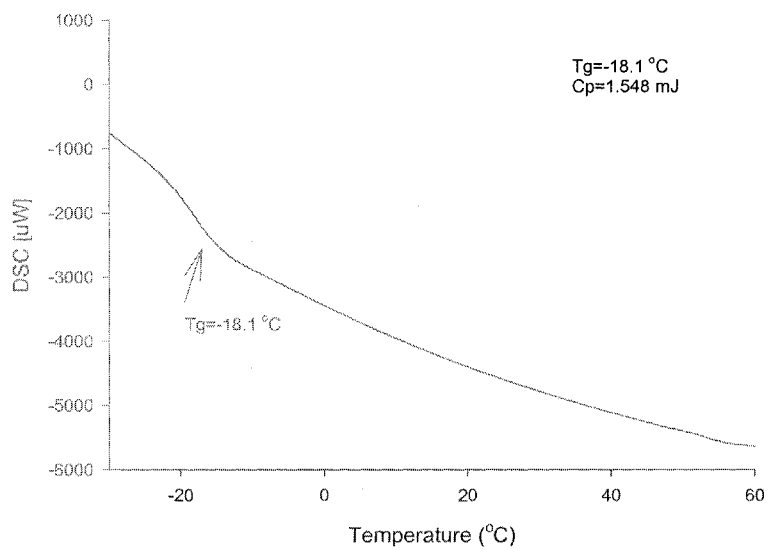


Figure 8: Differential Scanning Calorimetry of Elast 3

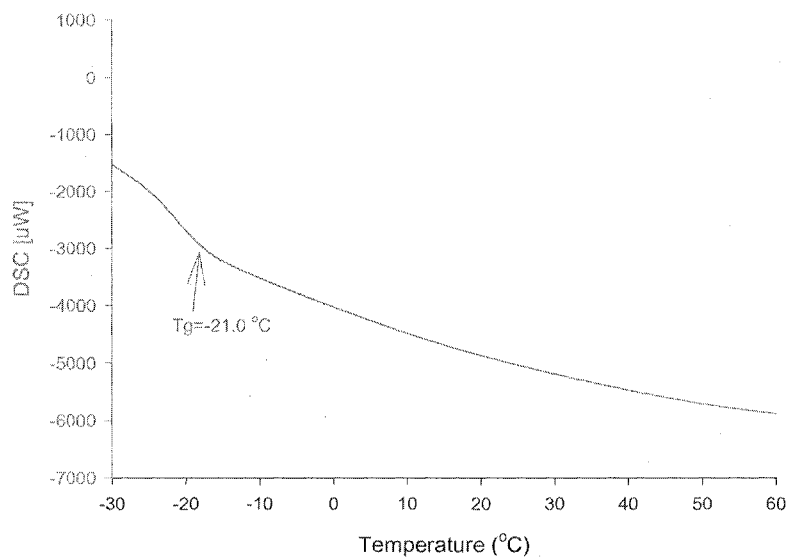


Figure 9: Differential Scanning Calorimetry of Elast 4

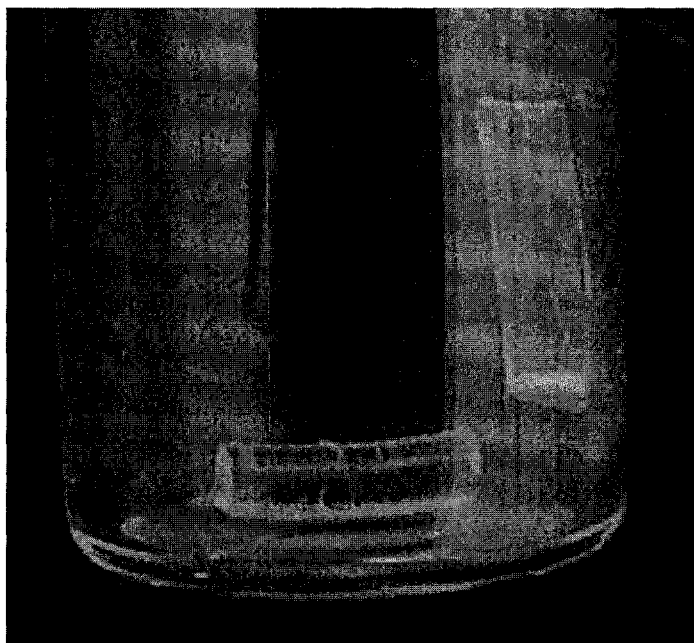


Figure 10: Elastomeric cylinders prepared using photo-crosslinking procedure detailed in chapter 3.